

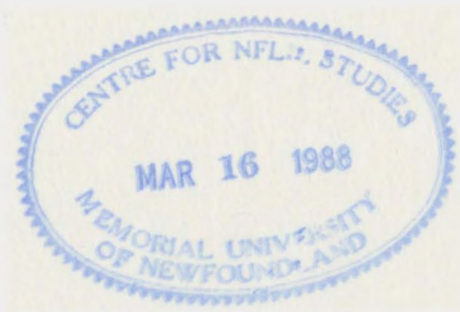
PETROCHEMISTRY OF MAFIC ROCKS FROM  
THE HARBOUR MAIN GROUP (WESTERN  
BLOCK), CONCEPTION BAY, AVALON  
PENINSULA, NEWFOUNDLAND

CENTRE FOR NEWFOUNDLAND STUDIES

**TOTAL OF 10 PAGES ONLY  
MAY BE XEROXED**

(Without Author's Permission)

KEVIN J. CAMERON



PETROCHEMISTRY OF MAFIC ROCKS  
FROM THE HARBOUR MAIN GROUP (WESTERN BLOCK),  
CONCEPTION BAY, AVALON PENINSULA, NEWFOUNDLAND

BY

© KEVIN J. CAMERON, B.Sc.

A thesis submitted to the school of Graduate  
Studies in partial fulfillment of the  
requirements for the degree of  
Master of Science

Department of Earth Sciences  
Memorial University of Newfoundland

February 1986

Permission has been granted to the National Library of Canada to microfilm this thesis and to lend or sell copies of the film.

The author (copyright owner) has reserved other publication rights, and neither the thesis nor extensive extracts from it may be printed or otherwise reproduced without his/her written permission.

L'autorisation a été accordée à la Bibliothèque nationale du Canada de microfilmer cette thèse et de prêter ou de vendre des exemplaires du film.

L'auteur (titulaire du droit d'auteur) se réserve les autres droits de publication; ni la thèse ni de longs extraits de celle-ci ne doivent être imprimés ou autrement reproduits sans son autorisation écrite.

ISBN 0-315-31004-9

## THE ROAD NOT TAKEN

Two roads diverged in a yellow wood,  
And sorry I could not travel both  
And be one traveller, long I stood  
And looked down one far as I could  
To where it bent into the undergrowth;

Then took the other, as just as fair,  
And having perhaps the better claim,  
Because it was grassy and wanted wear;  
Though as for that, the passing there  
Had worn them really about the same,

And both that morning equally lay  
In leaves no step had trodden black.  
Oh, I kept the first for another day!  
Yet knowing how way leads on to way,  
I doubted if I should ever come back.

I shall be telling this with a sigh  
Somewhere ages and ages hence:  
Two roads diverged in a wood, and I --  
I took the one less travelled by,  
And that has made all the difference.

Robert Frost

## ABSTRACT

Volcanic rocks and associated igneous intrusions outcropping in southern Conception Bay, central Avalon Peninsula, represent the upper portion of the late Precambrian (Hadrynian) Harbour Main Group. The Group here consists of three ash-flow tuff (ignimbrite) sequences, associated terrestrial sediments, and minor intrusive rocks, overlain by a thick succession of subaerial mafic lavas. Although the rocks have undergone moderate deformation, pristine igneous textures (eg. glass shard outlines and ophitic texture) are well preserved. Metamorphism has reached only lower greenschist (prehnite-pumpellyite) facies resulting primarily in a reconstitution of most of the primary phases. Plagioclase is replaced by epidote and prehnite and olivine by serpentine, chlorite, and iddingsite while pyroxene remains as a relict phase in most of the rock units.

The stratigraphy of the mafic sequence can be divided into three main rock units. The lower portion consists of lavas rich in clinopyroxene (augite) phenocrysts and displays subalkaline trends on various discrimination diagrams. The main part of the sequence is made up of flows containing pseudomorphed olivine and plagioclase phenocrysts in addition to plagiophyric mafic sills. The chemical affinities displayed here are subalkaline to transitional

trends. The stratigraphically highest lavas outcrop just south of the main map area and are characterised by a lack of phenocrystic phases and mildly alkaline chemical trends. Variations in selected major and trace element analysis indicate that these mafic rock units may be related to one another by some process of differentiation, probably involving fractionation of olivine, clinopyroxene, and plagioclase from an alkali basalt parental magma. Careful use of discrimination diagrams and field relations of associated rock units strongly indicate that these mafic rocks were erupted in a non-orogenic tensional tectonic environment such as an area undergoing strike-slip faulting (pull-apart basin), block-faulting, or possibly a combination of both of these (ie. a transtension regime). A modern day analogue may be the Basin and Range Province of the southwestern United States.

## ACKNOWLEDGEMENTS

I am indebted to Dr V.S. Papezik for his encouragement, advice, and patience throughout this study and for reteaching mineralogy to me. I deeply appreciate the guidance and patience of Dr. T. Rivers who continued as supervisor for this project after Dr. Papezik's untimely death. Many thanks to G. Andrews for providing major element geochemical analyses, D. Press and P. Finn for assistance with trace element analyses, H. Londerich for help with microprobe analysis, and J. Warford for preparing thin sections. I thank Brad Mercer for his able field assistance and for putting up with my nonsense during the rainy periods of that summer. Financial support from a Natural Sciences and Engineering Research Council operating grant to Dr. Papezik is greatly appreciated. Sincere thanks to the entire geological community at Memorial University for providing stimulating discussions and offering helpful hints on how to survive a winter in St. John's. Thanks to my family for suffering through my bad temper during the writing phase and to Janet for being a friend. A special note of thanks to C. Tory, Saint Mary's University, for taking time to explain the art of text editing using the VAX computer, to Dr. C. Elson, Dr. K. Mailer, and E. Hamilton of the Chemistry department, Saint Mary's for reminding me of deadlines and for pushing me to

finish the thesis. I would like to thank the Geology department of St. Mary's University for the use of their facilities. To anyone I may have overlooked, my sincere apologies: I just kept passing the open windows.

## TABLE OF CONTENTS

Chapter		Page
	ABSTRACT.....	ii
	ACKNOWLEDGEMENTS.....	iv
	LIST OF TABLES.....	x
	LIST OF FIGURES.....	xi
	LIST OF PLATES.....	xiii
1	INTRODUCTION.....	1
1.1	INTRODUCTION.....	1
1.2	LOCATION AND ACCESS.....	5
1.3	TOPOGRAPHY.....	9
1.4	PREVIOUS WORK.....	10
1.5	AGE OF HARBOUR MAIN GROUP.....	12
1.6	PRESENT STUDY.....	13
2	GEOLOGICAL SETTING.....	14
2.1	THE AVALON ZONE.....	14
2.2	STRATIGRAPHY OF THE AVALON PENINSULA.....	15
2.3	LOCAL STRATIGRAPHY.....	19
2.3.1	Ash-Flow Tuff Sequences.....	20
2.3.2	Blue Hills Sequence.....	26
2.3.3	Post-Harbour Main Group Rocks.....	45
2.4	STRUCTURE.....	46

## TABLE OF CONTENTS (continued)

Chapter		Page
3	PETROGRAPHY.....	51
3.1	INTRODUCTION.....	51
3.2	ASH-FLOW TUFF SEQUENCES.....	52
3.2.1	Mineralogy and Textures.....	52
3.2.2	Alteration.....	53
3.3	BLUE HILLS SEQUENCE.....	55
3.3.1	Pyroxene-phyric Lavas.....	55
3.3.2	Aphyric Basaltic Lavas.....	56
3.3.3	Plagiophyric Sills.....	65
3.4	ALTERATION OF MAFIC ROCKS.....	68
3.5	ASSOCIATED ROCKS.....	71
3.5.1	Porphyrite.....	71
3.5.2	Pyroclastic Units.....	72
3.5.3	Epiclastic Rocks.....	73
3.5.4	Mafic Dyke.....	73
4	GEOCHEMISTRY.....	75
4.1	INTRODUCTION.....	75
4.2	WHOLE ROCK CHEMISTRY.....	75
4.2.1	Major Oxides.....	83
4.2.2	Trace Elements.....	90

## TABLE OF CONTENTS (continued)

Chapter		Page
4.3	PYROXENE CHEMISTRY.....	107
5	RECOGNITION OF PRIMARY MAGMATIC AFFINITIES.....	118
5.1	INTRODUCTION.....	118
5.2	MAGMATIC AFFINITIES BASED ON WHOLE ROCK CHEMISTRY.....	118
5.2.1	Major Oxides.....	118
5.2.2	Trace Elements.....	125
5.3	MAGMATIC AFFINITIES BASED ON CLINO- PYROXENE COMPOSITION.....	136
6	RECOGNITION OF TECTONIC AFFINITIES.....	145
6.1	INTRODUCTION.....	145
6.2	TECTONIC AFFINITIES BASED ON WHOLE ROCK DATA.....	146
6.2.1	Major Oxides.....	146
6.2.2	Trace Elements.....	147
6.3	TECTONIC AFFINITIES BASED ON CLINO- PYROXENE COMPOSITION.....	158
6.4	DISCUSSION OF RESULTS.....	163
7	SUMMARY AND DISCUSSION.....	168
7.1	SUMMARY.....	168

# TABLE OF CONTENTS (continued)

Chapter	Page
7.2	POSSIBLE REGIONAL CORRELATIONS.....170
	REFERENCES.....174
	APPENDIX A ANALYTICAL METHODS.....190
A.1	SAMPLING PROCEDURE.....190
A.2	SAMPLE PREPARATION.....191
A.3	MAJOR OXIDE ANALYSIS (AND PHOSPHOROUS AND L.O.I.).....192
A.4	TRACE ELEMENT ANALYSIS.....193
A.5	RARE-EARTH ELEMENT ANALYSIS.....196
A.6	RELICT CLINOPYROXENE ANALYSIS.....200
	APPENDIX B CIPW NORMS.....201
	GEOLOGICAL AND SAMPLE LOCATION MAP.....Back Cover

## LIST OF TABLES

Table No.	Page
1. Generalised Precambrian stratigraphy, Avalon Peninsula.....	16
2. Major oxide and trace element chemistry.....	76
3. Rare-earth element chemistry.....	98
4. Analyses of relict clinopyroxenes.....	108
A-1. Precision of major oxide analysis.....	194
A-2. Precision of trace element analysis.....	197
A-3. Accuracy of trace element analysis.....	198
B-1. CIPW Norms.....	203

## LIST OF FIGURES

Figure No.	Page
1. Tectonostratigraphic zonation of Newfoundland.....	3
2. Regional geology of northeastern Avalon Peninsula...	6
3. Simplified geological map of study area.....	8
4. Schematic geological cross-section, study area.....	49
5. $\text{SiO}_2$ versus $\text{Zr/TiO}_2$ classification of mafic rocks..	85
6. Variation diagrams of major oxides versus differentiation index.....	88
7. Variation diagrams of trace elements versus differentiation index.....	92
8. Cr versus Ni content in mafic rocks.....	95
9a. Nb versus Y variation diagram.....	97
9b. Y, Nb versus Zr variation diagram.....	97
10. Chondrite-normalised rare-earth element patterns..	105
11. Compositional variation of relict clinopyroxenes..	112
12. $\text{SiO}_2$ , $\text{TiO}_2$ versus $\text{FeO/MgO}$ variation diagrams for clinopyroxenes.....	114
13. $\text{MgO}$ , $\text{TiO}_2$ versus $\text{Al}_2\text{O}_3$ content in clinopyroxenes..	117
14. Plot of alkali parameters.....	121
15. Alkali-silica plot.....	122
16. AFM diagram.....	124
17. Variation in Y/Nb ratio in various rock units.....	128
18. Distribution of $\text{TiO}_2$ versus Y/Nb ratio.....	131

## LIST OF FIGURES (continued)

Figure No.	Page
19. $P_2O_5$ versus Zr variation diagram.....	133
20. $TiO_2$ versus $Zr/P_2O_5$ variation diagram.....	135
21. Silica versus alumina content in relict clinopyroxenes.....	139
22. Al <sub>2</sub> versus $TiO_2$ content in clinopyroxenes.....	141
23. Magmatic parentage of Blue Hills Sequence using relict clinopyroxene compositions.....	143
24. $TiO_2$ versus FeO/MgO variation diagram.....	149
25. Zr/Y - Ti/Y discrimination diagram.....	151
26. $TiO_2$ versus Zr variation diagram.....	154
27. Zr/Y - Zr discrimination diagram.....	157
28. Ti versus V content.....	160
29. $SiO_2$ versus $TiO_2$ in relict clinopyroxenes.....	162
30. Tectonic character of Blue Hills Sequence using clinopyroxene compositions.....	165
31. Distribution of late Precambrian volcanic rocks in the Avalon Zone, northern Appalachians.....	171

## LIST OF PLATES

Plate No.	Page
1. Eutaxitic texture in ash-flow tuff units.....	22
2. Volcanogenic sediments interbedded with ash-flow tuff units.....	22
3. Conglomerate interbedded with ash-flow tuff units..	25
4. Example of porphyrite unit.....	25
5. Basalt flows, Blue Hills.....	29
6. Example of flow-top breccia.....	29
7. Amygduloidal/scoriaceous flow-top.....	31
8. Brecciated flow-top of 'aa' type, Blue Hills.....	31
9. Recent aa lava flow, Hawaii.....	33
10. Brecciation in a spiracle.....	33
11. Example of mottled texture of some mafic flows.....	36
12. Field exposure of plagiophyric sill unit.....	36
13. Chilled zone of plagiophyric sill unit.....	39
14. Angular mafic blocks in vent breccia.....	39
15. Phreatic(?) breccia exposed at Turk's Gut.....	42
16. Lahar breccia outcropping in Blue Hills.....	42
17. Air fall deposit, Blue Hills Sequence.....	44
18. Boulder conglomerate of basal Conception Group.....	44
19. Angular unconformity between Harbour Main Group and overlying Cambrian sediments.....	47
20. Glass shards in ash-flow tuff unit.....	54

## LIST OF PLATES (continued)

plate No.	Page
21. Glomeroporphyritic texture, pyroxene-phyric unit...	58
22. Altered plagioclase phenocryst with inclusions.....	58
23. Pseudomorphed olivine phenocrysts.....	61
24. Well-developed ophitic texture in mafic flows.....	61
25. Poikilophitic texture in mafic flows.....	63
26. Plagioclase laths displaying trachytic texture.....	63
27. Rosette of plagioclase laths, plagiophyric sill....	67
28. Diabasic texture, plagiophyric sill unit.....	67
29. Photomicrograph of chilled zone, plagiophyric sill.	70
30. Photomicrograph of porphyrite sample.....	70

*If a man will begin with certainties, he shall end in doubts; but if he will be content to begin with doubts, he shall end in certainties. -- Francis Bacon*

## CHAPTER 1

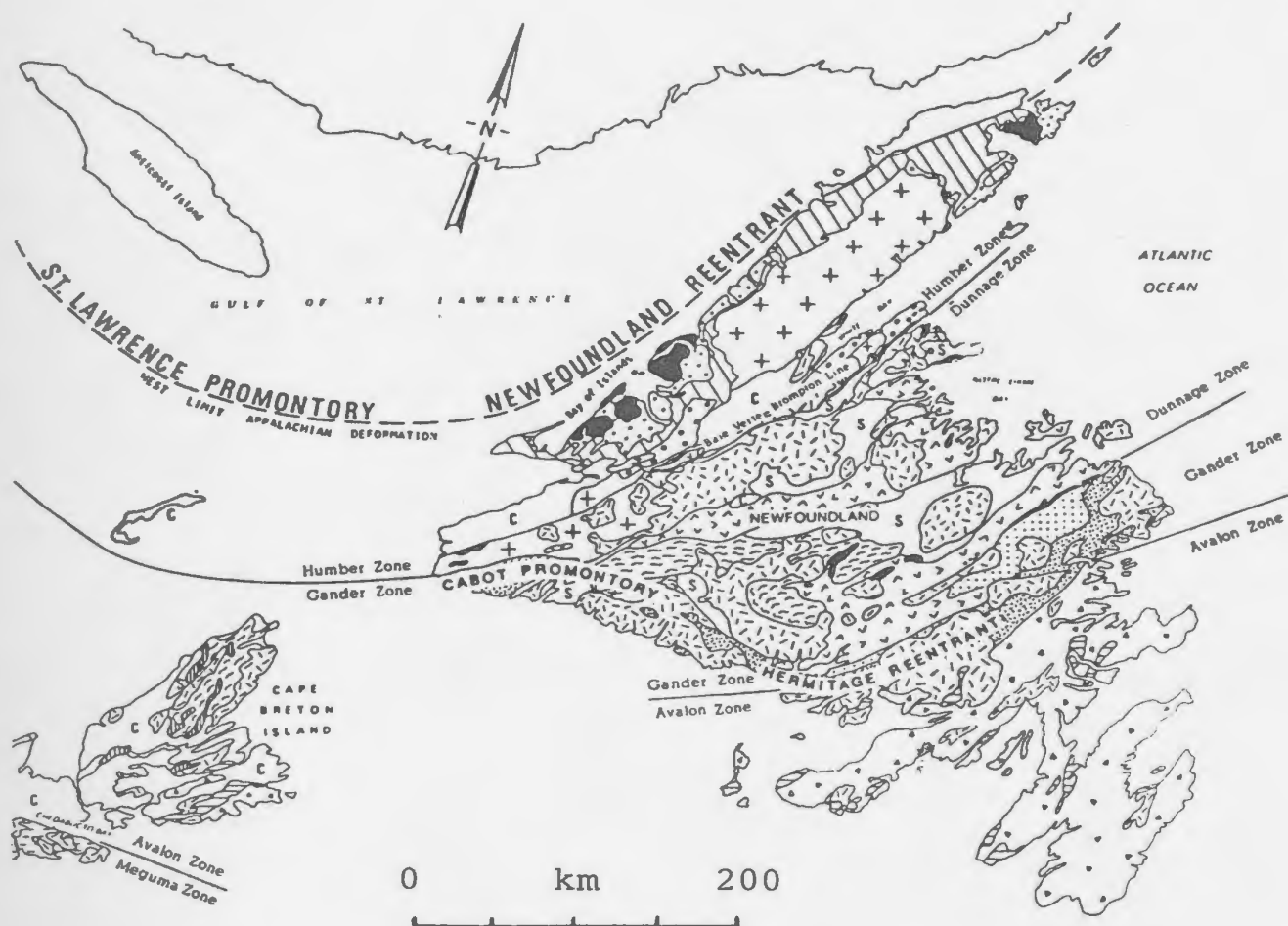
### INTRODUCTION

#### 1.1 INTRODUCTION

The Harbour Main Group is a sequence of slightly metamorphosed volcanic and sedimentary rocks located on the Avalon Peninsula, eastern Newfoundland (Fig. 1). The Group is part of the Avalon Zone of the Appalachian Orogen. In Newfoundland this zone consists of a sequence of late Precambrian volcano-sedimentary rocks overlain by both marine and continental sedimentary rocks of late Precambrian age. These rocks are conformably to unconformably overlain by shallow marine to terrestrial sedimentary rocks of lower to mid-Palaeozoic age. The entire sequence has been intruded by plutonic rocks ranging in age from late Proterozoic to Carboniferous (Williams, 1979).

The tectonic setting of this part of the Avalon Zone is not clearly understood and has been the subject of various interpretations. Papezik (1970), Strong et al. (1974),

FIGURE 1. Tectonostratigraphic zonation of Newfoundland  
(after Williams, 1978, 1979).



Granitic to dioritic and gabbroic intrusions (mainly Mid-Paleozoic but ranging in age from Late Precambrian to Jurassic)



Metamorphic rocks of unknown affinity (mainly Mid-Paleozoic)

#### SUCCESSOR BASINS OF APPALACHIAN OROGEN



**T** Terrestrial sedimentary and volcanic rocks related to opening of present Atlantic Ocean (Triassic-Jurassic)

**C** Late orogenic to post orogenic mainly terrestrial sedimentary and minor volcanic rocks (Carboniferous-Permian)

**S** Mainly clastic sediments and terrestrial volcanic rocks deposited in troughs and basins across vestiges and deformed margins of Iapetus (Middle Ordovician to Devonian)

#### HUMBER ZONE

ANCIENT CONTINENTAL MARGIN OF EASTERN NORTH AMERICA

#### DUNNAGE ZONE

VESTIGES OF IAPETUS OCEAN

#### GANDER ZONE

EASTERN MARGIN OF IAPETUS

#### AVALON ZONE

AFRICAN EUROPEAN ELEMENTS OF APPALACHIAN OROGEN

#### MEGUMA ZONE



Transported mainly ophiolitic rocks (Late Cambrian to Early Ordovician)



Transported mainly sedimentary rocks (Late Precambrian to Middle Cambrian)



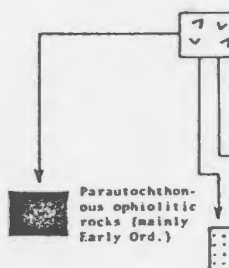
Mainly carbonate and overlying clastic sediments (Cambrian to M. Ordovician)



Clastic sediments and bimodal volcanic rocks (Late PC to Early Cambrian)



Grenvillian basement



Marine volcanic rocks, slate, chert, greywacke and melange (Mainly Ordovician)

Clastic sedimentary rocks (Early Ord. and Older)

Metamorphosed cover rocks and sialic basement



Shale, sandstone, minor limestone (Cambrian to Early Ordovician)



Sedimentary and volcanic rocks (Late Precambrian-Hadrynian)



Marbles and quartzites with assoc. gneisses and migmatites (Late PC and older)



Greywacke and slate (Early Ord. and older)

strong and Minatides (1975), Nixon and Papezik (1979) have suggested that the Harbour Main Group was formed during continental volcanism related to block-faulting in the late precambrian, in a manner analogous to that of the Basin and Range Province in the southwestern United States. However, Hughes (1970), Hughes and Brueckner (1971), Poole (1976), Rast et al. (1976) maintain that rocks of the Harbour Main Group were formed in either an oceanic island or island-arc type tectonic environment.

As the Harbour Main Group is the oldest known exposed rock unit on the Avalon Peninsula, the tectonic significance of these rocks is critical not only to an understanding of the geological evolution of this part of Newfoundland but also to models put forth for possibly equivalent rock units elsewhere in the Appalachian Orogen. In recent years petrochemistry has become an invaluable tool in defining tectonic settings of ancient volcanic rocks. Chemical work in previous studies of the Harbour Main Group was concerned mainly with silicic rocks which, however, do not have sufficiently distinctive signatures. Mafic volcanics were therefore selected in this study, in particular those in the western belt of the Group. These rocks are potentially suitable indicators of the magmatic and tectonic affinities of the igneous activity associated with this part of the Harbour Main Group.

## 1.2 LOCATION AND ACCESS

Major fault zones divide the Harbour Main Group into eastern, central and western blocks (Fig. 2). The eastern block consists predominantly of mafic volcanic rocks, including pillow lavas, massive flows, abundant pyroclastic and sedimentary rocks, and locally prominent acidic flows and plugs. The central block is dominated by the Holyrood Pluton with highly altered volcanic rocks along the contacts. Volcanic rocks of the Harbour Main Group attain their most typical development in the western block which consists of ash-flow tuffs (ignimbrites), massive basaltic flows, and volcanogenic sediments.

The present study area (Fig. 3) lies within that part of the Harbour Main Group defined by Papezik (1970) as the 'western block'. The area is located in southern Conception Bay, Avalon Peninsula, and is bounded by Colliers Bay on the east and north, Gasters Tear Fault on the southeast, and on the west by a major fault (Marysvale Fault) extending from Turks Gut in the north through the community of Marysvale southwestwards and curving around the west side of the Blue Hills. Also included in the present study is an inlier of Harbour Main rocks located near the community of Brigus Junction and straddling the Trans-Canada Highway in this area.

The area lies approximately 70 kilometres to the southwest of St. John's and is most efficiently reached by

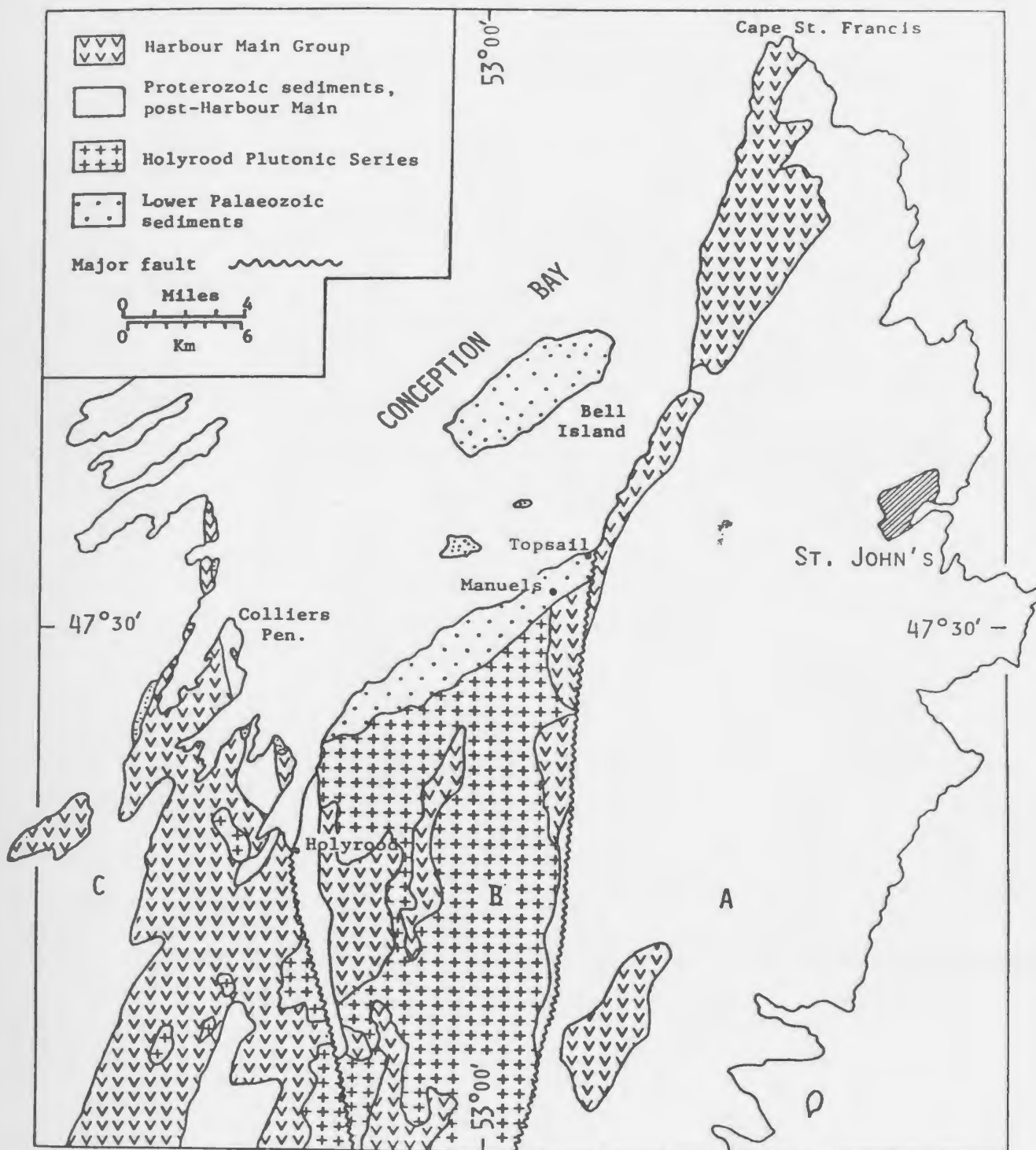


FIGURE 2. Regional geology of northeastern Avalon Peninsula. The area is divided into three main blocks: A - eastern, B - central, and C - western, by major north-northeasterly trending faults. See text for further description. Modified from Papezik, 1970.

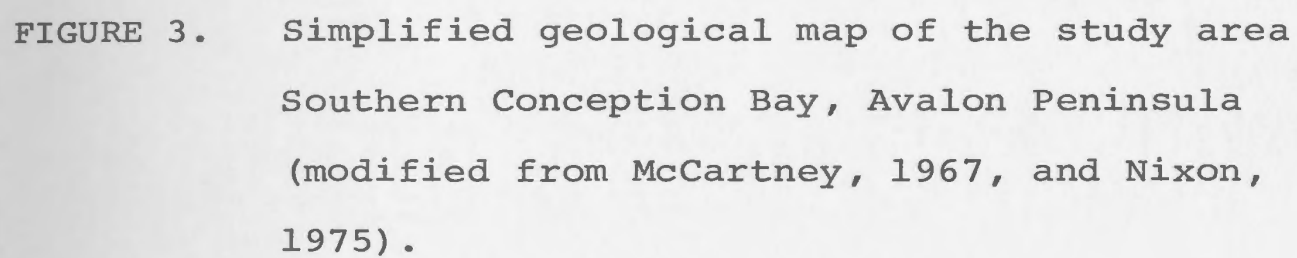
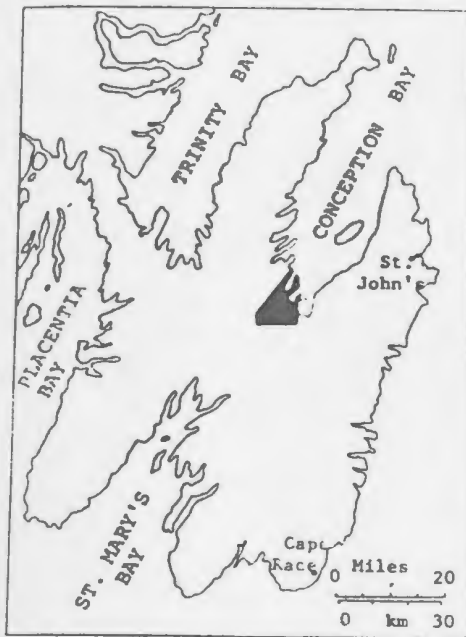
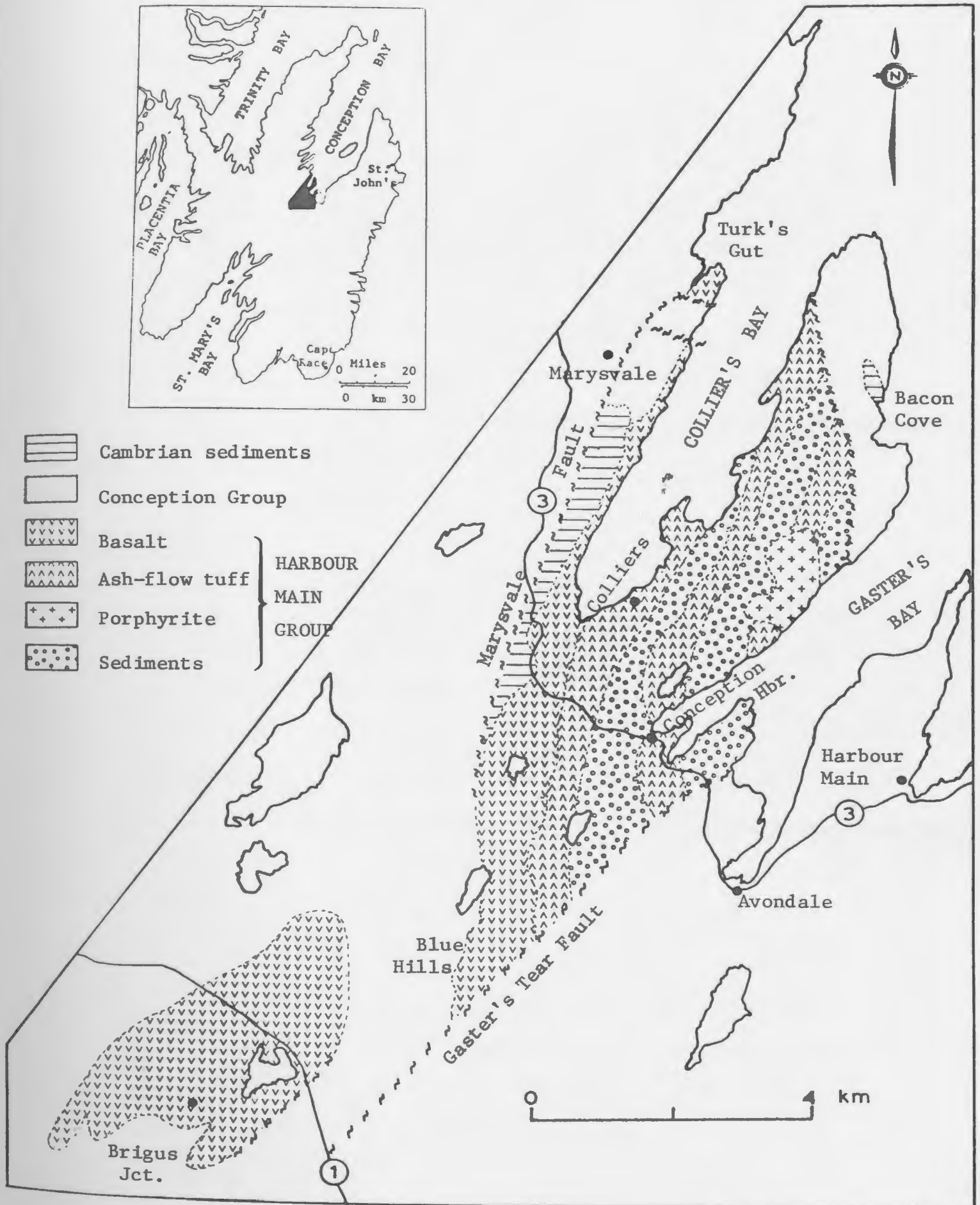
A small, dark, and mostly illegible map is located in the upper right quadrant of the page. It appears to be a geological map showing various landforms and possibly geological features, but the details are too faint to discern.

FIGURE 3. Simplified geological map of the study area  
Southern Conception Bay, Avalon Peninsula  
(modified from McCartney, 1967, and Nixon,  
1975).



- |  |                    |                            |
|--|--------------------|----------------------------|
|  | Cambrian sediments |                            |
|  | Conception Group   |                            |
|  | Basalt             | } HARBOUR<br>MAIN<br>GROUP |
|  | Ash-flow tuff      |                            |
|  | Porphyrite         |                            |
|  | Sediments          |                            |



travelling west on the Trans-Canada Highway (Route 1) and then north along the Avondale access road connecting to the Conception Bay Highway (Route 3). Local communities in the area include Avondale, Conception Harbour, Colliers, and Marysvale. The Brigus Junction inlier is reached by travelling west on Route 1, past the Avondale exit, to the secondary access road leading southward to this community which is 2 kilometres from the junction with Route 1. Numerous roads and trails provide easy access to most of the area.

### 1.3 TOPOGRAPHY

To a large extent the topography of the area is controlled by bedrock geology. The hills and ridges such as Finn Hill, Blue Hills, and the west shore of Colliers Bay are underlain by more resistant massive volcanic rocks, while the lower valley areas between these ridges are occupied predominantly by sedimentary rocks.

Glacial activity during the Pleistocene was the major force which shaped the present-day topography of the area as shown by whaleback ridges and perched erratic boulders. Glacially striated outcrops indicate that the ice moved in a general northerly direction. Glacial till is unevenly distributed and in places reaches a thickness of 8 metres, although many areas (eg. Blue Hills and the west shore of Colliers Bay) lack any surficial deposit. For a more

detailed account of glaciation in the area, the reader is referred to Henderson (1972).

#### 1.4 PREVIOUS WORK

Excellent and very detailed reports of previous geological work carried out in the area are given by McCartney (1967) and Nixon (1975). For the purpose of this study, the following summary of previous work is based primarily on Nixon (1975).

Work by A. Murray in 1868 and Murray and J.P. Howley between 1869 and 1883 resulted in a geological map of the Avalon Peninsula which was published in 1881. They classified the Precambrian intrusive rocks of the Avalon as "Laurentian gneiss, etc." and Harbour Main rocks as "metamorphic slate, sandstones, etc.". In 1919 A.F. Buddington, using chemical analyses, clarified the relations and petrology of the Avalonian Precambrian volcanic and plutonic rocks. He introduced the term 'Avondale volcanics' for the Harbour Main Group as they occur in Conception Bay. However, as the term Avondale had been used previously elsewhere, the rocks were renamed 'Harbour Main volcanics' by Howell (1925). Rose (1952) redefined the rocks involved and proposed the name 'Harbour Main Group'. This nomenclature was used in a series of G.S.C. publications by Hutchinson (1953), Jenness (1963), and McCartney (1967).

More recently, Papezik (1969, 1970) carried out the

first detailed studies of ash-flow deposits of the Harbour Main Group at Finn Hill on Colliers Peninsula. Based on chemical analyses of the volcanic rocks, he interpreted them as "a differentiated series from an alkali-olivine basalt parental magma in a post-orogenic tectonic setting of the Basin-Range type" (Papezik, 1969, p.1495). The same general conclusion was reached as a result of a more extensive study of the same area and was presented as a thesis at Memorial University of Newfoundland by Nixon (1975).

Hughes and Brueckner (1971) proposed a somewhat different model for the development of the late Precambrian Avalon Peninsula. They envisaged a calc-alkaline volcanic island archipelago involving contemporaneous volcanism (Harbour Main Group), sedimentation (Conception Group), and high-level granitoid plutonism (Holyrood plutonic series).

Within the past few years the Avalon Zone has again attracted geological interest as attempts are made to understand its role in the evolution of the Appalachian Orogen. A NATO advanced study focused on the Avalon and Meguma (Nova Scotia) Zones as part of the International Geological Correlation Programme. Williams (1984) refers to the Avalon Zone as a 'suspect terrane' and suggests the possibility that this zone may be a composite terrane which was assembled in late Precambrian times.

## 1.5 AGE OF HARBOUR MAIN GROUP

Harbour Main volcanics and some associated rocks have been dated by various methods. The oldest age reported for Harbour Main rocks is 1,500 Ma using a  $^{40}\text{Ar}/^{39}\text{Ar}$  technique (Stukas, 1977). This age is considerably older than any other obtained to date in the Avalon Peninsula, and may be a result of excess argon. An Rb-Sr whole-rock isochron age of  $568 \pm 29$  Ma for the Harbour Main volcanics is indicated by Fairbairn et al. (1966). Recent studies on zircons from an ash-flow tuff unit on Colliers Peninsula have yielded an uranium-lead discordant isochron age of  $606(+3.7, -2.9)$  Ma for the Harbour Main volcanics (Krogh et al., 1983), which is probably a realistic estimate of the age of eruption of these rocks. The sedimentary rocks of basal Cambrian age which unconformably overlie the volcanics probably have an age of 570 Ma as suggested by the time scale of Cowie (1964).

McCartney (1967) reports Rb-Sr isochron ages of  $574 \pm 11$  Ma and  $597 \pm 42$  Ma for plutonic rocks around Holyrood Bay. However, using the longer half-life of rubidium ( $^{87}\text{Rb} = 1.39 \times 10^{11}$  yr), Frith and Poole (1972) report an age of  $607 \pm 11$  Ma for the intrusion. Krogh et al. (1983), using abraded zircon cores, dated the Holyrood granite at  $620.5(+2.1, -1.8)$  Ma.

## 1.6 PRESENT STUDY

Field work was carried out during the summer and early autumn of 1982. This involved mapping an area of approximately 22 square kilometres. Field observations were recorded on forestry maps at a scale of 1:2500. This information was later replotted onto a base map at a scale of 1:12500.

Petrographic and geochemical studies were carried out in late 1982 and throughout 1983. Petrography was used as an aid in choosing least altered samples for major and trace element geochemical work.

These islands; the remnant peaks of a lost continent, roof of an old world, molten droppings from earth's bowels, gone cold; ribbed with rock, resisting the sea's corrosion for an age, and an age to come. -- A.R.D. Fairburn

## CHAPTER 2

### GEOLOGICAL SETTING

#### 2.1 THE AVALON ZONE

The Avalon Peninsula is situated in the eastern part of the Avalon Zone, which is the most easterly tectonostratigraphic zone of the Newfoundland Appalachians (Williams, 1979). The western boundary of the Avalon Zone is marked by a wide steep shear zone, the Dover-Hermitage Fault, which separates it from the Gander Zone (comprised essentially of polydeformed lower Palaeozoic rock units) (Fig. 1). The age and nature of the first movements of this fault are unknown, but the main movement is interpreted as Acadian (Dallmeyer et al., 1981). Movement on this fault was completed by 360 Ma (Dallmeyer, 1980) as a post-tectonic intrusion, the Ackley Granite, cuts both zones. The Avalon Zone, which can be traced geophysically in the offshore to the present continental margin (some 250 km) (Haworth and Lefort, 1979), is in excess of 700 kilometres wide. This distance is approximately twice the width of the rest of the

Appalachian orogenic belt.

Outside Newfoundland, 'Avalon-type' rocks have been reported in Nova Scotia (Schenk, 1971; Keppie, 1977), New Brunswick (Rast et al., 1976), parts of New England (Rodgers, 1970, 1972; Murray et al., 1978), the Carolinas (Wright and Seiders 1980; Long, 1979; Black, 1980) and Georgia (Whitney et al., 1978). Across the Atlantic Ocean equivalents of the Avalon Zone may be represented in the British Caledonides by the Arvonian volcanics of North Wales and the Longmyndian red beds and Uriconian volcanics of England (O'Brien, 1979). Possible correlatives of the Avalon Zone in Morocco have been described by Hughes (1972) and in other parts of western Africa by Schenk (1971), and Strong et al. (1978).

## 2.2 STRATIGRAPHY OF THE AVALON PENINSULA

The geology of the Avalon Peninsula has been reviewed in great detail in recent literature (eg. Williams, 1979; Williams et al., 1972, 1974; King et al., 1974; Rast et al., 1976; O'Brien et al., 1983). Therefore, the following section presents only a brief stratigraphic outline in order to provide a framework for later discussion. Table 1 outlines the stratigraphic relationships of rock units on the Avalon Peninsula.

The base of the stratigraphic section on the Avalon Peninsula is the Harbour Main Group (Howell, 1925;

TABLE 1. Generalised Precambrian stratigraphic sections, Avalon Peninsula, southeastern Newfoundland (after McCartney, 1967 and King, 1980). Stratigraphic sections not to scale.

PERIOD	WESTERN AVALON PENINSULA		CENTRAL AVALON PENINSULA		EASTERN AVALON PENINSULA	
	GROUP/ FORMATION	LITHOLOGY	GROUP/ FORMATION	LITHOLOGY	GROUP/ FORMATION	LITHOLOGY
CAMBRIAN	Random Fm.	Quartzite, arkose	Random Fm.	Quartzite, arkose		
PRECAMBRIAN (HADRYNIAN)			"AVALONIAN OROGENY"			
	Musgravetown Gp.	Red conglomerate, arkose, siltstones; probably of fluvial or deltaic origin	Hodgewater Gp.	Red arkose & siltstone of fluvial or deltaic origin	Signal Hill Gp.	Fluvial red conglomerate, arkose, and siltstones
	Connecting Point Gp.	Green & grey siltstones, slates, greywacke, cherty argillites of pelagic origin			St. John's Gp.	Deltaic black shales
			Conception Gp.	Pelagic greyish green siltstone, slate, greywacke	Conception Gp.	Pelagic greyish green siltstones, slate, greywacke, minor tuffaceous beds ? — ? — ? —
	Love Cove Gp.	Massive lava flows, volcanoclastics; terrestrial sediments	Harbour Main Gp.	Massive lava flows, pyroclastics, red terrestrial sediments	Harbour Main Gp.	Massive lava flows, pyroclastics, minor intrusives, red terrestrial sedts.

McCartney, 1967). Although stratigraphic relationships within the Group are complicated by faulting and are poorly understood, the major lithologies consist of subaerial felsic volcanic rocks (ash-flow tuffs, rhyolite flows and plugs), mafic flows with local pillow structures, and terrestrial volcanoclastic sediments. Nowhere is the base of the Group exposed, but McCartney (1967) estimated its thickness to be more than 1800 m.

The Harbour Main Group is overlain by the Conception Group, a 3-5 km thick flysch-like sequence of volcanoclastic sedimentary rocks representing widespread marine turbidite and pelagic sedimentation (King, 1980). The basal beds of the Conception Group are coarse to medium conglomerates and "suggest a near-shore, shallow-water sedimentary environment with sediment derived from nearby areas of older volcanic rocks and from partly unroofed granitic rocks" (McCartney, 1967, p.33). The basal beds are transitional into overlying greywackes, and are probably the products of the transition from a subaerial to a deep-water environment. The dominant rock-types in the Conception Group are grey-green and green siltstones, cherty argillites, slates, and greywackes with laminated cyclic, or graded bedding. Hughes (1972) reported isolated tuffaceous beds within the Conception Group which contain volcanic glass shards indicating active volcanism during the time of deposition. In addition, a single mafic flow within the Group (west shore of Holyrood Bay) and restricted thin beds of limestone were noted by McCartney

(1967).

The relationship between the Harbour Main and Conception Groups is controversial. The existence of a local angular unconformity in the northern Avalon Peninsula was interpreted by Rose (1952) and McCartney (1967) to represent an extensive erosional unconformity beneath the Conception Group. Hughes and Brueckner (1971) however, suggested that the presence of tuffaceous beds and lava flow within the Conception Group indicate a penecontemporaneous development with the Harbour Main Group. Detailed mapping in the southern Avalon Peninsula has shown that the Conception Group conformably overlies the Harbour Main Group (Williams and King, 1979).

The Conception Group is conformably overlain by a thick (8-9 km) sequence of molasse-like terrestrial and locally marine sedimentary rocks (King, 1980). In eastern Avalon Peninsula these rocks are referred to as the St. John's and Signal Hill Groups and the comparable Hodgewater Group is found in central Avalon Peninsula. They consist mainly of grey and red sandstones and siltstones grading into red conglomerates representing the development of a major coarsening-upwards sequence (King, 1980).

Cambro-Ordovician rocks occur as isolated outliers on the Avalon Peninsula. This sequence of platformal sediments, rich in Atlantic trilobite fauna, overlies the upper Proterozoic volcanic, sedimentary, and granitoid rocks. The basal Cambrian contact is variably an

unconformity, nonconformity, or disconformity in different locations in the Avalon Zone. In the east there is clearly an unconformity between the Cambrian and older rocks (eg. plate 19), but in the west, Greene and Williams (1974) suggest that Infracambrian rocks were transgressive into the Lower Cambrian. O'Brien et al. (1976) suggest a fault-modified disconformable contact between Infracambrian - Cambrian and Precambrian volcanic rocks on the Burin Peninsula.

### 2.3 LOCAL STRATIGRAPHY

This study is concerned with the west part of the western block of the Harbour Main Group. Figure 3 provides a simplified geological map of the area. Previous work by Papezik (1969, 1970) and Nixon (1975) has documented the geology and stratigraphy of the Group on Colliers Peninsula, immediately to the east of the present area. Based on preliminary work by Papezik, Nixon delineated three predominantly pyroclastic sequences, composed essentially of ash-flow tuffs with interbedded volcanogenic sediments. In order to introduce a discussion of the overlying basaltic sequence and to provide continuity from Nixon's study, a

brief summary of the ash-flow tuffs as they occur in the area is given below. The description of these units is taken from Nixon and Papezik (1979).

### 2.3.1 Ash-flow Tuff Sequences

The three ash-flow tuff units, from oldest to youngest (ie. east to west), have been referred to as the 'Bacon Cove, Weavers Hill, and Finn Hill ash-flow sequences'. The thickness of these sequences varies from about 250 m to 350 m. Lithologies vary from sequence to sequence, but generally consist of crystal and vitric tuffs usually reddish-grey or dark red in colour with varying amounts of lithic fragments. Many of the units are conspicuously rich in lens-like 'fiamme' structures (Plate 1) representing collapsed pumice fragments and/or lava clots. The pumice fragments are generally more abundant near the top of individual units. Variable degrees of welding are obvious in most of the units with crystal-rich, non-welded basal zones grading through partly-welded to strongly-welded centres to partly-welded to non-welded zones near the top of the unit.

plate 1

Example of eutaxitic ash-flow unit on Finn Hill, Colliers Peninsula. The grey, elongated lens-like bodies are 'fiamme' representing flattened pumice fragments. Scale is 15 cms.

Plate 2

Example of tuffaceous sandstones and siltstones interbedded with ash-flow tuff units on Colliers Peninsula. Way up is towards top of photo. Note 'flame' structures and shale chips in overlying sandier unit. Scale is 15 cms.



In all three sequences albite is the most abundant phenocryst mineral constituting 75% of the crystals in the Bacon Cove Sequence and decreasing amounts in the other two sequences. Quartz and biotite phenocrysts are also abundant in the Bacon Cove and Weavers Hill Sequences. However, these minerals are absent in the Finn Hill Sequence in which several units contain minor augite and rare chlorite pseudomorphs after olivine. Mafic rock fragments are noticeably more abundant in the Finn Hill Sequence. In most units both the size and proportion of the crystals decrease upwards.

Rock units associated with the ash-flow tuff sequences include volcanoclastic sediments, porphyritic intrusions, and diabase dykes. The sedimentary rocks occur as distinct zones/belts separating each of the three ash-flow sequences and overlying the Finn Hill Sequence. The rocks include red to reddish-brown tuffaceous sandstones and siltstones (Plate 2), displaying cross-stratification, graded bedding, and channel structures. Isolated beds of coarse conglomerate contain well-rounded, but poorly sorted cobbles and boulders of volcanic rocks (Plate 3).

Porphyritic intrusions occur sporadically throughout the ash-flow sequences as irregular stocks and thick lens-like sills or dykes. These 'porphyrites' (Nixon and Papezik, 1979) are green to grey in colour and consist mainly of stubby subhedral crystals of albite which are commonly in glomeroporphyritic intergrowths (Plate 4).

plate 3

Example of coarse conglomerate units interbedded with ash-flow tuff units, southern Conception Bay. Note well rounded, poorly sorted structure. All boulders are of ash-flow tuff composition. Hammer handle is 30 cm long.

Plate 4

Field exposure of 'porphyrite' unit of the Blue Hills sequence. Note the abundance of stubby altered plagioclase crystals. See Plate 30 for photomicrograph of this rock unit.



Field evidence, indicating the passive emplacement of porphyrite bodies into unconsolidated sediments, suggests that the intrusion was roughly contemporaneous with the formation of the volcanic and sedimentary rocks of the area. Other, probably unrelated, intrusive rocks in the area are steeply dipping, east-west trending greenish-grey diabase dykes.

### 2.3.2 Blue Hills Sequence

The name 'Blue Hills Sequence' is introduced here to describe the basalt flows and associated rocks which overlie the ash-flow tuff sequences and are exposed on the west shore of Colliers Bay and the Blue Hills to the south. Similar rock types occur as an inlier around the community of Brigus Junction (Fig. 3 and map in back pocket). McCartney (1967) regarded these mafic rocks as the youngest part of the Harbour Main Group and estimated the thickness of the volcanics to be about 300m. However, sections measured in the Blue Hills indicate a thickness much in excess of this, probably 600m.

The Blue Hills Sequence is separated from the ash-flow tuffs of the Finn Hill Sequence by a thick unit of sediments. Although the contact is not exposed anywhere in the map area, it is almost certainly a conformable contact as the mafic flows exhibit the same general attitude as the ash-flow sequences, that is, a north-south strike, facing

and dipping steeply west.

Rock types of this sequence include massive to amygduloidal subaerial mafic flows, pyroxene-phenocrystic lavas, plagiophyric sills, various breccias, and minor volcanoclastic sedimentary deposits. Exposures of the Blue Hills Sequence indicate that flows are of variable thickness ranging between 3 and 15 m (Plate 5). Contacts between individual flows are easily recognisable in the field by the presence of oxidised, locally scoriaceous and brecciated flow tops (Plates 5-8). In several places, flow tops are marked by 0.5 to 1 m thick fragmented zones (Plate 8). These breccia zones contain blocks and slightly rounded fragments of basalt similar to the underlying central parts of the flow, but are slightly more amygduloidal. The amygdules are variable in size and are irregularly shaped. These features are typical of aa flows (MacDonald, 1972) and are similar to features observed in recent Hawaiian aa flows (Plate 9).

Another interesting volcanological feature is found at the basal parts of some of the lava flows. Occasionally, where sediments underlie a flow, spiracles have developed. The spiracles are roughly conical in cross-section and measure about 1 m across at their base, narrowing upwards (Plate 10) and curving in the direction of flow movement. Within the spiracle the basalt consists of angular fragments of the host flow, indicating brecciation while still fluid. The brecciation probably resulted from generation of steam

plate 5

Example of outcrop in northern Blue Hills area displaying a series of basalt flows. The darker bands represent the oxidised tops of the lava flows. The flows face west (to the left) and dip approximately  $65^{\circ}\text{W}$ . For scale, note field assistant on outcrop, approximately one-third way down the centre of photo.




Plate 6

Example of scoriaceous fragments within oxidised flow top breccia. The fragile form of most fragments indicates that they are not far travelled. Outcrop along western shoreline, Colliers Bay. Pen is 15 cm long.

5



6



plate 7

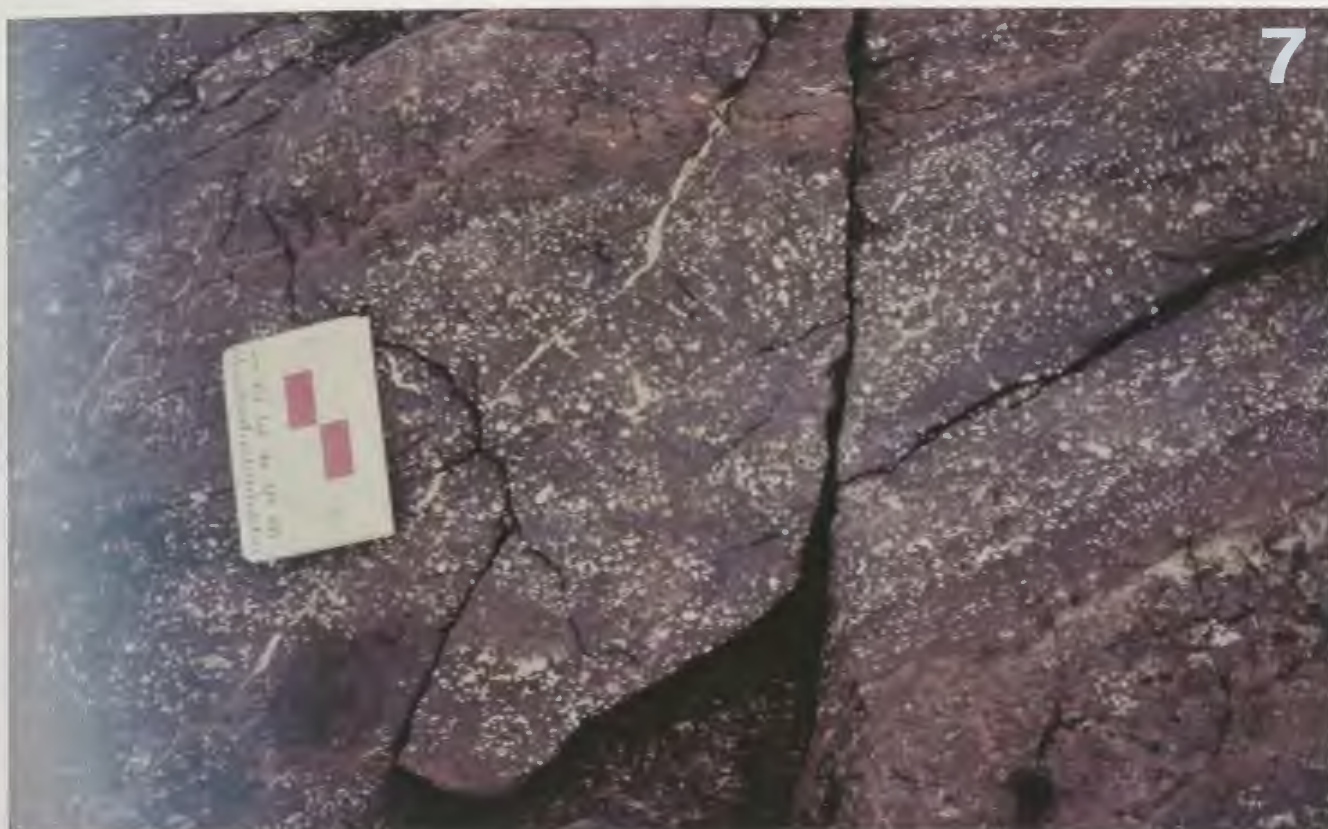
Example of highly amygduloidal-scoriaceous flow top displayed by some flows in the study area. Locality of outcrop is along the south shore of Colliers Bay. Amygdules here are filled predominantly by calcite.

48  
5

Plate 8

Oblique cross-sectional outcrop in southern area of the Blue Hills exhibiting brecciated flow top characteristic of 'aa' type lava. Brecciation grades downward into massive flow. Hammer handle is approximately 20 cm. long. Compare with Plate 9.

7



8



plate 9

Example of recent (approximately 100 years old) aa lava flow in Hawaii. Note the similarity of Plate 8 with the rubbly flow top grading into the massive portion of the flow. Field notebook is 15 cm long.

Plate 10

Example of brecciation within a spiracle developed in a lava flow on the west shore of Colliers Bay. The spiracle is conical in shape with its base at the lower right corner of photo, tapering upwards to the top left corner. Handle of hammer (30 cm) parallels the strike/base of flow which is out of the field of view of the photo, lower right. Note massive portion of same flow just above hammer head.

TOP



TOP



from the flow passing over underlying wet sediments.

The stratigraphically lower section of the Blue Hills Sequence consists of a series of pyroxene-phenocrystic lava flows. Rocks of this type occur along the eastern margin of the Blue Hills and at several places along the west shore of Colliers Bay. These rocks are characterised by abundant dark green, essentially unaltered clinopyroxene phenocrysts in a generally fine-grained matrix. The flows are intercalated with breccias containing large angular mafic blocks. This rock series is discussed further in the petrography and geochemistry sections.

The main series of the Blue Hills Sequence consists of reddish-brown, brown, or grey mafic lava flows which are generally aphanitic to fine-grained. The central parts of more massive flows contain pseudomorphed olivine phenocrysts which occur predominantly in the Blue Hills area, or plagioclase phenocrysts which are more common in flows along the west shore of Colliers Bay. However, both types occur throughout the entire study area. A few flows outcropping along the west shore of Colliers Bay differ slightly from the main lava type in that they are olivine microporphyritic with a strongly poikilitic groundmass (plagioclase laths enclosed in anhedral clinopyroxene grains). This texture imparts a spotted appearance to the outcrops (Plate 11).

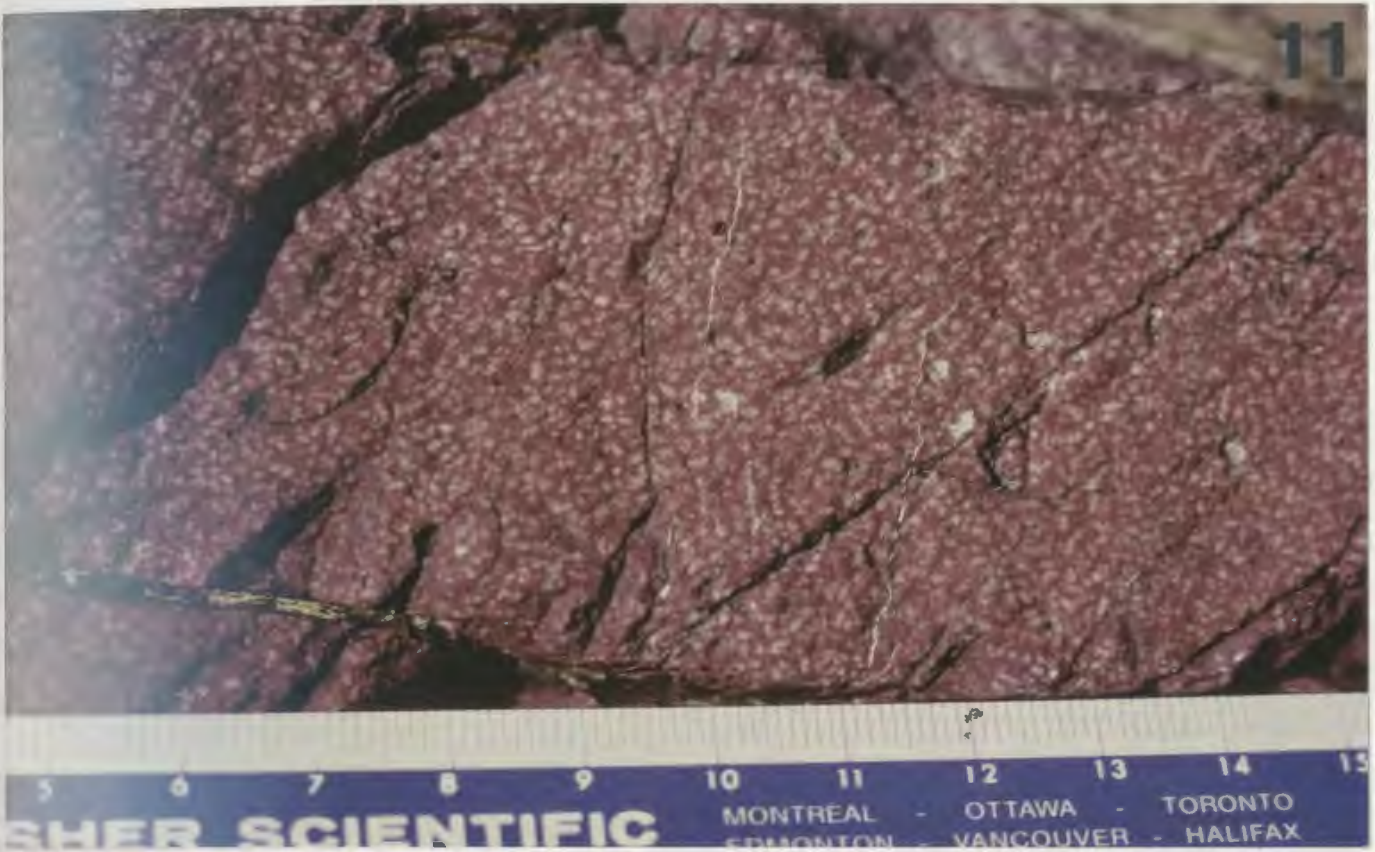
Coarse-grained feldspar-phyric basalts occur scattered throughout the area but are most common in the Blue Hills. Megascopically these rocks contain epidotised plagioclase

plate 11

Example of the mottled texture exhibited by some lava flows along the west shore of Colliers Bay. Although the photo was taken on the oxidised portion of the flow, the texture is characteristic of entire lava flow. For photomicrograph of texture, see Plate 25. Scale is in cm.

Plate 12

Example of field occurrence of plagiophyric sills from the Blue Hills Sequence. The plagioclase phenocrysts display a glomeroporphyritic texture (see Plate 27 for photomicrograph). The red spots are haematite pseudomorphs after olivine phenocrysts.



phenocrysts up to 1.5 cm long (Plate 12). Field relations and petrography suggest that these rocks are sills intrusive into the main series of lava flows. Margins of these sills are marked by dark brown, highly amygduloidal, chilled borders containing a few plagioclase phenocrysts (Plate 13). The amygdules are filled almost exclusively with prehnite (Plate 29). In most places the contact of these sills with the lava flows show signs of metasomatic alteration, changing parts of adjacent lava flows into bleached, baked zones. The sills are thicker than the lava flows and are generally 25-50 m across.

Various breccia units are present in the Blue Hills Sequence. The most common of these is mafic pyroclastic breccia. A spectacular example is exposed on a hilltop near Route 3 as it turns sharply west on the southwest side of Colliers Bay. Here the breccia consists of large angular blocks of fine-grained basalt set in a highly oxidised comminuted matrix (Plate 14). The exposure is roughly 'trough-shaped' and extends along strike for about 100 m. This feature may represent a vent breccia now exposed in cross-section. A similarly coarse mafic breccia is exposed at the northern tip of Turk's Head (at the northern extreme of the field area). Field relations at this locality, however, indicate that this was more likely a lava flow which encountered wet unconsolidated sediments and was subsequently brecciated by phreatic explosions. The inclusion of irregularly oriented 'patches and clots' of

plate 13

Example of the chilled border zone of the plagiophyric sill unit, Blue Hills Sequence. Note the distinct plagioclase laths and irregularly shaped amygdules, which are filled mainly with prehnite (see Plate 29).

Plate 14

Possible vent-breccia (see text for discussion) outcropping on a hilltop southwest of Colliers Bay. The breccia consists of large angular mafic blocks set in a fine-grained comminuted matrix, stained with iron oxide. Handle of hammer is 30 cm long.

TOP



laminated sediments caught between basalt blocks supports this interpretation (Plate 15).

A laharic breccia is exposed in discontinuous outcrop on the west side of a north-south trending valley in the central Blue Hills. The original thickness of this unit is unknown, as probably the bulk of it has been eroded to form the valley. The lahar consists of angular, subrounded, and rounded amygduloidal basalt fragments along with small plagioclase crystals all set in a reddish-brown gritty muddy matrix. The composition of the matrix and the lack of sorting among the fragments (Plate 16) suggest that this rock was deposited from a debris flow.

Minor pebble conglomerates, sandstones, and siltstones are sporadically intercalated with the basalt flows. These rocks are lithologically very similar to the sedimentary rocks interbedded with the underlying ash-flow tuff sequences; however, lithic fragments here consist predominantly of vesicular basalt. The sedimentary units generally occur as thin discontinuous lenses and probably represent deposition in small ponds or streams in depressions on the flow tops.

An unusual deposit occurs on the same hilltop as the vent (?) breccia described earlier. The unit consists of a stratified crystal-rich rock (Plate 17). The crystals consist almost entirely of euhedral to broken plagioclase grains averaging 1-2 mm in size. The unit occurs between basalt flows and, like the other sedimentary units, is

plate 15

Coarse angular (phreatic?) breccia exposed at the northern end of Turk's Gut. Note the portions of laminated red sediment caught between the grey mafic blocks. Pen is 15 cm long.

5

Plate 16

Example of a lahar breccia outcropping in the central Blue Hills. Amygduloidal mafic fragments are poorly sorted and are surrounded by a gritty muddy matrix.

TOP



plate 17

Exposure of stratified air-fall deposit, southwest Colliers Bay. This unit consists almost entirely of broken plagioclase crystals set in a fine-grained haematite matrix. Hammer handle (30 cm long) trends approximately north-south, with north towards the top of the photo.

Plate 18

Coarse boulder conglomerate exposed at Turk's Gut, northern end of study area. This unit represents basal Conception Group or uppermost Harbour Main Group (see text for discussion). All boulders are of mafic composition. The high degree of rounding and poor sorting suggest proximal conditions of deposition. The matrix consists of coarse (2-3mm) sand also of mafic composition. Viewed looking east. Conglomerate rests on mafic lavas which outcrop on the hillside just east of this exposure. Note hammer (handle is 30 cm long) near left centre of photo.

TOP



trough-shaped and at its widest is about 3 m thick. It is not certain whether this is an airfall or waterlain deposit. The almost euhedral crystals and their great abundance, however, may favour deposition from the air. If this is an airfall deposit, it indicates that explosive, ash-flow type eruptions were continuing during the initial stages of basalt eruption.

### 2.3.3 Post-Harbour Main Group Rocks

At Turk's Gut, in the northern part of the map area, basalt flows of the Harbour Main Group are immediately overlain by a spectacular coarse boulder conglomerate (Plate 18). McCartney (1967) referred to this unit as the basal zone of the Conception Group. However, recent discussion (H. Williams, pers. comm., 1983) suggests that the conglomerate may be the uppermost unit of the Harbour Main Group. However, if one accepts that the Conception Group is in conformable contact with the underlying Harbour Main Group, then the assignment of the conglomerate to one or the other group may be an argument in semantics. The conglomerate is composed entirely of well-rounded mafic rock fragments up to 1.5 m long set in a finer-grained sandy matrix also of mafic composition. The high degree of rounding of the boulders combined with the low degree of sorting most likely indicates proximal, high-energy conditions of deposition (S.A. Smith, pers. comm., 1982).

Elsewhere in the field area, the Conception Group consists of greenish-grey finely laminated siltstones and mudstones which weather to a characteristic buff to cream colour. Except for the conglomerate locality, the contact between the Harbour Main and Conception Groups is a fault, and is presumed to be so where exposed in the study area.

Within the map area, lower to middle Cambrian sedimentary rocks rest with marked unconformity on mafic volcanics of the Harbour Main Group. This relationship is superbly exposed on the clifftop west of Colliers Bay (Plate 19). The basal unit can be observed in patchy low outcrops in farmers' fields where conglomerate with angular mafic rock fragments in a coarse sandy red matrix fill low spots in the Precambrian volcanic regolith. The succession continues upwards with red thinly-bedded, fine-grained calcareous sandstones, red shales, and minor algal beds (McCartney, 1967). A black manganiferous horizon separates Lower and Middle Cambrian formations. The Cambrian succession is in fault contact with the Conception Group in the area.

## 2.4 STRUCTURE

There is a general consensus that the Avalon Zone was affected by two main orogenic events, a late Precambrian 'Avalonian' orogeny (Lilly, 1966; Hughes, 1970) and a younger Devonian (Acadian) orogeny. Each of these events

19



Plate 19

View, facing north, of essentially flat-lying lower to middle Cambrian sediments (left side of photo) resting unconformably on steeply west (left) dipping mafic lava flows of the Harbour Main Group (right side of photo). West side of Collier's Bay.

affected the Avalon Zone in different ways. The Avalonian deformation is most apparent in the east, where the Conception Group displays a vertical cleavage beneath a flat-lying Cambrian sequence (eg. Bacon Cove on Colliers Peninsula). On the other hand, the Acadian deformation is most intense in the west with asymmetric folding and southeast directed thrusting, and it dies out eastwards where lower Palaeozoic rocks, notably on Bell Island in Conception Bay, are essentially flat-lying and undeformed.

Within the map area the succession of ash-flow tuff sequences, sedimentary units, and mafic flows (all conformable and facing west) comprise the western limb of an open anticline whose north-south trending axis is located east of the present map area. The structural information from isolated outcrops in the area of Brigus Junction indicate that the inlier is a dome or a doubly plunging small anticline, with part of its eastern margin as a normal fault. The flows here represent the upper portion of the Blue Hills stratigraphy. Figure 4 presents a simplified representative cross-section of the map area.

The volcanic units lack penetrative deformation but some of the finer-grained intercalated sediments have developed a slight axial-planar cleavage. Occasionally 'bedding' surfaces of the volcanics show evidence of local shearing. Numerous high-angle faults trending generally northwest-southeast cut the volcanic and sedimentary rocks of the group. The fact that many of these faults do not cut

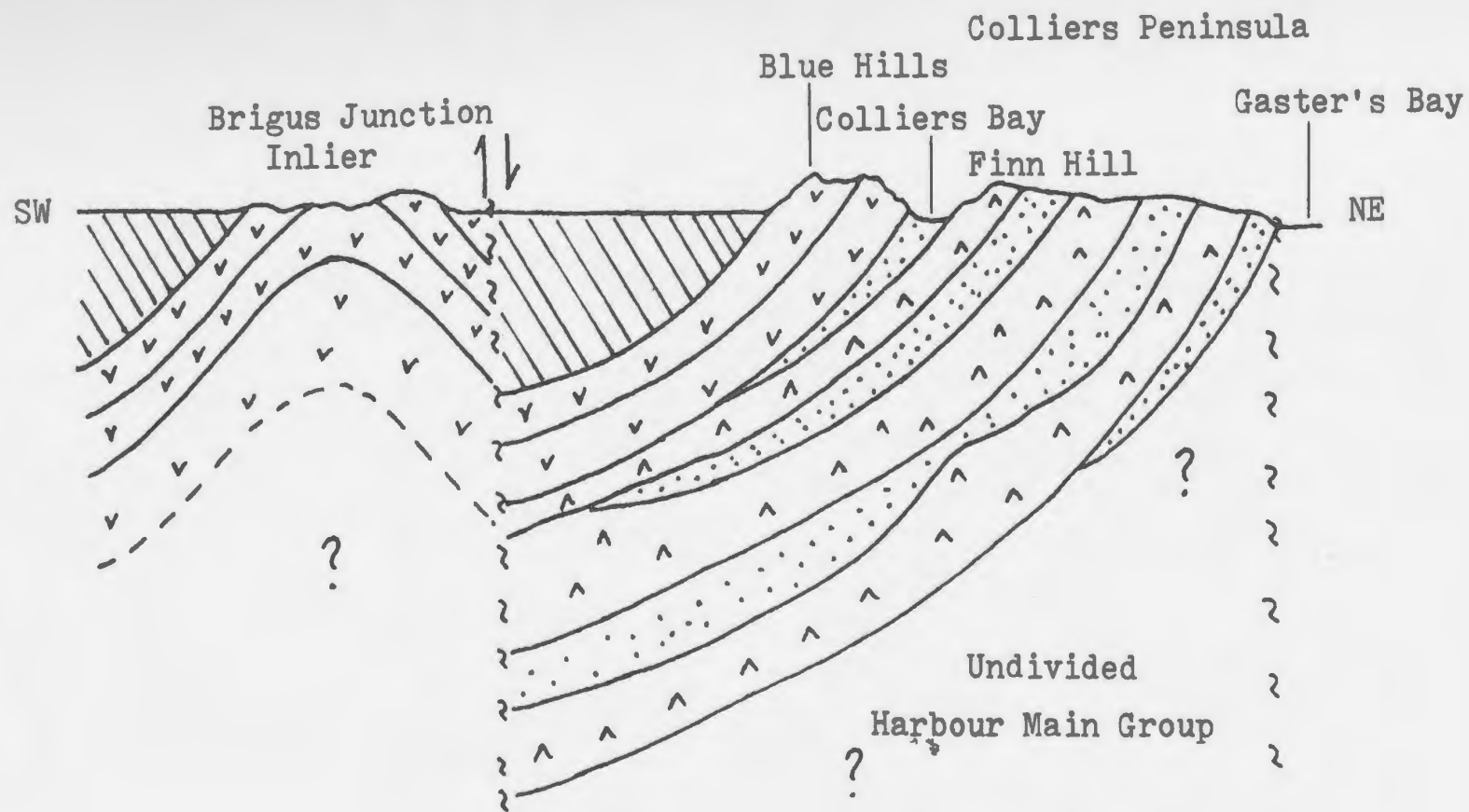
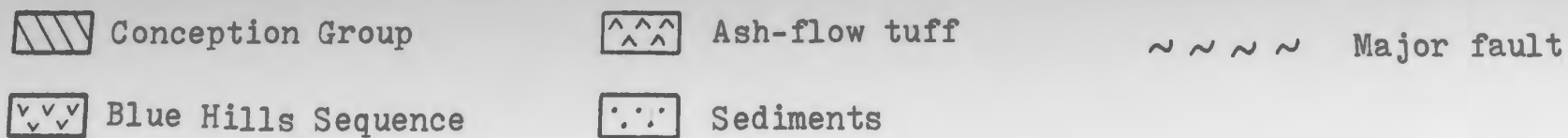


Figure 4. Schematic cross-section of rock units in the Blue Hills Sequence of the Harbour Main Group. Horizontal and vertical scales are not implied.

the entire succession of the Harbour Main Group (particularly well illustrated in the ash-flow tuff sequences) may indicate that some of these faults were penecontemporaneous with deposition of the volcanics. Large, steep boundary faults (eg. Marysvale Fault, Brigus Fault, Gasters Fault) are northeast-southwest trending and juxtapose rocks of the Harbour Main Group against Conception Group and Cambrian formations.

*To a pessimist every opportunity is an obstacle; to an optimist every obstacle is an opportunity. -- Anonymous*

## CHAPTER 3

### PETROGRAPHY

#### 3.1 INTRODUCTION

A wide variety of mineralogical and textural features are present in the complete succession of volcanics of the study area. On the basis of petrographic distinctions the rock types have been grouped into the following units: ash-flow tuffs, pyroxene-phyric basaltic flows, aphyric basaltic flows, plagiophyric sills, porphyrite, breccias, and sedimentary rocks. In the subsequent sections of this chapter each rock type is described in terms of its original mineralogy (as well as can be deduced) followed by a discussion on alteration. All the rock types considered here have been affected by low-grade (prehnite-pumpellyite facies) metamorphism and thus are appropriately referred to as 'metavolcanics'. Although the prefix 'meta-' will not appear in most of the following discussion it is implied throughout the text. The chemical significance of this alteration will be discussed in a subsequent chapter.

## 3.2 ASH-FLOW TUFF SEQUENCES

### 3.2.1 Mineralogy and Textures

The following is intended only as a summary of the meticulous petrography of these rocks carried out by Nixon (1975). For more detailed descriptions one is encouraged to consult this treatise. Generally speaking these rocks consist of crystal, vitric, and lithic tuffs with any combination of these three main components occurring in any single unit. The most common of these however, are crystal lithic tuffs. In all three ash-flow tuff sequences albite is the dominant phenocryst phase. Characteristic variations in the mineralogy between individual ash-flow sequences has been mentioned previously (Chapter 2).

Textures characteristic of ignimbrite cooling units (Ross and Smith, 1961) have been recognised in nearly all units of the tuff sequences. Individual units display distinct unwelded or incipiently welded basal zones grading upwards into welded zones and then unwelded tops. Pumice in the welded zones shows collapsed fiamme structure and often imparts a primary eutaxitic fabric to the rocks. The presence of welded zones in the units indicates that heat loss during extrusion was minor, thereby supporting an ignimbritic origin for these rocks. Vesiculation of the magma produced pumice and led to a nuée ardente mechanism of eruption.

The ignimbrites are composed of subhedral to anhedral plagioclase (albite), quartz, and biotite phenocrysts and pumice fragments embedded in a fine-grained felsic ash matrix principally composed of alkali feldspar, epidote, and chlorite. Quartz crystals are usually resorbed, showing rounding and intricate embayment; they invariably occur as alpha-quartz paramorphs after beta-quartz. The percentage of lithic fragments is variable and may range from rare to extremely abundant from one unit to the next. Cusp- and lune-shaped glass shards are generally abundant in individual units (Plate 20) and in some welded zones they may be so abundant and flattened as to give the rock a fluidal texture.

### 3.2.2 Alteration

By their very nature, ash-flow tuffs are predominantly glassy and devitrify with time. The pattern of devitrification textures in ignimbrites is highly variable, excellent descriptions and examples of which are given by Ross and Smith (1961). Despite the development of microspherulitic feldspar and perlitic cracks, the ash-flow tuff units of the Harbour Main Group are, for the most part, remarkably well preserved, considering their age. Distinct glass shards are readily identifiable as they are outlined with haematite dust. The glass shards themselves have been recrystallised to intergrowths of fibrous quartz and alkali

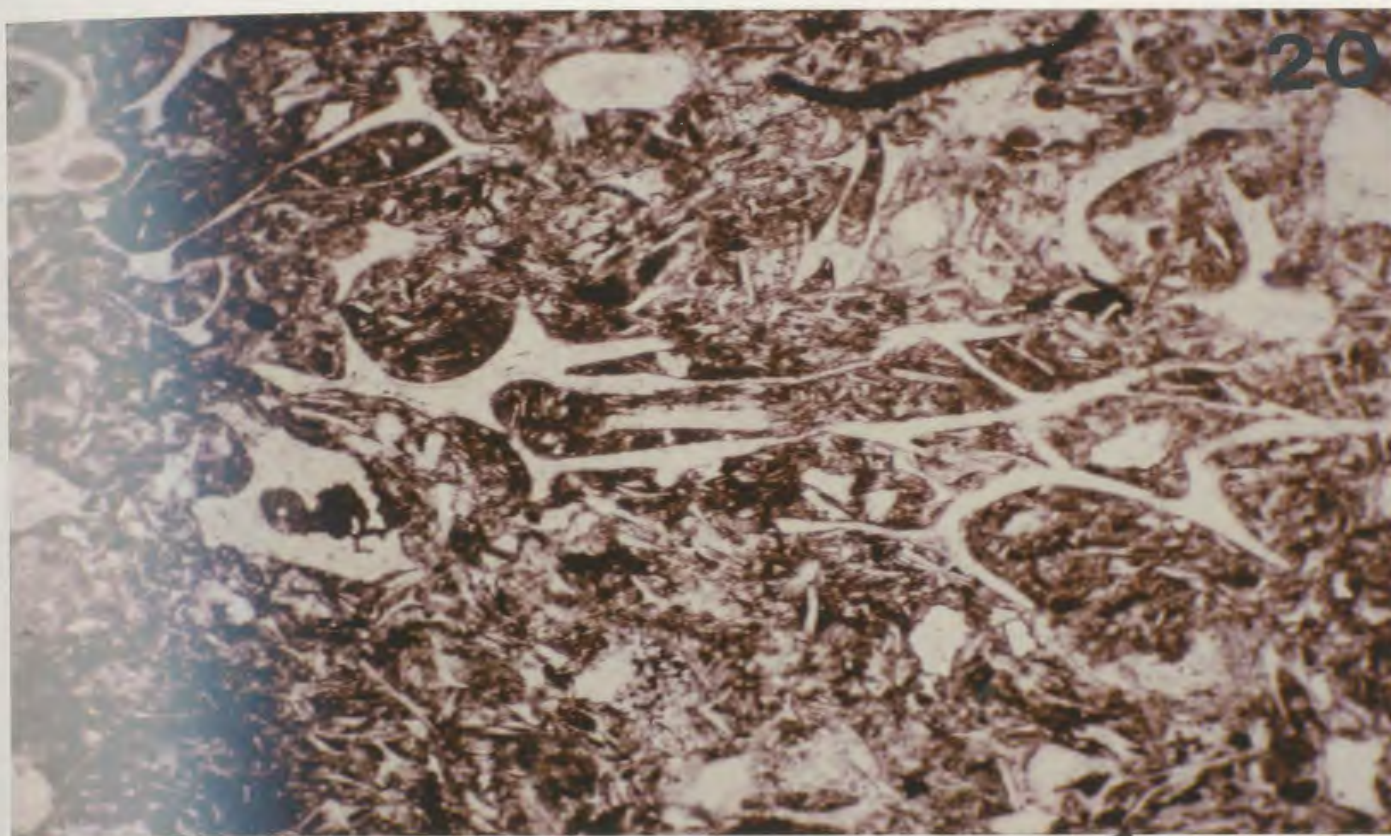


Plate 20

Photomicrograph of a representative sample of the ash-flow tuff units on Collier's Peninsula. Note the excellent preservation of cusp-shaped glass shards (now devitrified) set in an oxidised matrix. Plane-polarised light. (Field of view is approximately 1mm wide).

feldspar. A similar alteration is exhibited by the pumice fragments. Plagioclase grains are entirely of albitic composition but commonly retain relatively clear polysynthetic twinning. In places epidote and prehnite alteration overgrowths are quite pervasive. Biotite grains and phenocrysts have been largely altered to chlorite.

### 3.3 BLUE HILLS SEQUENCE

In general the meta-basalts of the Blue Hills Sequence display typical basaltic or diabasic textures with phenocrysts of olivine, plagioclase, and/or pyroxene in a groundmass of plagioclase laths, pyroxene and olivine granules, and opaque minerals. The mafic rocks of the Blue Hills Sequence can be petrographically divided into three main groups with distinctive mineralogical and textural features. The following sections describe these distinctions.

#### 3.3.1 Pyroxene-phyric Lavas

Lavas from the stratigraphically lower portion of the Blue Hills Sequence are characterised by the presence of abundant clinopyroxene phenocrysts. These lavas are restricted to the east side of the Blue Hills and a few isolated localities along the west shore of Colliers Bay.

Large colourless to pale green euhedral to subhedral

pyroxenes (augite) up to 0.5 cm in diameter are invariably twinned and occur either as single crystals or as glomeroporphyritic grains (Plate 21). The latter have irregular, rounded grain to grain contacts but have well-developed crystal faces towards the groundmass. Many of the pyroxenes display zoning.

Plagioclase phenocrysts occur as tabular, rather stubby crystals, usually singly but sometimes as clusters, averaging 0.2 cm in length and reaching a maximum of 1 cm. One particular sample (109-4) exhibits inclusions of augite and an anhedral opaque phase (probably magnetite) poikilolitically enclosed in larger plagioclase crystals (Plate 22). The plagioclase phenocrysts may have been originally zoned but secondary alteration has obscured definite evidence of this. Pseudomorphed olivine phenocrysts are rare in these rocks, but where they are observed they are replaced by iddingsite, chlorite, and haematite; thus indicating the earlier presence of olivine in these lavas.

The groundmass of these rocks is composed of a fine-grained mixture of highly altered plagioclase, pyroxene and magnetite granules, and chlorite.

### 3.3.2 Aphyric Basaltic Lavas

The main section of the mafic sequence consists of subaerial basaltic lavas. The chilled bases of these flows

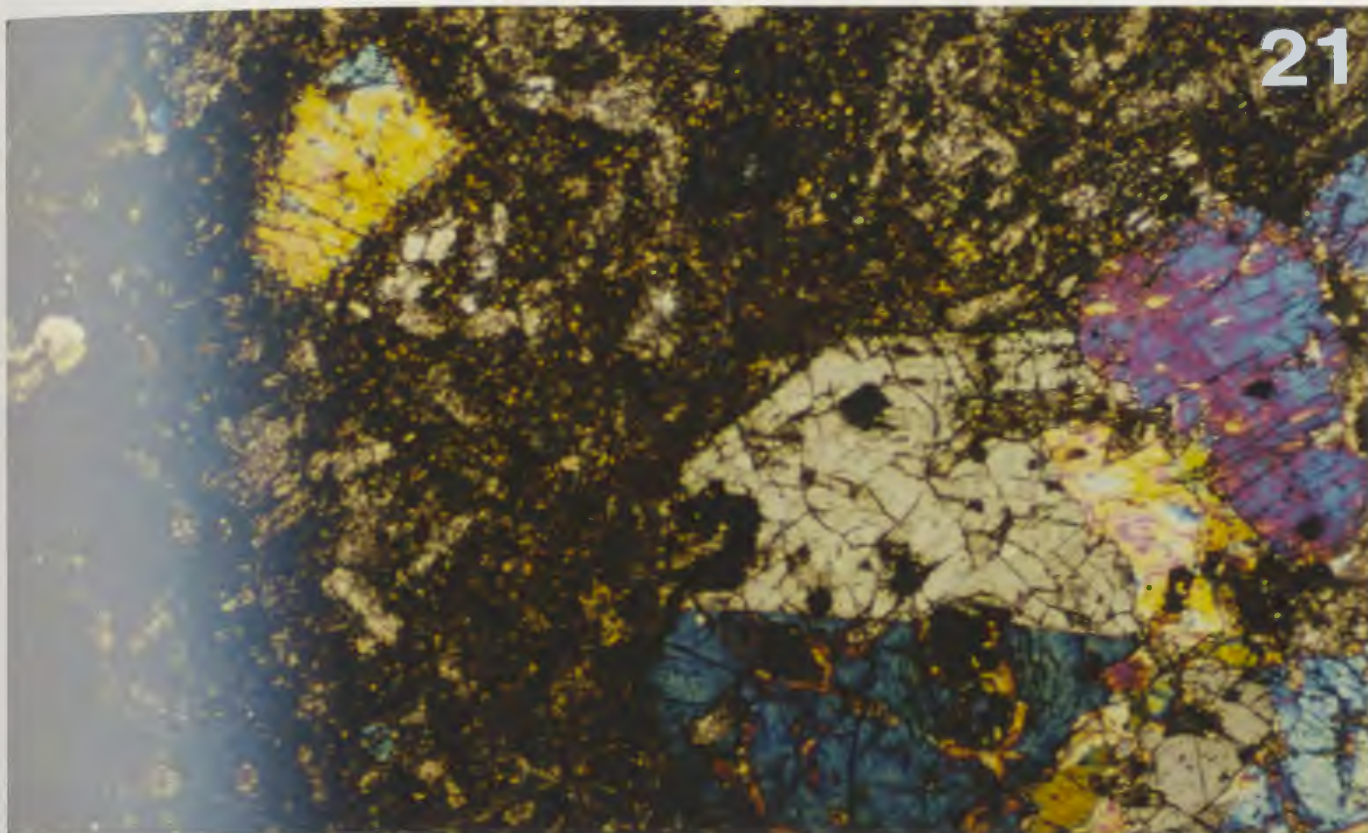
plate 21

Example of the glomeroporphyritic texture displayed by clinopyroxene phenocrysts in the stratigraphically lower pyroxene-phyric lavas of the Blue Hills Sequence. The phenocryst phases consist of Ca-rich augites which are often twinned and occasional pseudomorphed olivines. The matrix is composed of fine-grained opaques and altered plagioclase. Sample 108-3. Field of view is approximately 4.5 mm wide, X-nicols.

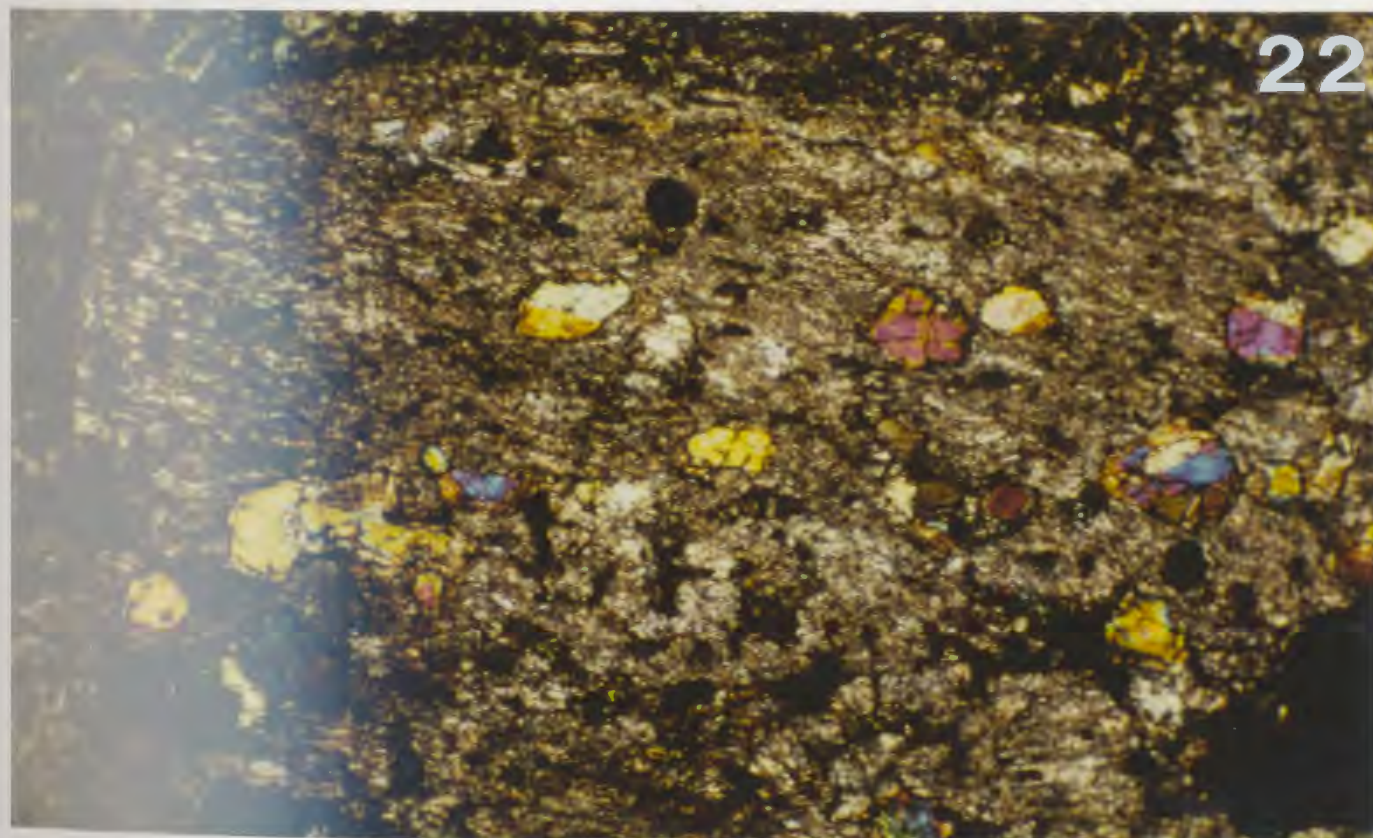
Plate 22

Photomicrograph showing an altered plagioclase phenocryst with inclusions of pyroxene and opaque material. Sample is from the pyroxene phyric unit. Sample 109-4. Field of view is approximately 2.5 mm wide, X-nicols.

21



22



are aphanitic or aphyric. They are quite often amygduloidal and sometimes display coalescing amygdules. The phaneritic central parts of the flows are medium- to fine-grained and often contain phenocrysts of olivine and/or plagioclase. The phenocrysts range in size from microphenocrysts (0.2 mm) to 2-4 mm. In many instances the phenocrysts are intergrown in clusters and display a glomeroporphyritic texture (Plate 23). In these flows clinopyroxene does not occur as a phenocryst phase, but is locally quite abundant (20-30 % of mode) in the groundmass of most flows where it ophitically to subophitically encloses plagioclase laths (Plate 24). Pyroxene in these basalt flows generally has a brownish tint and very often is slightly pink. In most flows from the Brigus Junction Inlier, the pyroxene is noticeably pleochroic pinkish-brown. Chemical analysis of these augites shows them to contain significant amounts of titanium (see Table 4, Ch. 4) and thus are titaniferous augites. The groundmass also contains plagioclase laths and olivine granules. No Ca-poor pyroxene has been recognised in any of the flows.

The 'spotted' texture exhibited by some flows along the west shore of Colliers Bay (see Plate 11) is essentially a variation of ophitic texture properly referred to as 'poikilophitic' (A.G.I. Glossary, 1972, p.552). Here plagioclase microlites are enclosed in large anhedral clinopyroxene grains (Plate 25).

In finer-grained flows and near the tops of many of the

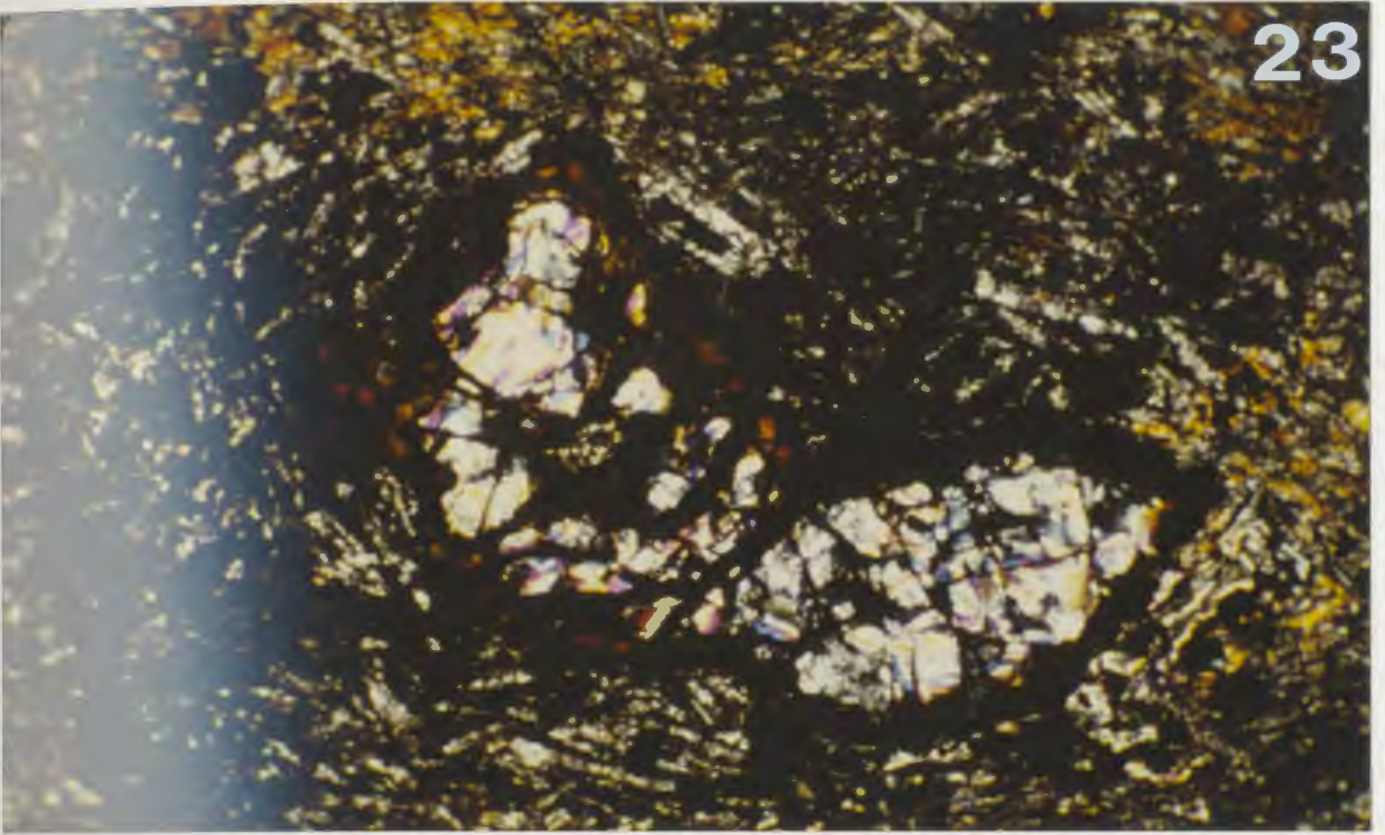
plate 23

Photomicrograph showing a cluster of pseudo-morphed euhedral olivine phenocrysts. The rims of the olivines are replaced by iddingsite and iron oxides with the core replaced mainly by prehnite. Note how the plagioclase microlites 'flow' around the olivine phenocrysts. Relict pyroxene is also present in the groundmass. Sample 170-1. Field of view is approximately 2.5 mm wide, X-nicols.

Plate 24

Photomicrograph displaying well developed ophitic texture between relict augite and altered plagioclase laths typically observed in lava flows from the main portion of the Blue Hills Sequence. The dark groundmass consists of altered olivine and opaque minerals. Sample 046-1. Field of view is approximately 2.5 mm wide, X-nicols.

23



24

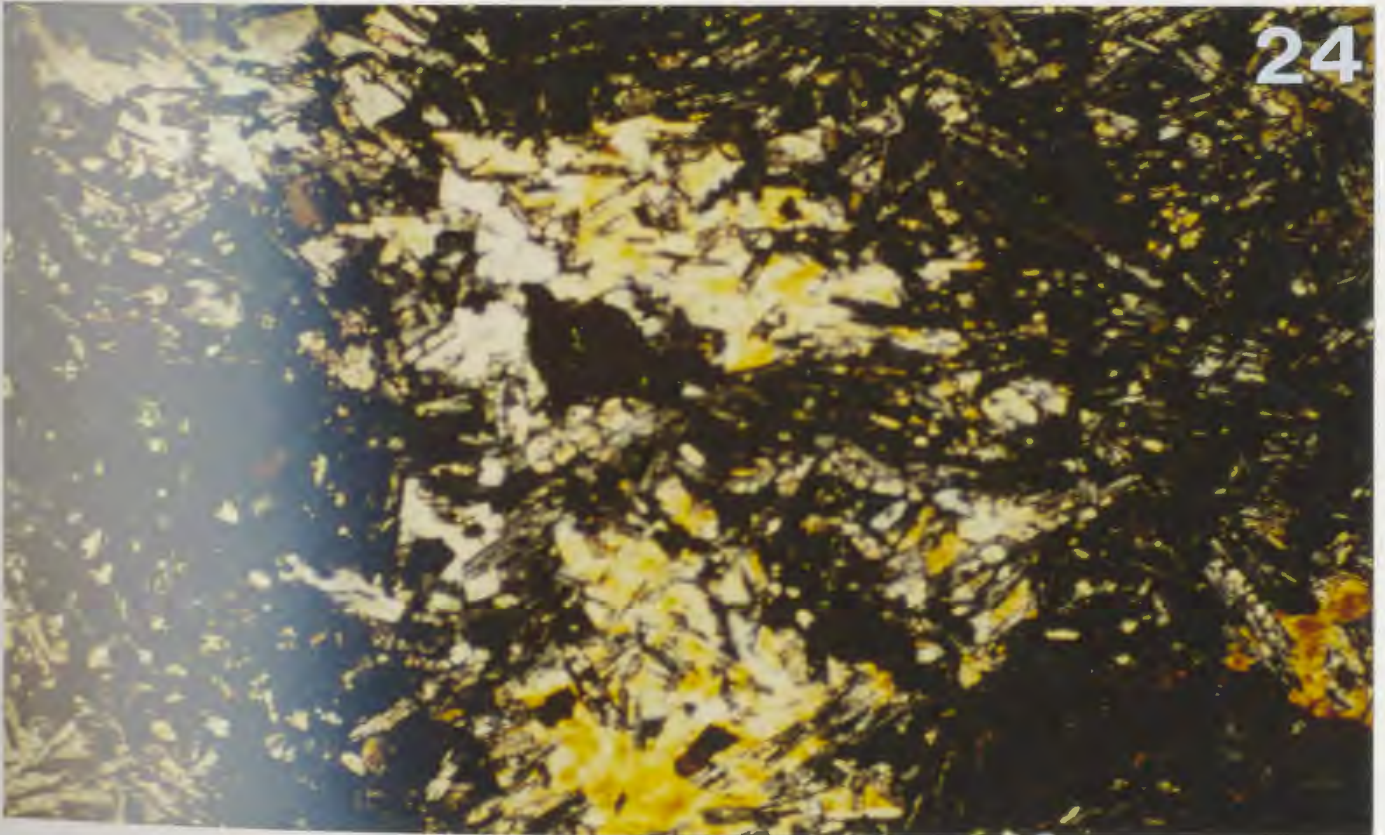
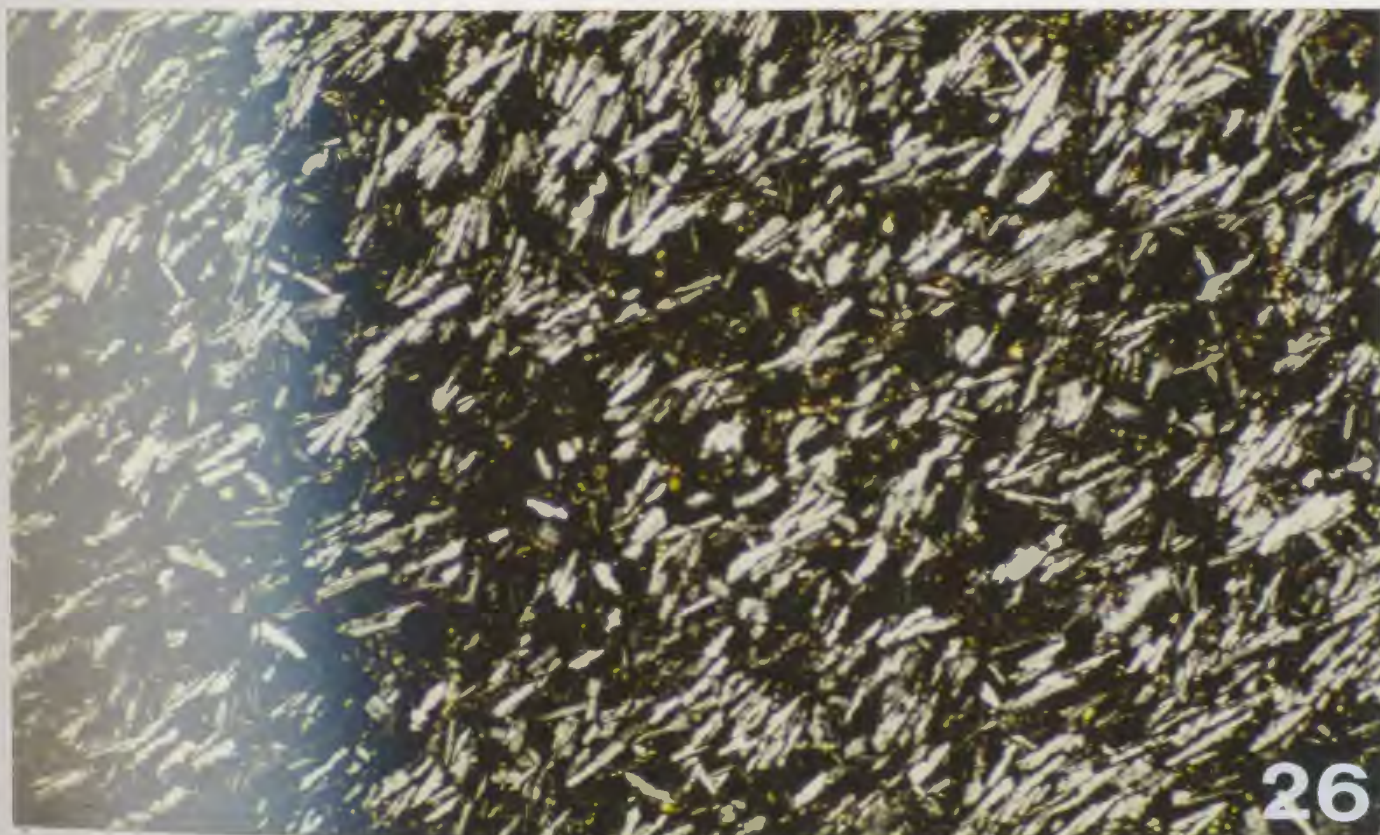
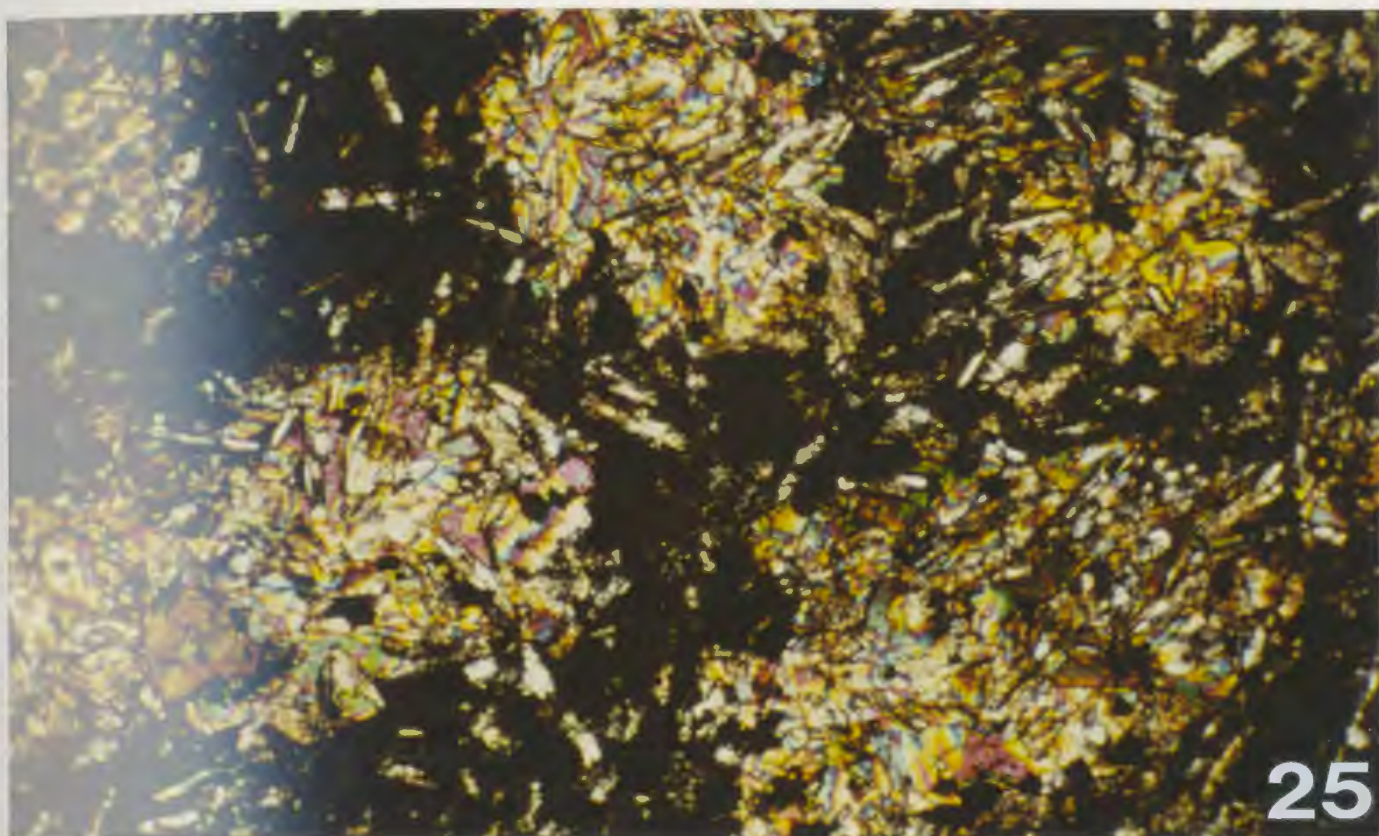


plate 25

Photomicrograph exhibiting poikilophitic texture observed in outcrop of Plate 11. Here, clusters of anhedral augite enclose mats of altered plagioclase microlites. The groundmass consists mainly of fine-grained opaque minerals. Sample 111-3. Field of view is approximately 2.5 mm wide, X-nicols.

Plate 26

Photomicrograph of altered plagioclase laths displaying a distinct alignment due to flow, imparting a trachytic texture. Clinopyroxene in these lavas occurs as orange and yellow granules disseminated throughout the groundmass. Sample 212-2. Field of view is approximately 2.5 mm wide, X-nicols.



flows, there is a parallel to sub-parallel alignment of plagioclase laths imparting a somewhat trachytic / pilotaxitic texture to these rocks (Plate 26). In some places the plagioclase laths are seen to 'flow' around olivine phenocrysts (Plate 23). In these same flows the groundmass plagioclase microlites very often display textures such as 'spikey' ends and sometimes glassy cores indicating rapid cooling - as would be expected near the flow tops of subaerial lavas.

Two thin sections examined could possibly be classified petrographically as andesite (eg. sample 058-1). Geochemical analysis (see Table 2, Ch.4) tends to support this classification. The rock contains microphenocrysts of plagioclase (which are locally zoned) and rare skeletal olivine pseudomorphs. However, the pervasive alteration in this rock, especially the obliteration of relict pyroxene, makes it difficult to be absolutely certain about this rock. As this rock type is restricted to a few isolated outcrops near the contact zone of the ash-flow tuffs with the overlying basalts, near the mouth of Colliers River, it is quite possible that it may be an intermediate volcanic representative of the transition from ash-flow tuff to truly basaltic volcanism.

The basaltic flows from Brigus Junction Inlier are characterised by the loss of prominent phenocryst phases and consist almost entirely of flow oriented plagioclase laths with titanomagnetite and very minor amounts of granular

clinopyroxene (Plate 26). Rare larger microphenocrysts of olivine (pseudomorphed) occur in a few samples. This rather abrupt change in petrography may mark the onset of fractionation in the basalts (see also geochemistry chapter). Minor amounts of sphene were observed in a few thin sections from this area.

### 3.3.3 Plagiophyric Sills

Mineralogically these rocks are very similar to the main series of lava flows, the only significant difference being the textural relationships between plagioclase, pyroxene, and olivine. Plagioclase dominates these rocks and occurs as subhedral to euhedral phenocrysts displaying seriate texture (Plate 28) ranging in length from 1 mm to 1 cm. Glomeroporphyritic texture is well developed here and 'rosettes' of radiating plagioclase phenocrysts are quite common (Plate 27). Pleochroic brown or pinkish-brown clinopyroxene (augite) occurs between the plagioclase phenocrysts in an intergranular texture and comprises approximately 10-20 % of the rock. Olivine pseudomorphs are abundant as phenocrysts (up to 3 mm) which are commonly in glomeroporphyritic arrangement. Pseudomorphed olivine is also present in the groundmass as microphenocrysts and granules.

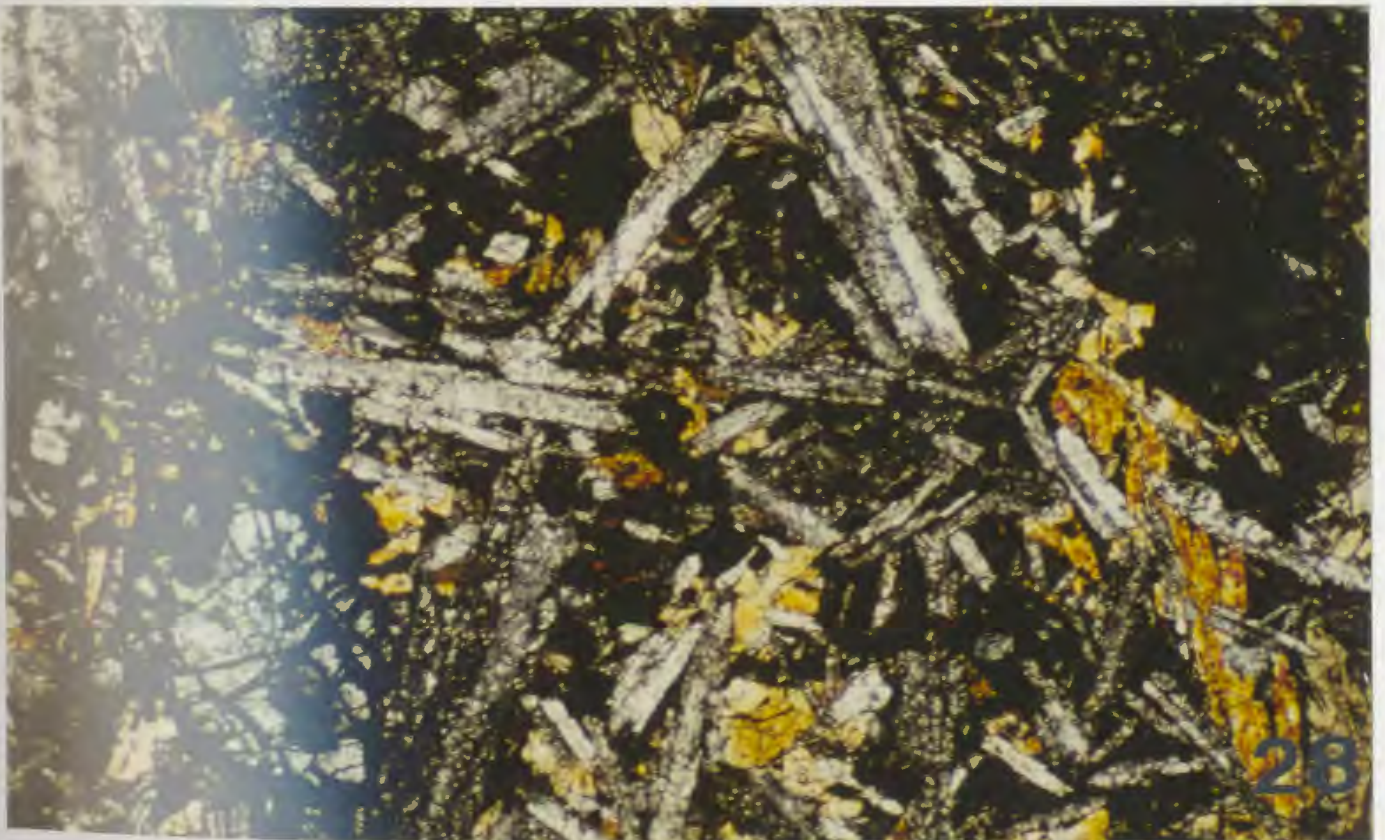
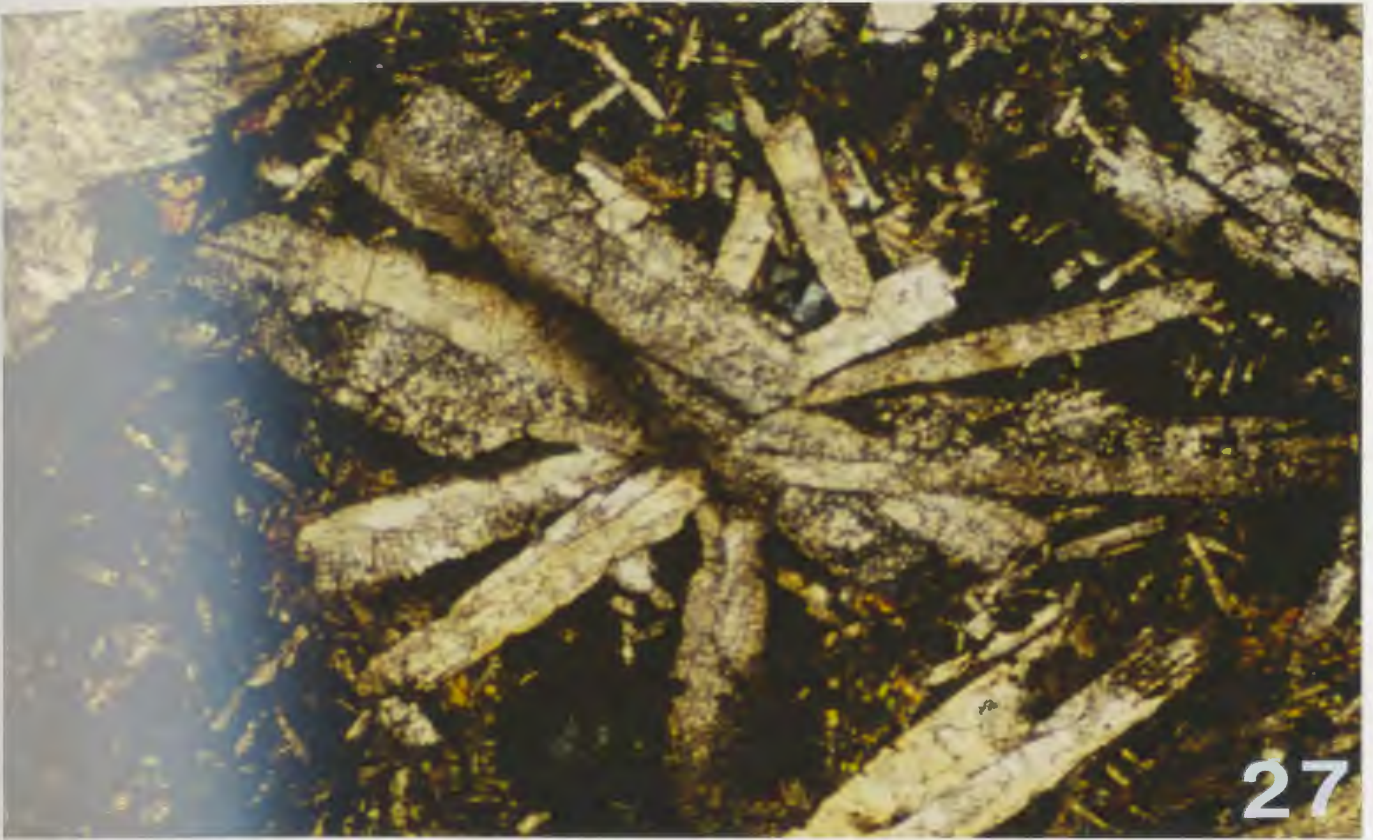
The chilled borders of the sills are fine-grained and amygduloidal with the amygdules filled primarily with

plate 27

Photomicrograph showing a rosette of plagioclase laths typical of these plagiophyric sills. The plagioclase is altered to albite, epidote, and/or prehnite. The groundmass consists of altered plagioclase microlites, anhedral relict clinopyroxene and olivine pseudomorphs. Sample 055-1. Field of view is approximately 4.5 mm wide, X-nicols.

Plate 28

Photomicrograph of plagiophyric sill unit of the Blue Hills Sequence. This sample represents a more even-grained diabasic texture of the sills with altered plagioclase laths displaying seriate texture. Relict clinopyroxene has a sub-ophitic to intergranular relationship with the plagioclase. Note the pseudomorphed olivine phenocryst replaced by haematite (rim) and chlorite (core) in lower left corner of photo. Sample 081-4A. Field of view is approximately 4.5 mm wide, X-nicols.



prehnite and minor quartz (Plate 29). Plagioclase phenocrysts (up to 3 mm) and microlites as well as olivine pseudomorphs are set in an opaque groundmass. No relict pyroxene was observed here.

### 3.4 ALTERATION OF MAFIC ROCKS

The mafic rocks in the study area have undergone partial alteration giving rise to secondary minerals such as epidote, albite, prehnite, minor pumpellyite, and chlorite. These rocks thus represent sub-greenschist (prehnite-pumpellyite) facies metamorphism (Papezik, 1974).

Plagioclase is generally very altered and replaced by prehnite or albite pseudomorphs (eg. Plates 27-30). Olivine is completely pseudomorphed, being replaced by pleochroic iddingsite, chlorite, haematite, and opaque minerals (Plates 23 and 28). Clinopyroxene is virtually unaltered and remains as 'pristine' grains in most of the thin sections examined (eg. Plates 21, 24, 25, and 28).

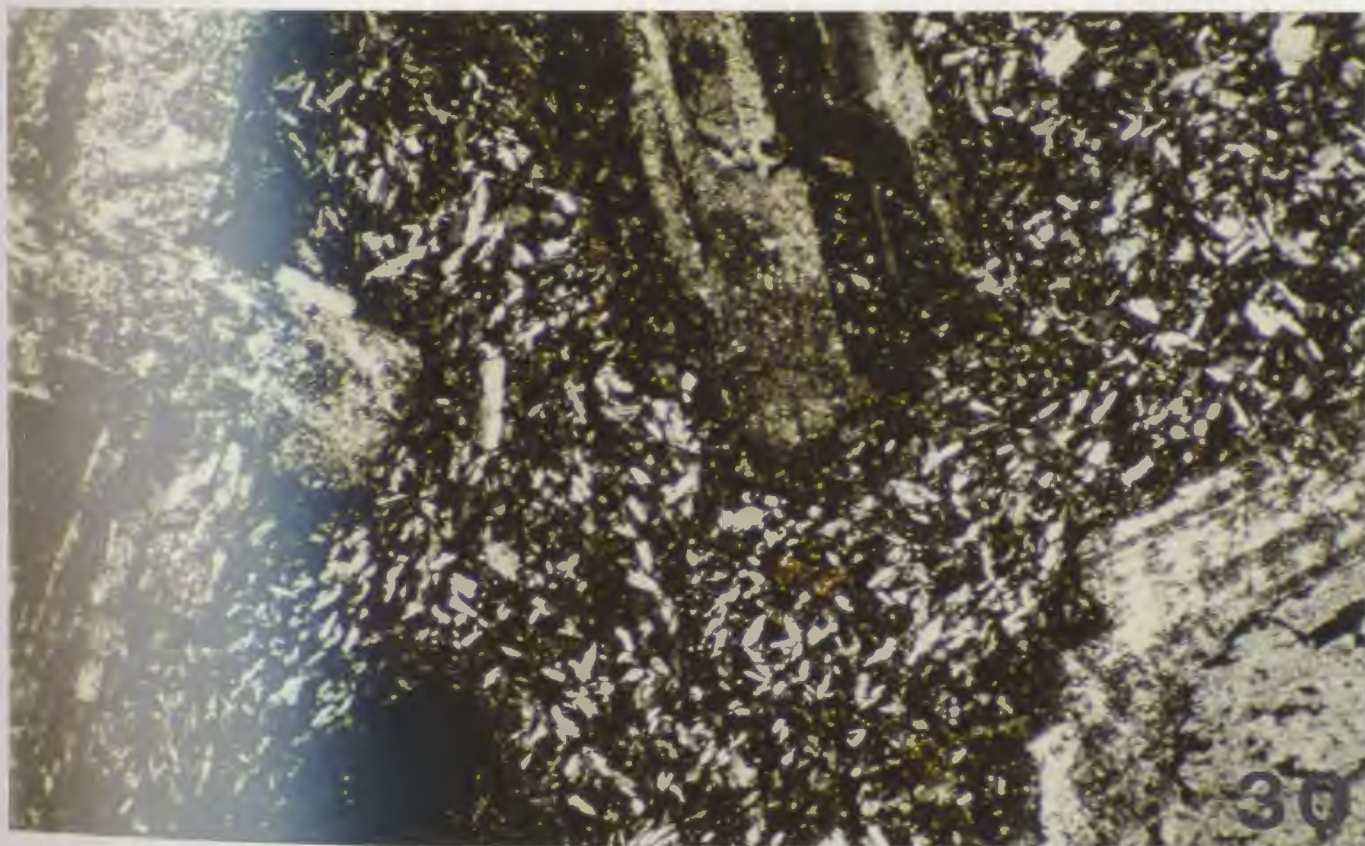
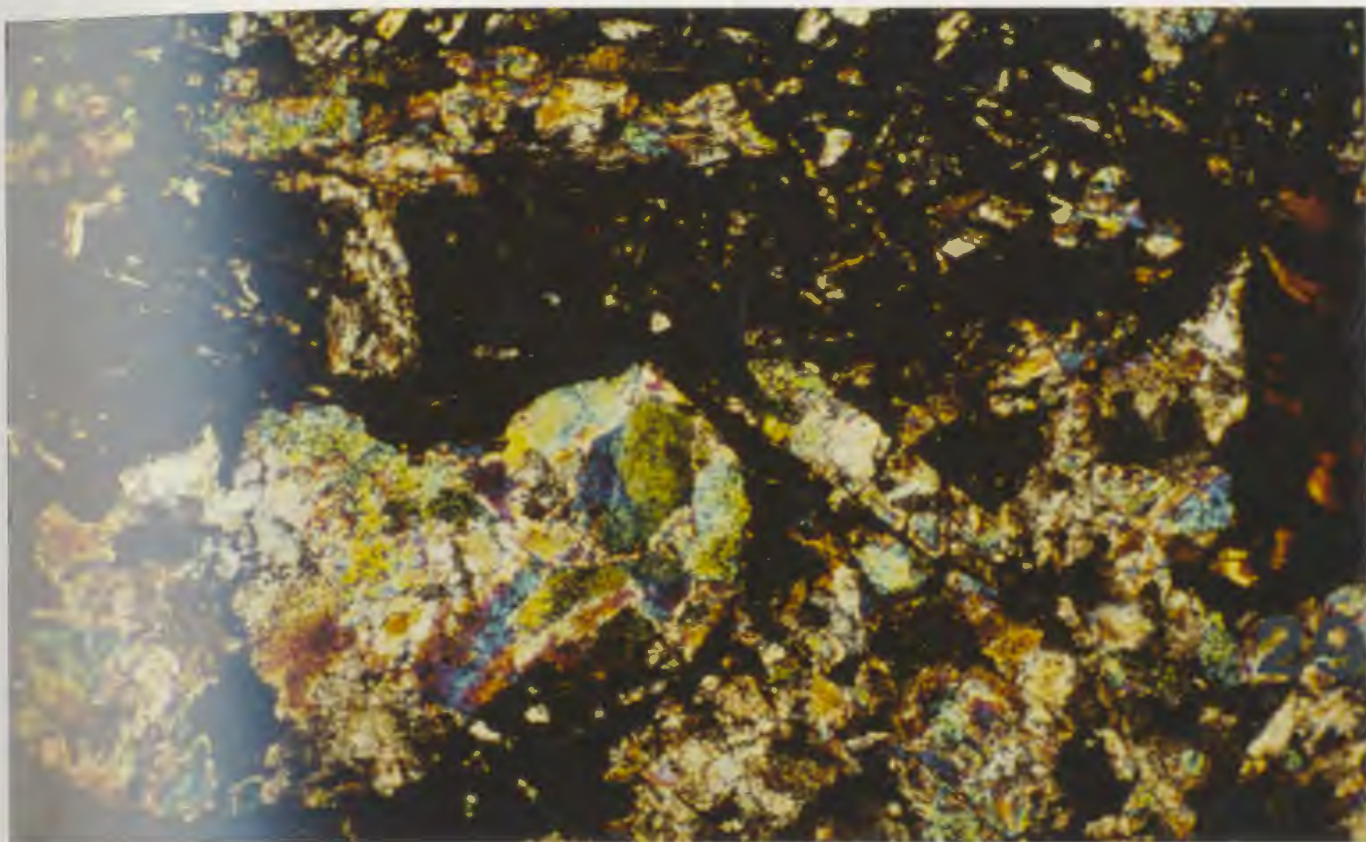
As noted above, the mafic rocks are in places amygduloidal. For the most part, the amygdules are filled with prehnite, minor pumpellyite, and quartz (eg. Plates 13 and 29). Near the contact with the overlying Cambrian sediments, calcite becomes the prime constituent of the amygdules. One peculiarity encountered in several lava flows with amygdules is a zoning of amygdule-filling materials. Invariably the bottom of the amygdule is

Plate 29

Photomicrograph of chilled border of plagiophyric sill (see Plate 12). Amygdules, such as the one which occupies the lower left quarter of this plate, consist primarily of prehnite with minor amounts of quartz. Plagioclase laths are highly altered to epidote and/or prehnite (upper portion of photo and parallel to top edge). Field of view is approximately 2.5 mm wide, X-nicols.

Plate 30

Photomicrograph of a sample from a 'porphyrite' intrusion within the map area (see Plate 4). Plagioclase crystals display a bimodal grain size, and are in part highly altered to albite and epidote. Some of the phenocrysts retain polysynthetic twinning and distinct zoning. Field of view is approximately 2.5 mm wide, X-nicols.



composed of haematite, followed upwards by prehnite, quartz, and calcite. Because the meniscus of each mineral component is sub-parallel and is in turn parallel to the attitude of the flow-base, it is likely that the vesicles were filled soon after eruption while they were still in a sub-horizontal position. Amygdules of this type proved to be a valuable 'way-up' indicator in many instances during field work.

Leucoxene is locally present in several of the thin sections, particularly from flows of the Brigus Junction Inlier. It occurs as a cloudy, whitish area around some of the opaque minerals, suggesting the presence of ilmenite in these rocks.

### 3.5 ASSOCIATED ROCKS

#### 3.5.1 Porphyrite

These basic intrusives are characterised by subhedral to euhedral tabular aggregates of altered plagioclase crystals up to 0.5 cm in length, commonly exhibiting faint remnants of zoning and rare inclusions of devitrified glass and opaque material (Plate 30). In thin section this rock resembles an example of porphyritic andesite described by Moorhouse (1970). Occasional olivine phenocrysts are pseudomorphed by opaque minerals. Although no relict pyroxene was observed in samples from the present study

area, Nixon (1975) reports minor amounts in specimens he collected from a porphyrite body on the east side of Colliers Peninsula as well as another near the town of Colliers. The groundmass of the porphyrite is composed of tiny microlites of plagioclase set in a very fine-grained dusty opaque matrix.

### 3.5.2 Pyroclastic Units

The breccias of the Blue Hills Sequence consist of a variety of mafic fragments in a fine- to medium-grained, haematized matrix. The mafic fragments consist of scoriaceous, vesicular/amygduloidal, plagiophyric, and aphanitic basalts, all being petrographically similar to rocks within the Blue Hills Sequence. Felsic volcanic rock fragments are rare in the mafic breccias. Highly altered plagioclase occurs as phenocrysts and also as a groundmass phase.

The air-fall deposit described earlier (Section 2.3.3) is typified by broken to subhedral plagioclase (albite) grains (comprising 75-80 % of the rock) 1mm to 0.1 mm in size set in a fine-grained haematized matrix of volcanic dust. Rare basaltic rock fragments are also present. Poorly developed graded bedding is evident on a mm scale.

Mafic tuffs are noticeably absent from the study area.

### 3.5.2 Epiclastic Rocks

The fine-grained clastic sedimentary rocks of the Blue Hills Sequence contain crystal fragments as well as rock fragments ranging in size from sand and silt to cobbles and pebbles in a predominantly silty or clay matrix. The rock fragments, which are generally of vesicular basalt, are subrounded to angular, and are usually poorly sorted and probably were derived as cinders and blocks from the loose, rubbly flow tops of the lavas. Well-rounded felsic volcanic fragments (welded crystal tuffs) are the main constituents of a pebble conglomerate unit occurring between two mafic flows on the east side of Turks Head.

The sedimentary rocks constitute a very minor percentage of the Blue Hills Sequence and are generally petrographically similar to the sandstones and siltstones of the underlying ash-flow tuff sequences. However, there is a greater proportion of mafic detritus as cobbles and pebbles in the sediments of the Blue Hills Sequence.

### 3.5.3 Mafic Dyke

One thin section of a greenish-grey mafic dyke was examined from the study area. The most obvious feature of this rock is the total absence of olivine pseudomorphs. Pale green clinopyroxene (augite) subophitically encloses plagioclase laths which are slightly less altered than

plagioclase in the basalt flows. Chlorite is abundant (3-5 %) and occurs intersertal to the plagioclase laths. The rock is fine-grained and has an overall equigranular texture with no phenocrysts. Opaque minerals are predominantly magnetite with characteristic euhedral shapes and account for ~ 10 % of the thin section.

*The purpose of classification is not to set forth final and indisputable truths but rather to afford stepping stones towards better understanding. -- L.C. Graton*

## CHAPTER 4

### GEOCHEMISTRY

#### 4.1 INTRODUCTION

This chapter is divided into two main sections. The first deals with the results of whole rock (major and trace-element) chemistry on a suite of 66 mafic samples from the western belt of the Harbour Main Group (see Ch. 1). In addition, 34 of these samples were analysed for rare-earth elements. The second part of the chapter presents chemical data for relict pyroxenes in the mafic rocks. Descriptions of the various analytical techniques, together with accuracy and precision data, can be found in Appendix A.

#### 4.2 WHOLE ROCK CHEMISTRY

Major oxides and trace element analyses of samples are presented in Table 2. The samples are grouped according to petrographic similarities discussed in Chapter 3. As will

TABLE 2. MAJOR OXIDE AND TRACE ELEMENT CHEMISTRY, BLUE HILLS SEQUENCE, HARBOUR MAIN GROUP

PYROXENE-PHYRIC LAVAS										
	058-1	014-1	108-3	109-4	118-1	119-3	132-2	197-1	235-1	236-1
SiO <sub>2</sub> (%)	53.60	48.20	49.70	49.60	54.40	53.10	48.90	49.60	46.30	48.90
TiO <sub>2</sub>	1.00	1.46	0.78	1.04	1.32	1.39	1.36	1.20	1.45	1.64
Al <sub>2</sub> O <sub>3</sub>	18.20	18.40	15.90	17.70	15.60	15.80	17.60	17.70	18.10	15.70
Fe <sub>2</sub> O <sub>3</sub> **	8.64	10.09	10.19	10.40	10.21	9.77	9.77	9.75	10.03	10.16
MnO	0.25	0.17	0.19	0.17	0.18	0.16	0.15	0.20	0.16	0.20
MgO	4.93	5.40	7.48	6.23	4.44	4.30	6.00	7.23	6.48	6.26
CaO	1.61	8.71	8.91	5.56	5.68	5.64	6.46	4.29	5.60	7.08
Na <sub>2</sub> O	6.68	3.22	2.30	4.09	3.83	4.60	4.13	2.92	3.52	4.96
K <sub>2</sub> O	0.81	2.05	1.42	2.14	2.64	1.99	1.77	4.26	2.95	0.47
P <sub>2</sub> O <sub>5</sub>	0.32	0.24	0.18	0.29	0.39	0.38	0.33	0.34	0.32	0.38
L.O.I.	3.03	2.20	2.74	2.97	1.69	1.85	2.78	3.25	4.61	2.89
Total	99.12	100.14	99.79	100.19	100.38	98.98	99.25	100.74	99.52	98.64
Rb (ppm)	22	62	33	76	56	41	56	129	91	10
Sr	194	752	658	729	604	619	768	539	455	229
Ba	308	1559	939	1062	894	660	463	3326	727	114
Y	31	24	19	18	32	33	25	30	26	28
Zr	129	112	73	60	144	144	101	129	113	133
Nb	9	4	5	5	6	7	3	7	5	5
V	167	268	241	291	252	270	270	268	278	276
Cr	0	66	134	38	6	16	84	69	85	63
Ni	0	26	62	41	19	15	41	50	30	40
Ga	15	19	18	19	18	18	19	15	20	19
FeO*/MgO	1.58	1.68	1.23	1.50	2.07	2.04	1.47	1.21	1.38	1.46
Y/Nb	3.40	6.00	3.80	3.60	5.33	4.71	8.33	4.29	5.20	5.60
Ti/V	40.56	33.55	20.15	22.25	32.12	31.97	31.53	27.74	32.99	37.14

Notes: Fe<sub>2</sub>O<sub>3</sub>\*\* is total iron as Fe<sub>2</sub>O<sub>3</sub>; FeO\* is total iron as FeO.

TABLE 2 (continued).

## APHYRIC BASALTIC LAVAS

	022-1	035-5	037-1	039-1	046-1	048-1	053-1	067-1	073-1	076-3
SiO <sub>2</sub> (%)	48.20	47.70	46.20	47.20	46.40	46.30	48.00	48.30	45.70	46.20
TiO <sub>2</sub>	1.18	1.05	1.01	1.24	1.25	1.31	0.99	1.30	1.57	1.58
Al <sub>2</sub> O <sub>3</sub>	17.60	17.30	19.30	18.40	17.50	17.60	17.70	17.10	17.70	17.60
Fe <sub>2</sub> O <sub>3</sub> **	10.84	10.10	9.45	10.52	10.49	10.91	9.87	11.03	11.65	11.24
MnO	0.22	0.16	0.18	0.17	0.17	0.16	0.16	0.18	0.19	0.18
MgO	5.71	6.81	6.50	7.96	7.51	7.96	7.06	7.21	7.80	8.19
CaO	5.40	7.31	7.04	2.61	8.56	7.06	8.38	7.71	6.80	6.40
Na <sub>2</sub> O	3.43	3.66	2.86	4.09	2.53	3.22	2.84	2.53	3.00	3.20
K <sub>2</sub> O	1.95	1.44	2.85	2.53	1.46	1.76	1.70	1.55	1.67	1.68
P <sub>2</sub> O <sub>5</sub>	0.23	0.21	0.25	0.24	0.31	0.42	0.23	0.33	0.34	0.41
L.O.I.	3.46	3.28	4.97	4.48	2.89	3.41	2.97	2.59	3.19	3.48
Total	98.22	99.02	100.61	99.44	99.07	100.11	99.90	99.83	99.61	100.16
Rb(ppm)	48	35	101	70	26	41	35	33	43	37
Sr	696	839	742	555	573	775	650	534	491	422
Ba	1510	461	787	1627	754	705	564	625	666	780
Y	22	18	22	22	20	24	20	22	32	33
Zr	91	67	88	92	111	116	86	113	140	148
Nb	5	5	3	5	7	7	5	7	7	9
V	274	240	238	297	216	254	217	226	251	249
Cr	79	74	64	92	145	145	82	120	93	84
Ni	26	112	76	89	104	104	89	99	109	103
Ga	17	14	23	17	15	15	16	16	19	18
FeO*/MgO	1.71	1.33	1.31	1.19	1.26	1.23	1.26	1.38	1.34	1.23
Y/Nb	4.40	3.60	7.40	4.40	2.90	3.40	4.00	3.10	4.60	3.67
Ti/V	29.32	26.48	25.95	27.45	36.91	33.75	23.48	32.10	33.92	39.73

Notes: Fe<sub>2</sub>O<sub>3</sub>\*\* is total iron as Fe<sub>2</sub>O<sub>3</sub>; FeO\* is total iron as FeO.

TABLE 2 (continued).

## APHYRIC BASALTIC LAVAS

	082-2	87-2	092-1	092-2	100-2	101-5	102-3	104-1	111-2	111-3
SiO <sub>2</sub> (%)	47.00	45.70	47.30	46.80	47.90	48.30	47.60	48.90	47.40	46.50
TiO <sub>2</sub>	1.38	1.55	1.71	1.26	1.41	1.22	1.18	1.14	1.27	1.42
Al <sub>2</sub> O <sub>3</sub>	16.40	17.70	17.10	16.80	17.10	16.20	16.90	17.00	17.50	16.80
Fe <sub>2</sub> O <sub>3</sub> **	11.28	11.75	12.65	11.43	10.99	10.74	11.09	10.36	10.95	11.20
MnO	0.19	0.17	0.16	0.17	0.22	0.17	0.17	0.17	0.17	0.19
MgO	8.03	7.81	6.15	7.93	7.89	6.69	7.87	7.15	7.96	8.18
CaO	9.36	5.69	8.88	8.14	4.84	8.00	6.12	6.44	7.11	8.91
Na <sub>2</sub> O	2.38	3.76	2.97	3.10	3.76	3.76	3.87	3.51	3.13	2.18
K <sub>2</sub> O	0.86	1.48	0.92	1.44	2.07	1.47	1.16	2.13	1.51	0.61
P <sub>2</sub> O <sub>5</sub>	0.34	0.50	0.35	0.31	0.53	0.25	0.29	0.23	0.29	0.36
L.O.I.	2.96	3.41	2.29	3.14	3.70	3.06	3.36	3.20	2.98	2.93
Total	100.18	99.52	100.48	100.52	100.41	99.86	99.61	100.23	100.27	99.28
Rb(ppm)	20	33	20	30	59	40	27	49	33	15
Sr	553	694	546	577	1103	770	708	671	608	513
Ba	357	729	333	429	924	574	613	796	434	311
Y	25	26	28	24	28	22	21	22	18	24
Zr	100	121	120	107	130	103	76	95	90	110
Nb	5	7	6	5	7	5	5	6	6	7
V	258	283	261	239	246	208	278	232	233	267
Cr	173	110	57	187	105	165	177	114	131	159
Ni	141	110	87	147	67	139	124	113	115	149
Ga	17	21	15	16	21	16	16	17	18	19
FeO*/MgO	1.26	1.35	1.85	1.30	1.25	1.44	1.27	1.30	1.24	1.23
Y/Nb	5.00	3.71	4.67	4.80	4.00	4.40	4.20	3.67	3.00	3.43
Ti/V	33.23	34.53	39.97	32.86	35.82	36.60	26.74	30.49	33.96	36.82

Notes: Fe<sub>2</sub>O<sub>3</sub>\*\* is total iron as Fe<sub>2</sub>O<sub>3</sub>; FeO\* is total iron as FeO.

TABLE 2 (continued).

## APHYRIC BASALTIC LAVAS

	115-1	125-1	135-2	136-1	136-2	137-1	138-1	140-3	163-2	166-1
SiO <sub>2</sub> (%)	45.00	47.40	46.60	47.80	47.20	45.60	45.60	48.60	44.90	45.90
TiO <sub>2</sub>	1.45	1.39	1.27	1.07	1.18	1.13	1.29	1.36	1.62	1.18
Al <sub>2</sub> O <sub>3</sub>	17.10	17.10	17.60	17.80	17.90	18.30	18.20	17.10	17.20	17.60
Fe <sub>2</sub> O <sub>3</sub> **	12.04	11.21	11.30	10.17	10.82	10.47	9.91	10.84	13.12	11.23
MnO	0.25	0.13	0.21	0.14	0.14	0.17	0.14	0.19	0.22	0.20
MgO	9.46	7.48	8.06	6.67	7.48	8.22	6.59	5.47	8.26	7.96
CaO	6.73	7.83	5.83	8.46	6.04	5.88	8.85	7.27	6.79	6.76
Na <sub>2</sub> O	2.66	3.12	3.74	3.93	3.68	2.85	2.67	4.00	3.11	3.38
K <sub>2</sub> O	1.44	1.35	1.63	0.96	2.01	2.93	2.54	1.88	1.66	1.50
P <sub>2</sub> O <sub>5</sub>	0.28	0.48	0.33	0.22	0.25	0.27	0.32	0.39	0.34	0.37
L.O.I.	3.84	2.90	3.83	3.46	3.38	3.83	3.93	2.88	3.91	4.05
Total	100.25	100.39	100.40	100.68	100.08	99.65	100.04	99.98	101.12	100.13
Rb(ppm)	30	25	43	27	56	93	90	43	48	50
Sr	472	959	775	587	761	659	356	658	663	639
Ba	660	443	1198	220	777	1517	837	1035	808	693
Y	24	22	25	16	15	20	21	28	29	17
Zr	105	110	93	59	66	78	89	112	128	82
Nb	5	7	5	0	2	5	5	6	9	6
V	287	229	322	186	281	251	230	241	288	261
Cr	167	132	115	51	63	70	101	84	128	138
Ni	138	101	116	78	87	112	71	42	92	125
Ga	16	22	21	19	21	16	16	18	21	13
FeO*/MgO	1.15	1.35	1.26	1.37	1.30	1.15	1.35	1.78	1.43	1.27
Y/Nb	4.80	3.14	5.00	--	7.50	4.00	4.20	4.67	3.22	2.83
Ti/V	31.75	37.70	24.76	35.78	26.24	28.42	35.19	35.07	34.97	28.48

Notes: Fe<sub>2</sub>O<sub>3</sub>\*\* is total iron as Fe<sub>2</sub>O<sub>3</sub>; FeO\* is total iron as FeO.

TABLE 2 (continued).

## APHYRIC BASALTIC LAVAS

	169-1	169-2	172-2	173-1	185-1	186-1	221-2	225-2	228-1	229-1
SiO <sub>2</sub> (%)	46.70	48.20	46.40	44.70	48.40	47.10	46.20	47.20	47.90	45.20
TiO <sub>2</sub>	1.48	1.20	1.40	1.32	1.34	1.45	1.04	1.22	1.14	1.14
Al <sub>2</sub> O <sub>3</sub>	16.70	16.60	16.90	15.90	16.50	16.00	17.80	17.60	17.20	17.40
Fe <sub>2</sub> O <sub>3</sub> **	11.91	10.46	11.51	11.66	11.53	11.71	10.95	10.80	11.10	10.97
MnO	0.16	0.17	0.22	0.16	0.18	0.21	0.15	0.17	0.15	0.18
MgO	7.74	7.21	8.59	6.68	7.74	9.45	7.57	8.44	8.56	10.59
CaO	7.15	6.81	5.96	10.88	4.65	4.56	6.95	6.64	4.60	5.52
Na <sub>2</sub> O	3.11	3.59	3.15	2.89	3.93	4.04	3.57	3.43	4.04	2.91
K <sub>2</sub> O	1.73	2.16	1.72	1.15	1.77	1.14	1.35	1.52	1.54	1.65
P <sub>2</sub> O <sub>5</sub>	0.26	0.37	0.31	0.47	0.01	0.38	0.18	0.26	0.25	0.23
L.O.I.	2.76	3.16	3.78	3.54	3.53	4.30	3.23	3.45	3.93	4.14
Total	99.70	99.93	99.94	99.35	99.58	100.34	98.79	100.73	100.41	99.93
Rb(ppm)	57	82	38	19	42	29	34	49	64	51
Sr	431	760	598	314	1126	665	697	737	649	552
Ba	519	848	977	584	1781	809	605	898	242	584
Y	29	25	27	26	26	21	17	15	15	12
Zr	109	99	108	94	120	108	66	68	63	64
Nb	10	4	7	6	9	7	0	4	3	3
V	247	265	267	236	275	280	279	292	287	236
Cr	194	134	122	108	98	144	63	64	60	62
Ni	119	77	96	100	63	132	93	85	78	81
Ga	17	18	20	16	10	12	19	18	14	16
FeO*/MgO	1.38	1.31	1.21	1.57	1.34	1.11	1.30	1.15	1.17	0.93
Y/Nb	2.90	6.25	3.86	4.33	2.89	3.00	--	3.75	5.00	4.00
Ti/V	37.38	28.28	33.01	35.31	30.74	32.33	23.64	25.66	24.65	30.23

Notes: Fe<sub>2</sub>O<sub>3</sub>\*\* is total iron as Fe<sub>2</sub>O<sub>3</sub>; FeO\* is total iron as FeO.

TABLE 2 (continued).

APHYRIC BASALTIC LAVAS					BRIGUS JUNCTION LAVAS				
	232-1	234-1	239-1	240-1	144-1	145-1	145-2	146-1	150-1
SiO <sub>2</sub> (%)	46.70	47.20	47.80	48.00	45.30	46.40	46.10	45.30	44.90
TiO <sub>2</sub>	1.33	1.10	1.16	1.20	1.74	2.36	2.53	2.31	2.22
Al <sub>2</sub> O <sub>3</sub>	16.70	18.40	16.20	15.80	16.60	15.50	14.60	13.10	13.20
Fe <sub>2</sub> O <sub>3</sub> **	11.01	9.39	10.11	10.67	11.78	13.43	14.66	16.30	16.30
MnO	0.16	0.14	0.21	0.18	0.21	0.20	0.16	0.31	0.35
MgO	7.81	7.85	9.07	8.26	8.79	6.77	5.74	6.60	6.08
CaO	7.56	5.96	4.20	5.26	7.46	7.40	6.08	6.82	7.84
Na <sub>2</sub> O	3.94	2.85	2.98	3.68	2.72	3.01	3.12	3.62	2.43
K <sub>2</sub> O	0.73	3.42	3.58	2.55	2.03	2.22	3.09	1.52	3.07
P <sub>2</sub> O <sub>5</sub>	0.34	0.30	0.27	0.31	0.51	0.69	0.67	0.76	0.73
L.O.I.	3.84	3.90	3.48	3.51	3.64	2.55	2.70	2.88	2.38
Total	100.12	100.51	99.06	99.42	100.78	100.53	99.45	99.52	99.50
Rb (ppm)	21	125	81	73	65	69	77	37	85
Sr	674	505	632	884	386	325	565	429	355
Ba	730	697	645	802	605	543	1004	493	2079
Y	21	17	25	25	32	36	37	33	39
Zr	90	81	108	105	136	191	247	247	228
Nb	6	0	7	5	10	13	16	20	16
V	264	224	236	260	253	320	301	361	344
Cr	135	66	195	203	88	60	65	0	0
Ni	121	77	145	136	105	86	80	12	22
Ga	15	13	12	18	17	19	17	22	22
FeO*/MgO	1.27	1.08	1.00	1.16	1.21	1.78	2.29	2.22	2.41
Y/Nb	3.50	--	3.57	5.00	3.20	2.77	2.31	1.65	2.44
Ti/V	31.34	30.51	30.74	28.82	42.89	45.71	51.98	39.69	39.91

Notes: Fe<sub>2</sub>O<sub>3</sub>\*\* is total iron as Fe<sub>2</sub>O<sub>3</sub>; FeO\* is total iron as FeO.

TABLE 2 (continued).

	BRIGUS JCT.		SILLS				DYKE
	210-1	212-2	055-1	070-1	081-4A	118-4	202-1
SiO <sub>2</sub> (%)	45.80	45.90	46.30	46.70	46.60	46.10	50.80
TiO <sub>2</sub>	2.22	2.38	1.26	1.51	1.24	1.15	1.60
Al <sub>2</sub> O <sub>3</sub>	14.20	14.30	18.10	17.80	18.20	17.50	15.40
Fe <sub>2</sub> O <sub>3</sub> **	15.23	14.82	10.99	11.03	11.33	11.61	13.25
MnO	0.47	0.38	0.18	0.18	0.16	0.17	0.18
MgO	6.58	5.80	8.04	8.42	6.79	7.23	4.17
CaO	5.46	5.24	5.44	6.30	6.44	8.86	7.32
Na <sub>2</sub> O	3.09	4.04	3.96	3.23	2.96	3.60	2.80
K <sub>2</sub> O	3.14	1.88	1.32	1.50	2.75	0.51	2.30
P <sub>2</sub> O <sub>5</sub>	1.19	1.21	0.41	0.48	0.36	0.28	0.50
L.O.I.	2.36	3.71	3.80	3.61	3.10	3.70	1.80
Total	99.74	99.66	99.80	100.76	99.93	100.71	100.12
Rb(ppm)	87	38	30	32	82	14	55
Sr	172	244	791	489	466	579	458
Ba	1051	638	501	816	641	491	959
Y	38	34	25	31	20	20	37
Zr	271	237	115	143	109	78	171
Nb	27	22	8	6	7	7	13
V	283	294	277	184	258	267	330
Cr	0	0	86	89	84	179	0
Ni	0	1	113	144	115	128	12
Ga	20	19	21	20	19	18	22
FeO*/MgO	1.61	2.30	1.23	1.18	1.50	1.44	2.86
Y/Nb	1.41	1.55	3.13	5.17	2.86	2.86	2.85
Ti/V	47.03	50.57	28.57	51.15	29.74	26.94	29.61

Notes: Fe<sub>2</sub>O<sub>3</sub>\*\* is total iron as Fe<sub>2</sub>O<sub>3</sub>; FeO\* is total iron as FeO.

be shown, these petrographic distinctions correspond to chemical variations between sample groups. In the following discussions, the principles of Wise (1982) are not employed.

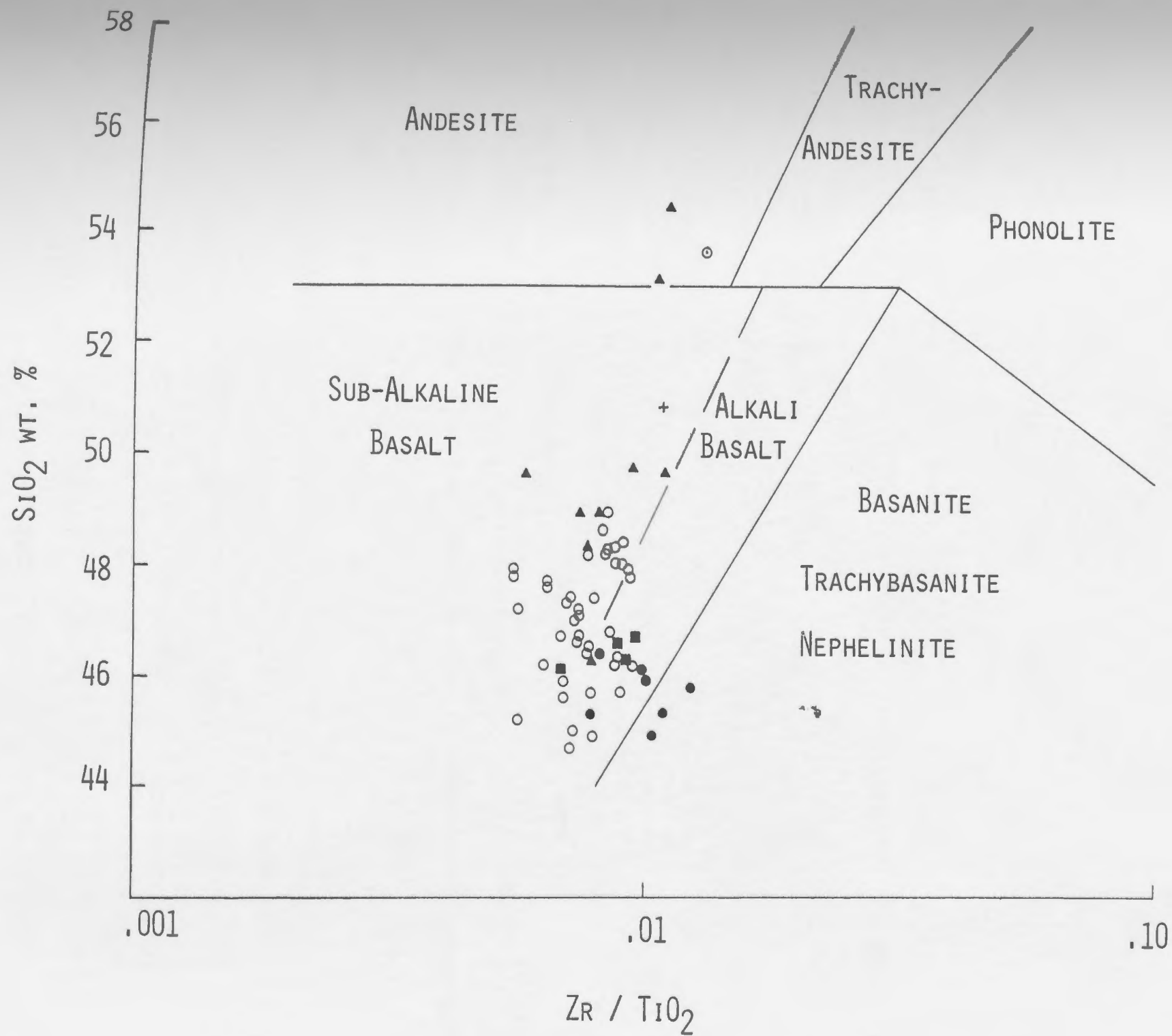
#### 4.2.1 Major Oxides

$\text{SiO}_2$  values range from 54.5 to 44.5 wt.% and generally decrease with increasing stratigraphic position. On a plot of  $\text{SiO}_2$  -  $\text{Zr/TiO}_2$  (Fig. 5) the samples are classified as andesites (058-1, 118-1, 119-3), sub-alkaline basalts (majority of samples), alkali basalts, and a few basanites (samples from the stratigraphically higher Brigus Junction Inlier).

This general classification of the rock units is also reflected in their normative compositions (Appendix B). A significant proportion of the analysed samples contain normative nepheline, particularly most of the stratigraphically higher lavas, which is a reflection of the alkalinity of these rocks. The high normative apatite in samples from the Brigus Junction Inlier reinforces their alkaline character. With the exception of the analysed mafic dyke, one sample (118-1) contains normative quartz (1.36 wt.%) which is a result of its high  $\text{SiO}_2$  content. The remainder of the analyses contain normative olivine ranging in content from 2.53 wt.% (108-3) to 28.23 wt.% (229-1). This correlates well with the abundance of pseudomorphed olivine grains recognised in the petrography. The high

FIGURE 5. Classification of mafic rocks within Blue Hills Sequence based upon their  $\text{SiO}_2$  content and the  $\text{Zr/TiO}_2$  ratio. Field boundaries after Winchester and Floyd (1977).

Symbols for samples:  $\odot$ , 058-1;  $\blacktriangle$ , pyroxene-phyric basaltic lavas;  $\bigcirc$ , aphyric basalt lavas;  $\bullet$ , Brigus Junction Inlier lavas;  $\blacksquare$ , sills;  $+$ , dyke.

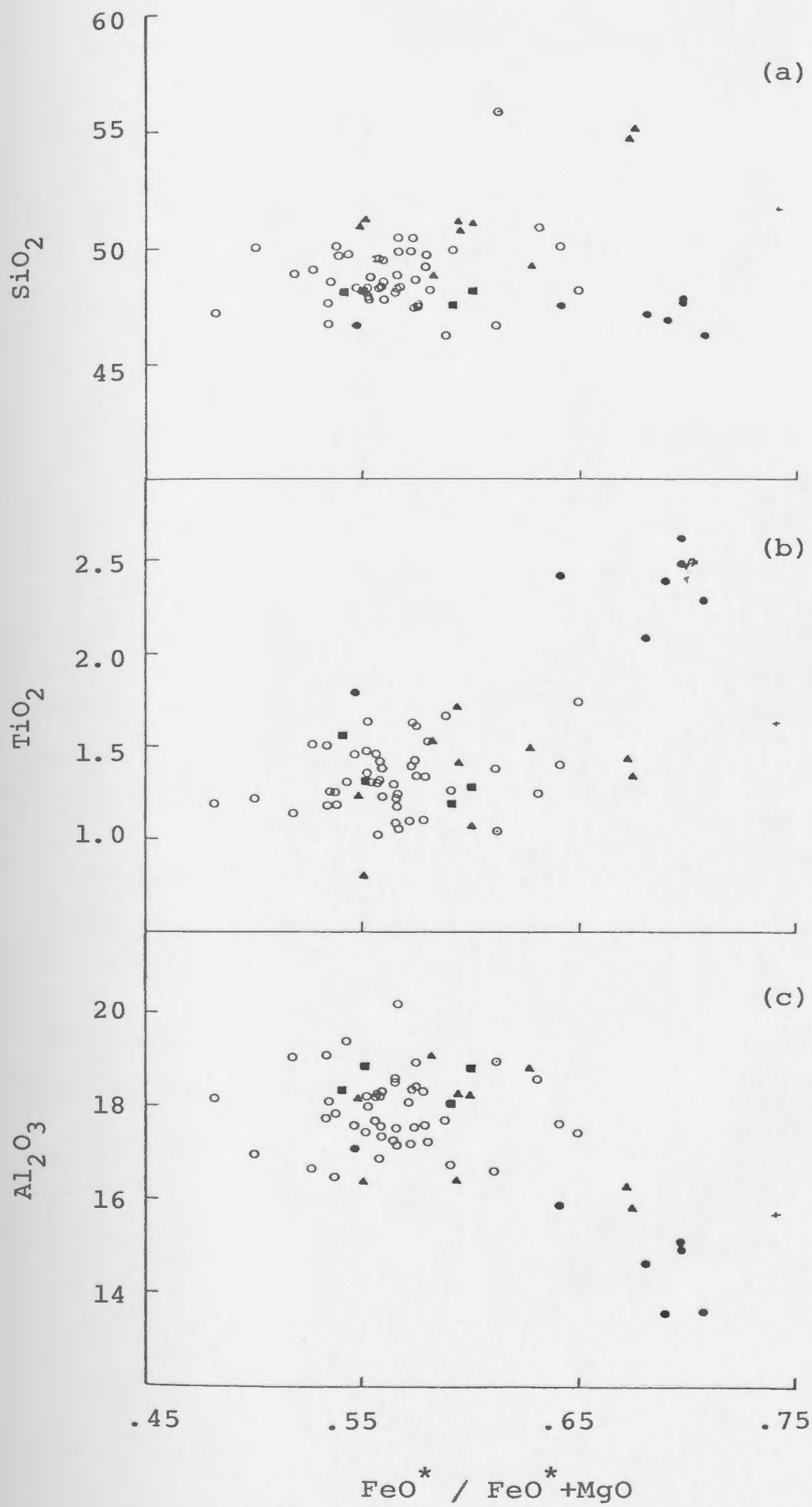


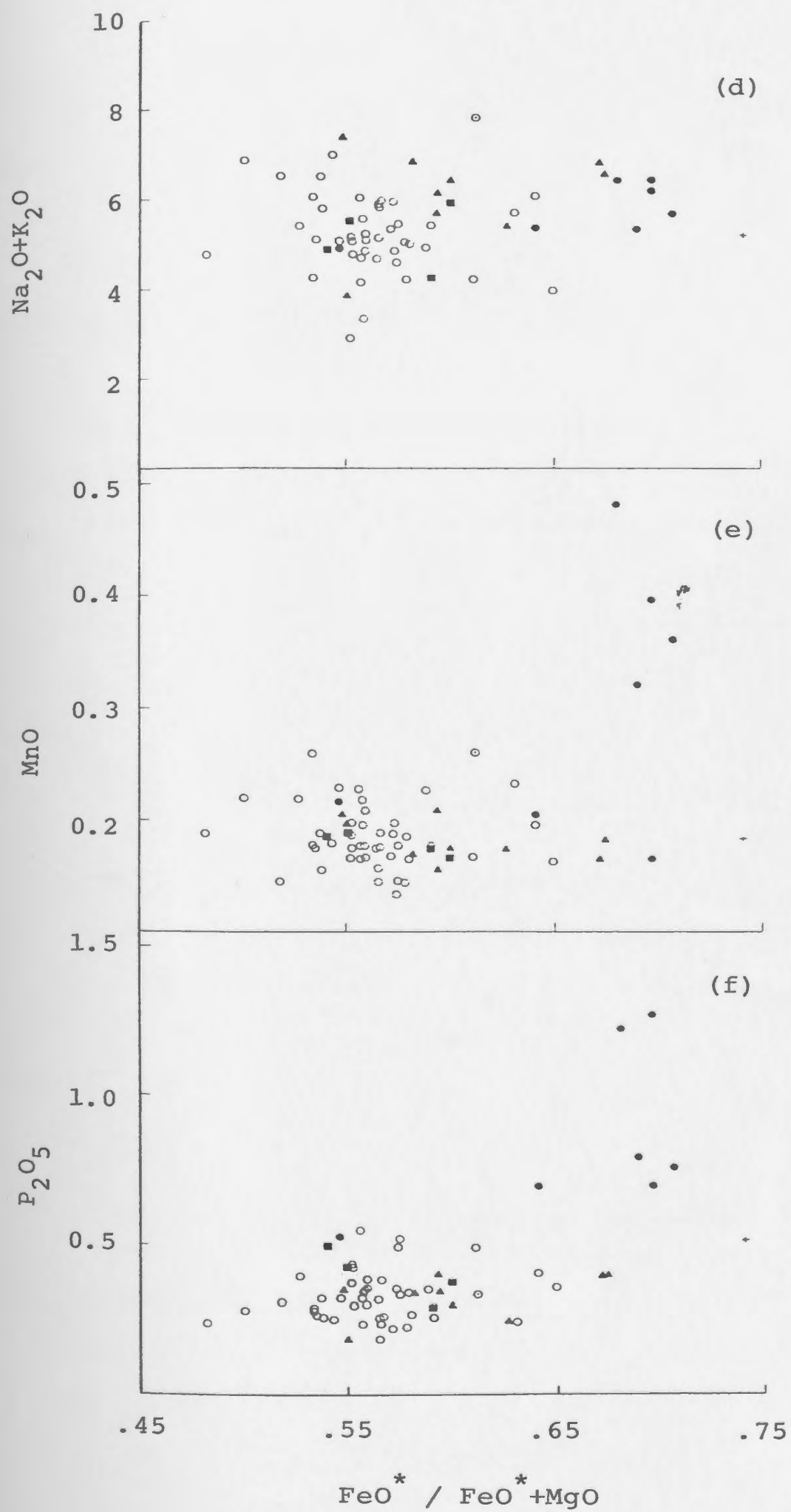
alumina content of some of the samples shows up as normative corundum.

One of the first problems encountered in this study was to establish whether the different mafic rocks are genetically related to each other by some process of fractionation. The first necessity is to choose a suitable parameter as an index of progressive crystallisation. The approach taken here is similar to that of Thompson et al. (1980) where the ratio  $\text{FeO}^*/\text{FeO}^* + \text{MgO}$  ( $F/F+M$ ) is used as abscissa for comparative plots of mafic rocks of the Blue Hills Sequence. This is a reasonable index of differentiation for basalts and should indicate if the magma from which the basalts were derived differed substantially at their time of genesis. In addition, this ratio is slightly more sensitive to subtle compositional changes than the conventional  $\text{FeO}^*/\text{MgO}$  ratio.

The major element variations occurring with increasing  $\text{FeO}^*/\text{FeO}^* + \text{MgO}$  define trends on Figure 6 that may be interpreted as a consequence of fractional crystallisation. In general,  $\text{SiO}_2$  shows little variation over the range of  $F/F+M$  ratios while  $\text{TiO}_2$  displays a continual enrichment with increasing  $F/F+M$  ratio which could reflect a combination of plagioclase, olivine, and clinopyroxene fractionation. The high  $\text{Al}_2\text{O}_3$  contents and slight positive europium anomalies (see Fig. 10) in these rocks almost certainly reflect the high modal plagioclase abundance. The derivation of basalts with high  $\text{Al}_2\text{O}_3$  also requires either clinopyroxene + olivine

FIGURE 6.  $\text{SiO}_2$ ,  $\text{TiO}_2$ ,  $\text{Al}_2\text{O}_3$ ,  $\text{Na}_2\text{O} + \text{K}_2\text{O}$ ,  $\text{MnO}$  and  $\text{P}_2\text{O}_5$  versus  $\text{FeO}^*/\text{FeO}^*+\text{MgO}$  of the Blue Hills Sequence mafic rocks (all oxides in weight percent, anhydrous values;  $\text{FeO}^*$  is total iron as  $\text{FeO}$ ). Symbols for samples:  $\odot$ , 058-1;  $\blacktriangle$ , pyroxene-phyric basaltic lavas;  $\bigcirc$ , aphyric basalt lavas;  $\bullet$ , Brigus Junction Inlier lavas;  $\blacksquare$ , sills;  $+$ , dyke.





ratio, as represented by lavas from the Brigus Junction Inlier (Figure 6(c)), may be caused by plagioclase-dominated crystal fractionation.

$P_2O_5$  and MnO both show a positive correlation with increasing F/F+M ratio with a sudden increase of both in lavas from the Brigus Junction Inlier. The high  $P_2O_5$  values are reflected in relatively high contents of normative apatite (Appendix B). For the most part, normative apatite ranges between 0.5 and 1.0 wt.%, but much higher values occur in samples from the Brigus Junction Inlier with one sample (212-2) reporting 2.97 wt.% normative apatite.

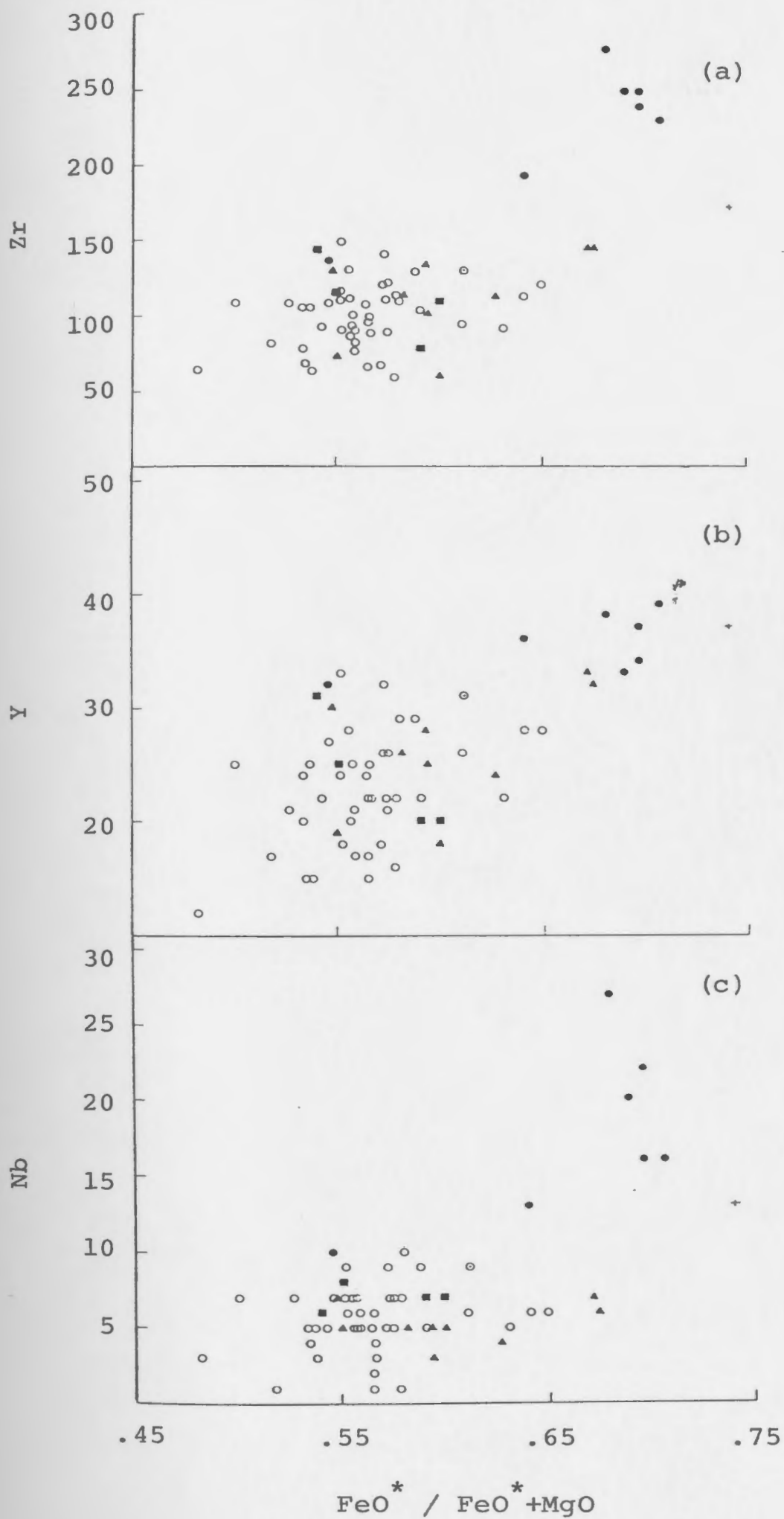
Figure 6 shows that there is considerable overlap in compositions of the rock units within the Blue Hills Sequence and this suggests that these lavas may be related by fractionation. However, the generally higher contents of  $TiO_2$ ,  $FeO^*$ , MnO,  $P_2O_5$  and lower  $Al_2O_3$  and MgO in the stratigraphically higher lavas of the Brigus Junction Inlier may be derived by extensive fractionation of the same parent or possibly from a separate magma source.

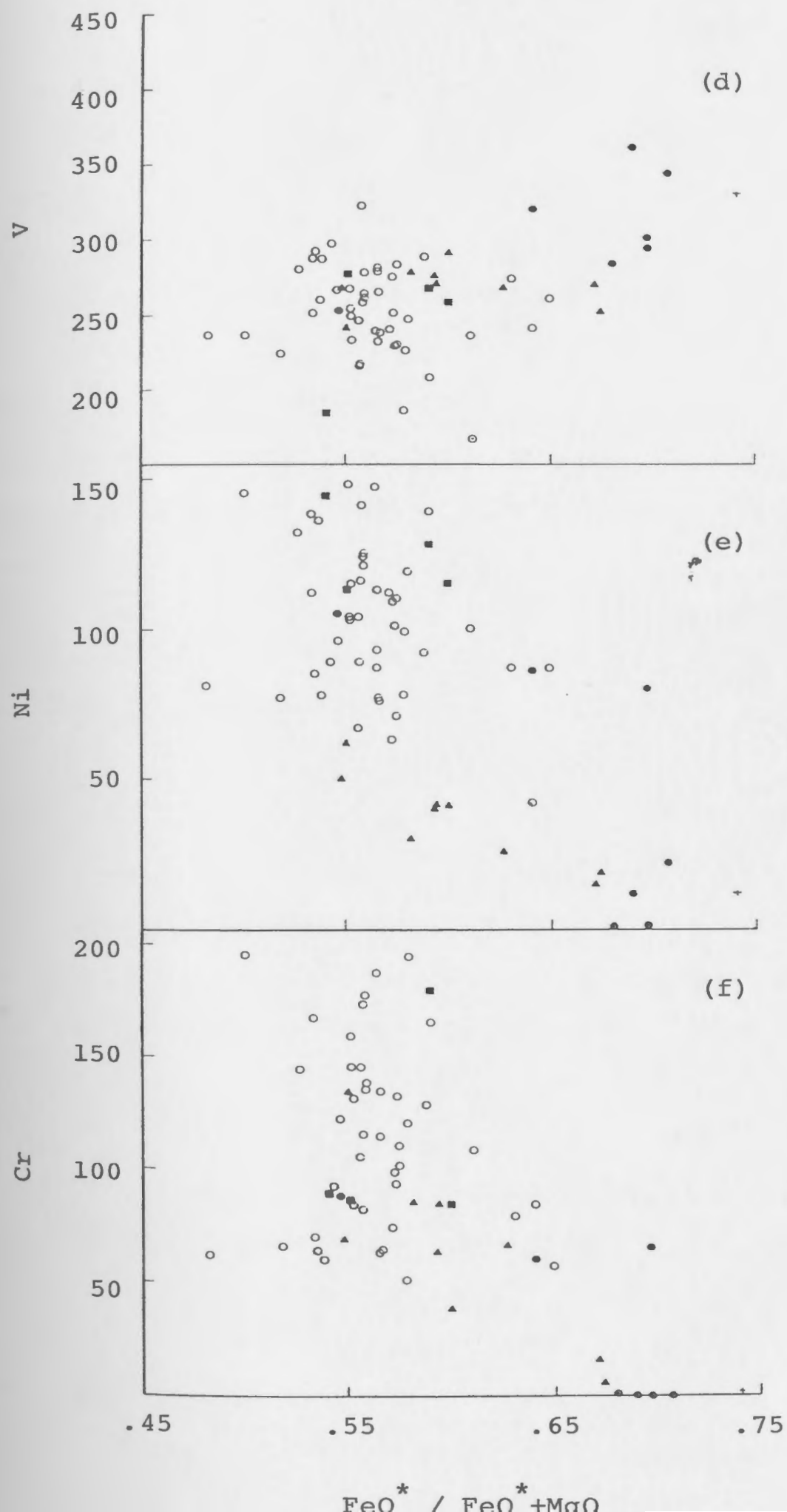
#### 4.2.2 Trace Elements

In Figure 7 selected trace elements are plotted against the differentiation index. The elements Y, Zr, Nb, and to a lesser extent V, exhibit higher concentrations with increasing F/F+M ratio while Ni and Cr decrease markedly. The first set of trace elements are all incompatible

FIGURE 7. Zr, Y, Nb, V, Ni and Cr (all values in ppm)  
versus  $\text{FeO}^*/\text{FeO}^*+\text{MgO}$  for mafic members of the  
Blue Hills Sequence.

Symbols for samples:  $\odot$ , 058-1;  $\blacktriangle$ , pyroxene-  
phyric basaltic lavas;  $\bigcirc$ , aphyric basalt lavas;  
 $\bullet$ , Brigus Junction Inlier lavas;  $\blacksquare$ , sills;  
+, dyke.





elements having higher affinity (expressed in terms of distribution coefficients) for a liquid/melt than for any major rock-forming minerals. The incompatible elements display a general increase with elevation in the volcanic stratigraphy. Extensive fractional crystallisation leads to residual liquids highly enriched in incompatible elements and severely depleted in Ni and Cr. A plot of Cr versus Ni (Fig. 8) indicates a positive correlation between these elements, the Brigus Junction lavas having particularly low concentrations of both. Because Ni is strongly enriched in olivine, its concentration falls rapidly during fractional crystallisation.

The variation of incompatible elements (eg. Nb, Zr, Y) is orderly and the good linear correlations obtained between pairs of these (Fig. 9) can be explained if the various rock units were derived from a common magmatic source involving fractional crystallisation of olivine, plagioclase, and clinopyroxene. Other minor minerals may also be important at later stages of fractionation. Because the Zr/Y ratio rises rapidly at higher Zr concentrations (Fig. 27, Ch. 6) it is likely that a Y-bearing mineral (possibly apatite) started to fractionate from the more evolved compositions. The fractionation of apatite may explain the enriched incompatible element content of the Brigus Junction Inlier lavas.

Rare-earth element (REE) contents of representative samples are presented in Table 3. The chondrite-normalised

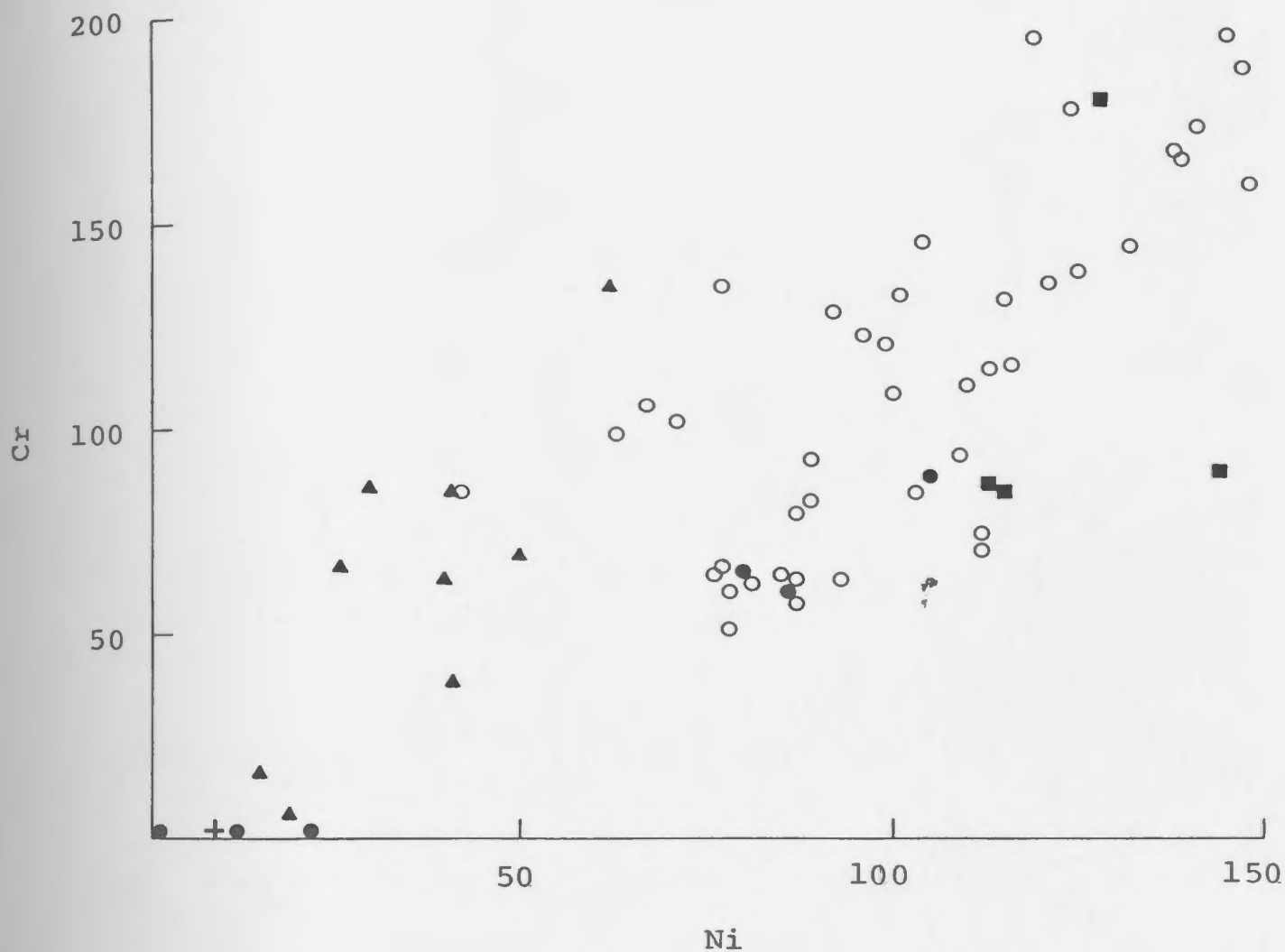


FIGURE 8. Plot of Cr versus Ni contents in mafic rocks of the Blue Hills Sequence. Symbols for samples:  
 ⊙, 058-1; ▲, pyroxene-phyric basaltic lavas;  
 ○, aphyric basalt lavas; ●, Brigus Junction  
 Inlier lavas; ■, sills; +, dyke.

FIGURE 9 (a). Plot of Nb versus Y in rocks of the Blue Hills Sequence.

FIGURE 9 (b), (c). Plot of Y and Nb versus Zr for members of the Blue Hills Sequence.

Symbols for samples:  $\odot$ , 058-1;

$\blacktriangle$ , pyroxene-phyric basaltic lavas;

$\circ$ , aphyric basalt lavas;  $\bullet$ , Brigus

Junction Inlier lavas;  $\blacksquare$ , sills;

+, dyke.

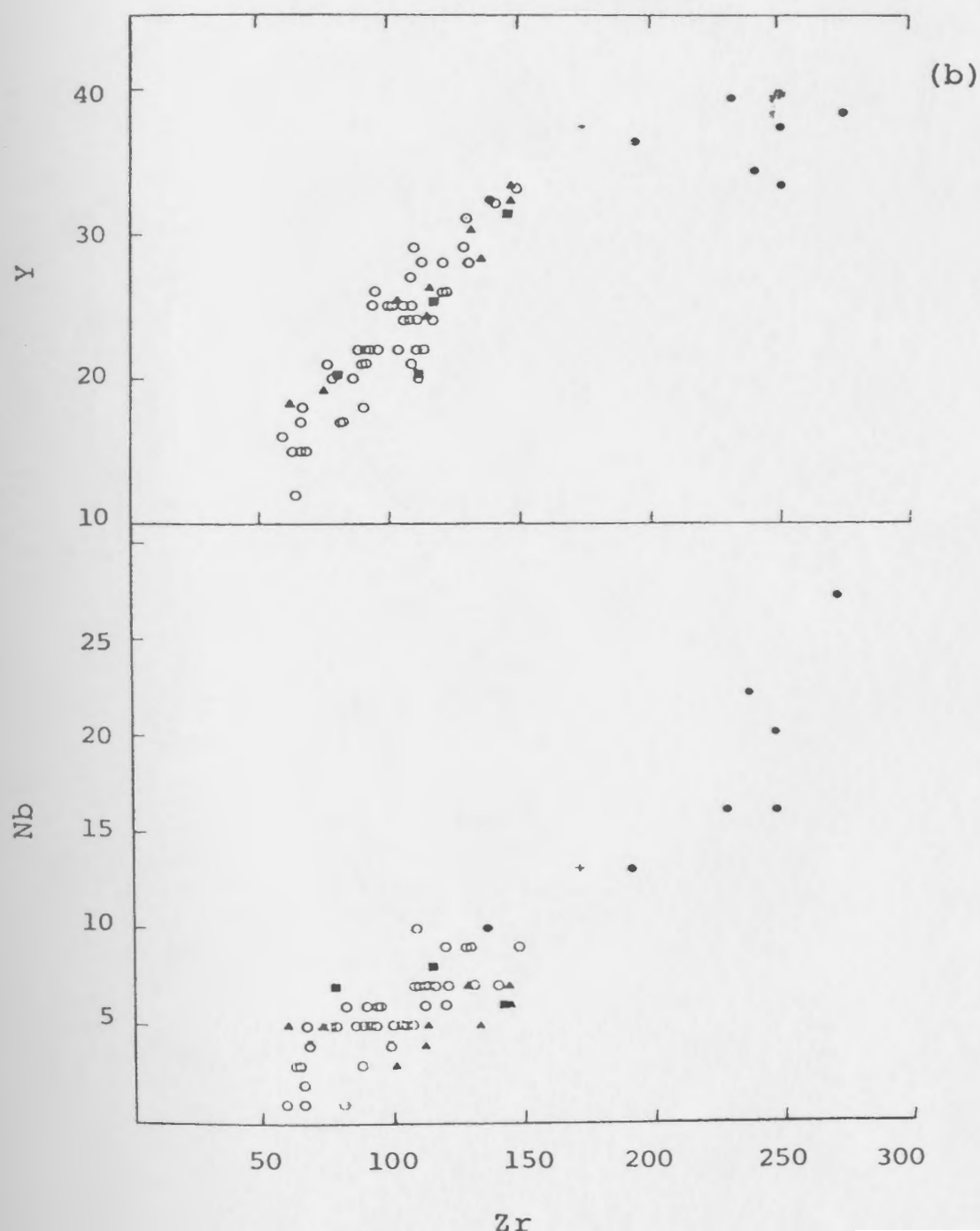
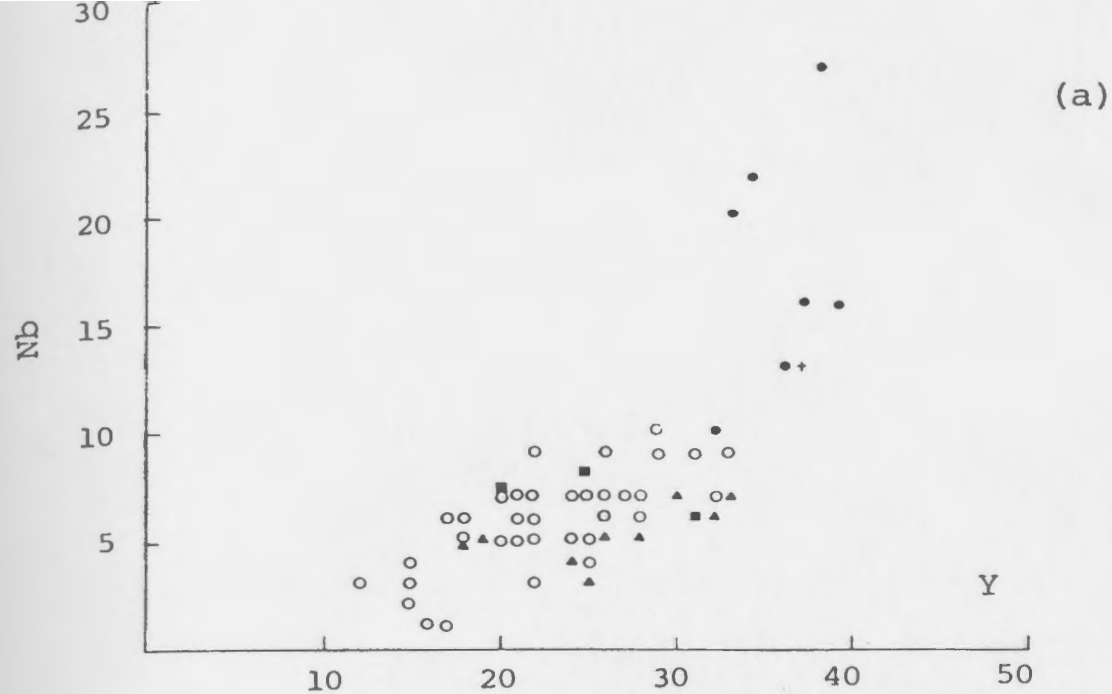


TABLE 3. RARE-EARTH ELEMENT GEOCHEMISTRY, BLUE HILLS SEQUENCE, HARBOUR MAIN GROUP

	PYROXENE-PHYRIC LAVAS						
	014-1	108-3	109-4	118-1	132-2	197-1	235-1
La (ppm)	2.09	6.37	3.73	7.02	7.68	9.41	4.89
Ce	8.76	19.11	15.05	21.76	25.81	26.31	17.55
Pr	1.74	2.86	2.22	3.38	4.18	3.47	3.12
Nd	8.80	14.24	11.53	15.68	20.35	15.75	17.31
Sm	2.72	3.68	3.17	3.99	5.56	4.26	5.12
Eu	1.00	1.27	1.15	1.42	2.27	1.04	1.96
Gd	3.14	3.20	2.97	4.20	4.97	3.58	5.50
Dy	2.88	2.32	2.27	3.62	4.28	3.44	4.83
Er	1.58	1.24	1.28	1.95	2.07	1.83	2.34
Yb	1.38	1.17	0.86	1.80	0.80	1.11	1.16
Σ REE	34.09	55.46	44.23	64.82	77.97	70.20	63.78
Σ LREE (Ce + Nd + Sm)	20.28	37.03	29.75	41.43 <sup>1/2</sup>	51.72	46.32	39.98
(La/Nd)*	0.45	0.85	0.61	0.85	0.72	1.13	0.54
(Nd/Yb)*	2.23	4.23	4.66	3.03	8.83	4.94	5.21

\*Note: (La/Nd) and (Nd/Yb) are ratios after the elements of interest have been normalised to chondritic values of Taylor et al., 1977.

TABLE 3 (continued).

## APHYRIC BASALTIC LAVAS

	022-1	035-5	046-1	053-1	058-1	076-3	082-2
La (ppm)	2.00	5.58	4.69	10.44	9.83	5.69	12.50
Ce	7.56	17.73	15.90	35.10	30.59	20.50	37.66
Pr	1.57	2.95	2.52	5.57	4.68	3.39	5.98
Nd	7.53	13.74	12.65	26.05	20.05	16.54	24.15
Sm	2.07	3.81	3.21	6.45	5.42	4.59	5.90
Eu	0.94	1.38	1.53	1.92	1.52	1.56	2.31
Gd	2.65	3.82	3.56	6.23	4.90	4.74	5.45
Dy	2.21	2.86	3.08	4.65	3.69	3.78	4.61
Er	1.27	1.29	1.59	1.91	1.79	1.96	2.12
Yb	0.89	0.70	1.12	0.67	1.40	1.40	1.11
Σ REE	28.69	53.86	49.85	98.99	83.87	64.15	101.79
Σ LREE (Ce + Nd + Sm)	17.16	40.86	31.76	67.60 <sup>a</sup>	56.06	41.63	67.71
(La/Nd)*	0.50	0.77	0.70	0.76	0.93	0.65	0.98
(Nd/Yb)*	2.96	6.87	3.95	13.63	4.98	4.11	7.54

\*Note: (La/Nd) and (Nd/Yb) are ratios after the elements of interest have been normalised to chondritic values of Taylor et al., 1977.

TABLE 3 (continued).

APHYRIC BASALTIC LAVAS							
	092-2	101-5	111-3	115-1	125-1	136-2	169-1
La (ppm)	5.17	8.91	14.30	5.26	9.27	3.34	4.84
Ce	17.98	30.11	42.23	20.16	26.29	11.36	17.48
Pr	3.00	4.74	5.76	3.27	4.06	1.91	2.74
Nd	14.98	23.09	27.62	15.96	17.40	9.38	13.91
Sm	4.18	5.78	6.82	4.06	4.23	2.48	3.91
Eu	1.46	1.85	2.54	1.57	1.68	1.14	1.15
Gd	3.94	4.87	6.50	4.61	4.27	2.58	4.28
Dy	3.12	4.01	5.36	3.59	3.21	2.15	3.77
Er	1.49	1.73	2.57	1.80	1.58	0.99	1.87
Yb	0.97	0.75	1.19	1.13	1.29	0.90	1.37
$\Sigma$ REE	56.29	85.84	114.89	61.41	73.28	36.23	55.32
$\Sigma$ LREE (Ce + Nd + Sm)	37.14	58.98	76.67	40.18 <sup>a</sup>	47.92	23.22	35.30
(La/Nd)*	0.65	0.73	0.98	0.62	1.01	0.67	0.66
(Nd/Yb)*	5.38	10.69	8.07	4.90	4.71	3.65	3.54

\*Note: (La/Nd) and (Nd/Yb) are ratios after the elements of interest have been normalised to chondritic values of Taylor et al., 1977.

TABLE 3 (continued).

APHYRIC BASALTIC LAVAS							
	172-2	185-1	221-2	225-2	228-1	232-1	240-1
La (ppm)	1.49	1.76	3.32	4.88	8.25	11.39	4.60
Ce	8.16	11.18	12.63	18.86	25.91	34.86	15.03
Pr	1.73	2.33	2.01	3.72	4.05	5.71	2.57
Nd	8.95	11.62	10.67	17.12	21.19	28.36	14.32
Sm	3.07	3.36	2.92	5.08	5.90	8.14	4.42
Eu	1.19	1.27	0.93	1.86	2.16	2.98	1.75
Gd	3.20	3.50	3.01	4.68	5.48	8.26	4.85
Dy	2.95	2.98	2.30	3.91	4.50	6.88	4.29
Er	1.65	1.62	1.00	1.68	2.17	2.03	1.78
Yb	1.14	1.28	0.68	0.67	1.25	0.77	0.83
$\Sigma$ REE	33.53	40.90	39.47	62.46	80.86	109.38	54.44
$\Sigma$ LREE (Ce + Nd + Sm)	20.18	26.16	26.22	34.61 <sup>a</sup>	53.00	71.36	33.77
(La/Nd)*	0.32	0.29	0.59	0.54	0.74	0.76	0.61
(Nd/Yb)*	2.73	3.16	5.50	8.96	5.89	12.84	6.03

\*Note: (La/Nd) and (Nd/Yb) are ratios after the elements of interest have been normalised to chondritic values of Taylor et al., 1977.

TABLE 3 (continued).

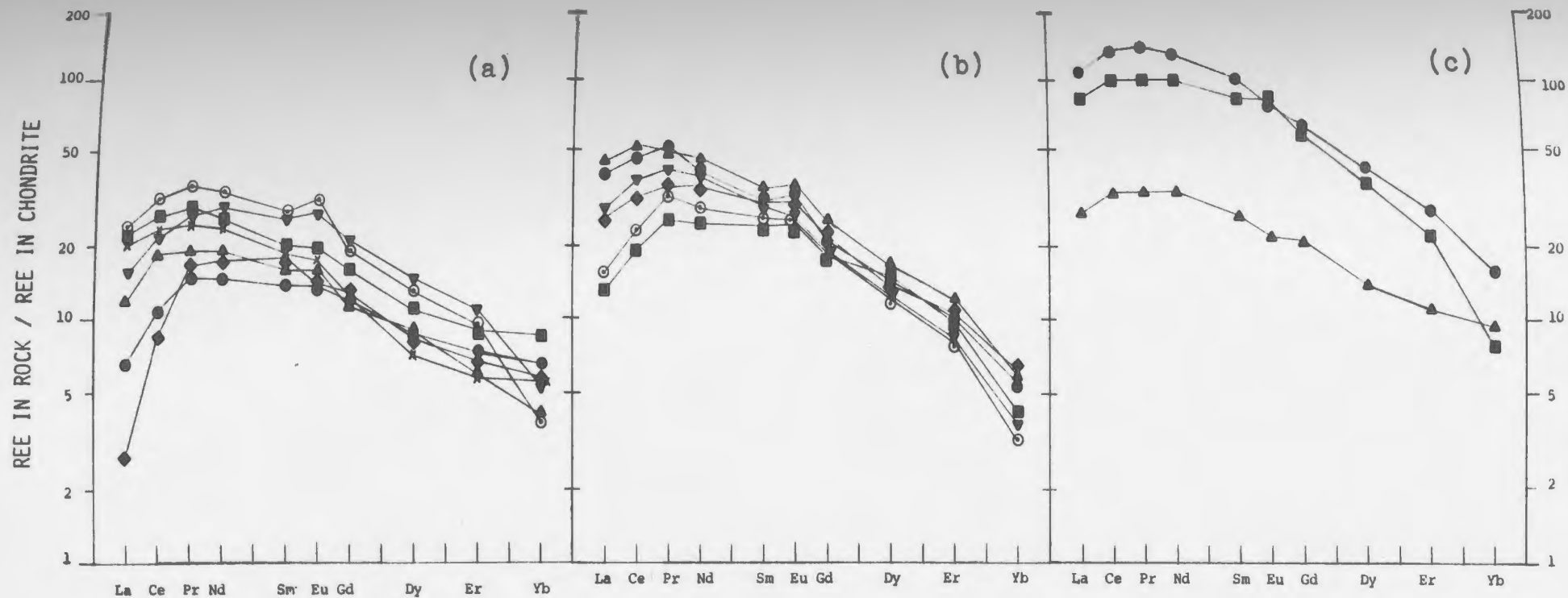
	BRIGUS JUNCTION			SILLS	
	145-1	146-1	212-2	070-1	081-4A
La (ppm)	8.56	26.13	34.57	4.19	4.48
Ce	27.04	83.33	110.70	14.91	15.90
Pr	3.88	12.40	16.41	2.64	2.92
Nd	20.10	60.92	78.47	13.12	12.86
Sm	5.31	16.37	20.45	3.80	3.91
Eu	1.59	5.92	5.78	1.49	1.30
Gd	5.50	15.18	16.58	4.07	3.72
Dy	4.46	11.80	13.46	3.87	3.29
Er	2.34	4.73	6.07	1.89	1.55
Yb	1.96	1.63	3.32	1.64	0.87
$\Sigma$ REE	80.74	238.41	305.81	51.62	50.80
$\Sigma$ LREE (Ce + Nd + Sm)	52.45	160.62	209.62	31.83	32.67
(La/Nd)*	0.81	0.81	0.83	0.60	0.66
(Nd/Yb)*	3.57	13.00	8.25	2.79	5.15

\*Note: (La/Nd) and (Nd/Yb) are ratios after the elements of interest have been normalised to chondritic values of Taylor et al., 1977.

REE plots (Fig. 10) of the samples are all convex upwards. There are several explanations for this peculiar pattern. Weathering and low-grade metamorphism could have caused the loss of some of the light rare-earth elements (LREE). Detailed descriptions of such processes have been reported by Morrison et al. (1978), Wood et al. (1976), Humphris et al. (1978), and Hellman et al. (1977, 1979).

Although precautions were taken to sample only the freshest portion of flows for analytical purposes, and further screening during petrography and pulverising eliminated other possible weathered specimens, it is difficult to accurately assess the effect of low-grade metamorphism which has affected this suite of rocks. As mentioned earlier (see Ch. 3) much of the primary mineralogy of these rocks has been altered to secondary phases. These changes could have caused a loss of LREE resulting in the depleted patterns of Figure 10. That all of the REE patterns are sub-parallel suggests that the metamorphism probably affected most of the lava stratigraphy to more or less the same extent. Therefore, although the patterns in Figure 10 probably do not reflect the original absolute LREE content of the samples, they most likely are representative of the relative contents and as such indicate that there is a relative LREE enrichment upwards in the stratigraphy. As the HREE are less susceptible to alteration, it is unlikely that this portion of the REE patterns has been significantly modified by post-burial

FIGURE 10. Chondrite-normalised rare-earth element (REE) patterns of selected representative samples from the (a) pyroxene-phyric basaltic lavas; (b) aphyric basalt lavas; and (c) Brigus Junction Inlier lavas of the Blue Hills Sequence. REE were determined using the thin film technique of Eby (1972) as modified by Fryer (1977). REE data are normalised to the Chondritic values of Taylor et al. (1977).



Symbol

Sample

⊙

132-2

■

118-1

×

108-3

▼

235-1

▲

109-4

●

014-1

◆

197-1

Symbol

Sample

▲

111-3

●

082-2

▼

101-5

◆

228-1

⊙

225-2

■

166-1

Symbol

Sample

●

212-2

■

146-1

▲

145-1

processes.

As presented in Table 3 there is an increase in total REE content with increase in stratigraphy. Figure 10 shows that the heavy rare-earth elements (HREE), Dy to Yb, patterns are coincident and/or subparallel, indicating that they have not been fractionated from one another. The LREE (La to Sm) form a divergent, fan-shaped pattern indicating that they have been fractionated from one another. This effect is to be expected if the fractionation is controlled by a crystalline phase such as clinopyroxene because its partition coefficient increases from La to Eu but stays nearly constant from Gd to Yb. It is unlikely that garnet played an important role in the REE fractionation process because the fan-shaped pattern is restricted to the LREE, whereas the partition coefficients for garnet increase dramatically from Ce all the way to Yb (Leeman et al., 1980).

In summary, the chemical data presented here suggests that the different units from the Blue Hills Sequence could have been derived from a common parental magma (probably of alkali-basalt composition) which underwent progressive fractional crystallisation of clinopyroxene, olivine, and plagioclase. The enrichment of incompatible elements in the Brigus Junction Inlier lavas may be due to extensive fractionation of the magma. A further possibility is that these uppermost lavas were generated from a different source.

### 4.3 PYROXENE CHEMISTRY

Results of electron microprobe analyses carried out on relict pyroxene grains from representative thin sections are presented in Table 4. Pyroxenes from the mafic rocks of the Blue Hills Sequence are all Ca-rich augites (Fig. 11). However, two distinct compositional trends are present. Clinopyroxenes from the stratigraphically lower pyroxene-phyric lavas display relatively constant variations in WO, EN and FS components. On the other hand, the remainder of the analysed clinopyroxenes (with the exception of the mafic dyke) display a range of FS and EN contents with only minor variation in WO. These variations may be due to changes in the composition of the melt during the early stages of crystallisation with the formation of phenocrysts in the earliest erupted lavas.

Variations in pyroxene chemistry parallel and reinforce similar changes in whole rock major and trace element compositions for the various units within the Blue Hills Sequence. Although there is some overlap between all units and geochemical boundaries are more or less gradational, there are exceptions. The pyroxene-phyric lavas are characterised by higher  $\text{SiO}_2$ ,  $\text{MgO}$ , and  $\text{Cr}_2\text{O}_3$  contents than pyroxenes from the other units. In addition, the pyroxene-phyric lavas are noticeably low in  $\text{TiO}_2$  contents, with none above 1 wt.%, and they are slightly lower in  $\text{FeO}^*$  and  $\text{MnO}$ .

TABLE 4. ANALYSES OF RELICT PYROXENES, BLUE HILLS SEQUENCE, HARBOUR MAIN GROUP

PYROXENE-PHYRIC LAVAS									
	014-1	083-3	108-3	109-4A	109-4B	109-4C	109-4D	118-1	132-2
SiO <sub>2</sub> (%)	51.43	51.38	52.15	51.85	51.82	51.61	52.55	50.36	51.42
TiO <sub>2</sub>	0.79	0.89	0.42	0.63	0.65	0.63	0.56	0.96	0.71
Al <sub>2</sub> O <sub>3</sub>	3.34	2.97	3.22	2.32	2.69	2.55	2.29	4.39	3.66
Cr <sub>2</sub> O <sub>3</sub>	0.22	0.14	0.19	0.01	0.03	0.08	0.03	0.13	0.27
FeO*	6.94	8.45	8.21	12.22	10.08	10.52	10.24	9.59	7.17
MnO	0.12	0.17	0.20	0.12	0.17	0.16	0.13	0.21	0.14
NiO	0.03	0.00	0.02	0.03	0.01	0.03	0.01	0.03	0.02
MgO	15.75	15.84	16.79	15.35	15.80	16.08	16.11	15.56	15.65
CaO	20.16	20.29	19.49	16.82	17.98	17.52	17.46	18.96	21.16
Na <sub>2</sub> O	0.35	0.36	0.29	0.37	0.35	0.38	0.37	0.34	0.35
Total	99.13	100.49	100.98	99.86	99.61	99.60	99.85	100.53	100.55
NUMBER OF IONS ON THE BASIS OF 6 OXYGENS									
Si	1.910	1.898	1.905	1.910	1.889	1.908	1.911	1.864	1.891
Al iv	0.090	0.102	0.095	0.062	0.070	0.075	0.053	0.136	0.109
Al vi	0.059	0.027	0.043	0.040	0.052	0.036	0.046	0.055	0.048
Ti	0.021	0.023	0.010	0.017	0.017	0.017	0.015	0.026	0.019
Cr	0.006	0.003	0.005	0.000	0.001	0.002	0.001	0.003	0.007
Mg	0.871	0.872	0.915	0.854	0.876	0.893	0.889	0.858	0.858
Fe 2+	0.215	0.260	0.250	0.381	0.314	0.327	0.317	0.296	0.220
Mn	0.003	0.004	0.005	0.007	0.005	0.005	0.006	0.006	0.003
Ca	0.802	0.802	0.762	0.673	0.717	0.699	0.693	0.751	0.833
Na	0.024	0.025	0.019	0.026	0.024	0.027	0.019	0.023	0.024
FeO*/MgO	0.441	0.533	0.489	0.796	0.638	0.654	0.636	0.616	0.458

Note: FeO\* is total iron as FeO.

TABLE 4 (continued).

## APHYRIC BASALTIC LAVAS

	046-1	067-1	073-1	076-3	080-1	082-2	087-2A	087-2B	101-5
SiO <sub>2</sub> (%)	51.52	50.52	50.75	49.59	48.72	50.79	49.26	47.98	50.57
TiO <sub>2</sub>	1.01	1.25	1.42	1.85	1.67	1.06	1.83	2.23	1.03
Al <sub>2</sub> O <sub>3</sub>	2.85	2.91	2.75	3.30	3.90	2.76	3.63	4.09	2.75
Cr <sub>2</sub> O <sub>3</sub>	0.17	0.07	0.05	0.01	0.02	0.03	0.00	0.00	0.09
FeO*	8.97	9.79	9.85	11.73	10.81	9.50	11.83	11.26	9.32
MnO	0.19	0.18	0.23	0.23	0.18	0.19	0.25	0.26	0.20
NiO	0.00	0.02	0.00	0.00	0.01	0.02	0.04	0.00	0.01
MgO	15.65	14.84	14.82	12.78	13.50	15.71	12.82	12.48	15.08
CaO	19.81	19.65	20.18	20.26	19.86	18.92	20.19	20.40	19.52
Na <sub>2</sub> O	0.31	0.34	0.43	0.47	0.43	0.34	0.41	0.52	0.32
Total	100.49	99.57	100.48	100.22	99.10	99.34	100.26	99.21	98.90

## NUMBER OF IONS ON THE BASIS OF 6 OXYGENS

Si	1.903	1.893	1.889	1.871	1.851	1.901	1.858	1.831	1.904
Al iv	0.097	0.107	0.111	0.129	0.149	0.099	0.142	0.169	0.096
Al vi	0.027	0.021	0.009	0.017	0.025	0.022	0.018	0.015	0.025
Ti	0.027	0.035	0.039	0.052	0.047	0.029	0.051	0.063	0.028
Cr	0.004	0.002	0.001	0.000	0.000	0.000	0.000	0.000	0.002
Mg	0.862	0.829	0.823	0.718	0.764	0.876	0.720	0.710	0.846
Fe 2+	0.276	0.306	0.306	0.370	0.343	0.296	0.373	0.358	0.292
Mn	0.005	0.005	0.006	0.006	0.005	0.005	0.007	0.008	0.005
Ca	0.784	0.789	0.804	0.818	0.808	0.759	0.815	0.833	0.787
Na	0.021	0.024	0.030	0.033	0.030	0.024	0.030	0.038	0.023
FeO*/MgO	0.573	0.660	0.665	0.918	0.801	0.605	0.923	0.902	0.618

Note: FeO\* is total iron as FeO.

TABLE 4 (continued).

	APHYRIC BASALTIC LAVAS					BRIGUS JUNCTION	
	102-3	140-3	166-1	169-2	172-2	144-3A	144-3B
SiO <sub>2</sub> (%)	50.8	50.74	50.15	50.25	49.82	50.64	49.99
TiO <sub>2</sub>	1.32	1.31	1.48	1.21	1.38	1.68	2.04
Al <sub>2</sub> O <sub>3</sub>	3.13	2.41	3.43	3.17	3.45	2.82	3.49
Cr <sub>2</sub> O <sub>3</sub>	0.06	0.10	0.09	0.21	0.13	0.00	0.02
FeO*	9.87	10.75	11.63	10.12	10.16	8.96	9.10
MnO	0.16	0.22	0.22	0.23	0.17	0.13	0.18
NiO	0.01	0.00	0.03	0.03	0.00	0.02	0.00
MgO	14.81	14.51	13.56	14.52	14.59	14.51	13.82
CaO	18.31	18.98	19.74	20.17	20.18	19.13	19.35
Na <sub>2</sub> O	0.36	0.33	0.34	0.29	0.34	0.37	0.43
Total	98.83	99.36	100.68	100.21	100.22	98.27	98.42
NUMBER OF IONS ON THE BASIS OF 6 OXYGENS							
Si	1.908	1.910	1.876	1.879	1.864	1.911	1.889
Al iv	0.092	0.090	0.124	0.121	0.136	0.089	0.111
Al vi	0.046	0.016	0.026	0.018	0.015	0.036	0.045
Ti	0.037	0.036	0.041	0.034	0.038	0.047	0.058
Cr	0.001	0.002	0.002	0.005	0.003	0.000	0.001
Mg	0.829	0.814	0.756	0.809	0.813	0.816	0.778
Fe 2+	0.311	0.338	0.363	0.316	0.317	0.282	0.288
Mn	0.004	0.006	0.006	0.006	0.004	0.003	0.006
Ca	0.737	0.766	0.790	0.808	0.808	0.772	0.784
Na	0.026	0.023	0.024	0.021	0.024	0.026	0.032
FeO*/MgO	0.666	0.741	0.858	0.697	0.696	0.618	0.658

Note: FeO\* is total iron as FeO.

TABLE 4 (continued).

	SILLS				DYKE
	055-1	070-1	081-4A	118-4	202-1
SiO <sub>2</sub> (%)	48.99	50.00	49.99	49.41	51.07
TiO <sub>2</sub>	1.64	1.61	1.44	1.43	0.82
Al <sub>2</sub> O <sub>3</sub>	3.77	3.29	3.33	3.77	2.18
Cr <sub>2</sub> O <sub>3</sub>	0.01	0.05	0.02	0.05	0.00
FeO*	11.82	10.28	10.45	10.26	14.05
MnO	0.24	0.20	0.17	0.20	0.33
NiO	0.00	0.04	0.03	0.03	0.02
MgO	13.05	13.89	14.27	13.80	14.32
CaO	20.43	20.53	18.85	20.61	17.71
Na <sub>2</sub> O	0.42	0.47	0.38	0.33	0.28
Total	100.37	100.37	98.93	99.88	100.79
NUMBER OF IONS ON THE BASIS OF 6 OXYGENS					
Si	1.847	1.871	1.889	1.860	1.916
Al iv	0.153	0.129	0.111	0.140	0.084
Al vi	0.014	0.016	0.022	0.027	0.012
Ti	0.046	0.045	0.040	0.040	0.023
Cr	0.000	0.001	0.000	0.001	0.000
Mg	0.734	0.774	0.803	0.773	0.800
Fe 2+	0.373	0.321	0.317	0.322	0.440
Mn	0.006	0.005	0.005	0.005	0.010
Ca	0.825	0.822	0.763	0.831	0.711
Na	0.030	0.033	0.027	0.023	0.020
FeO*/MgO	0.906	0.740	0.732	0.743	0.981

Note: FeO\* is total iron as FeO.

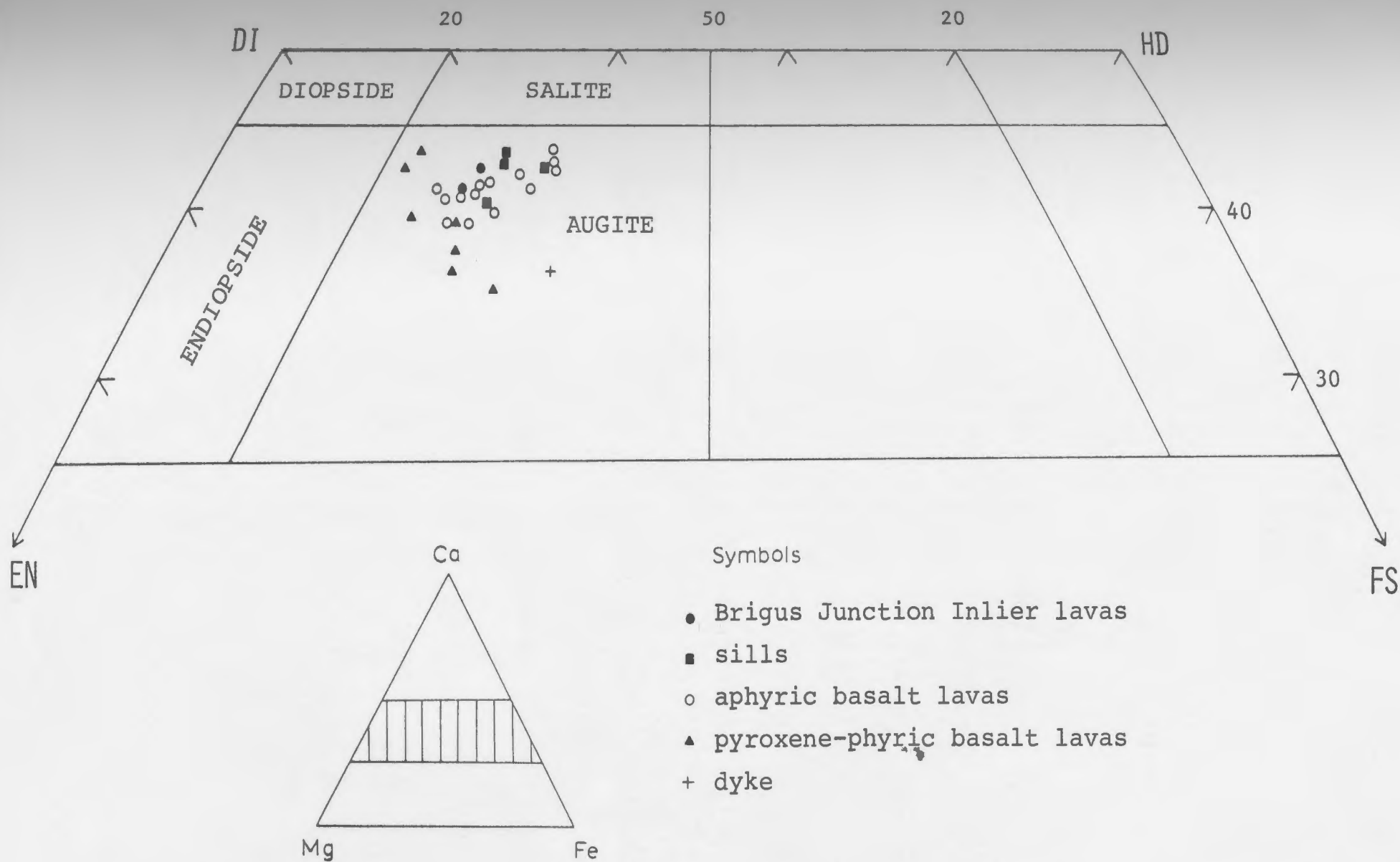
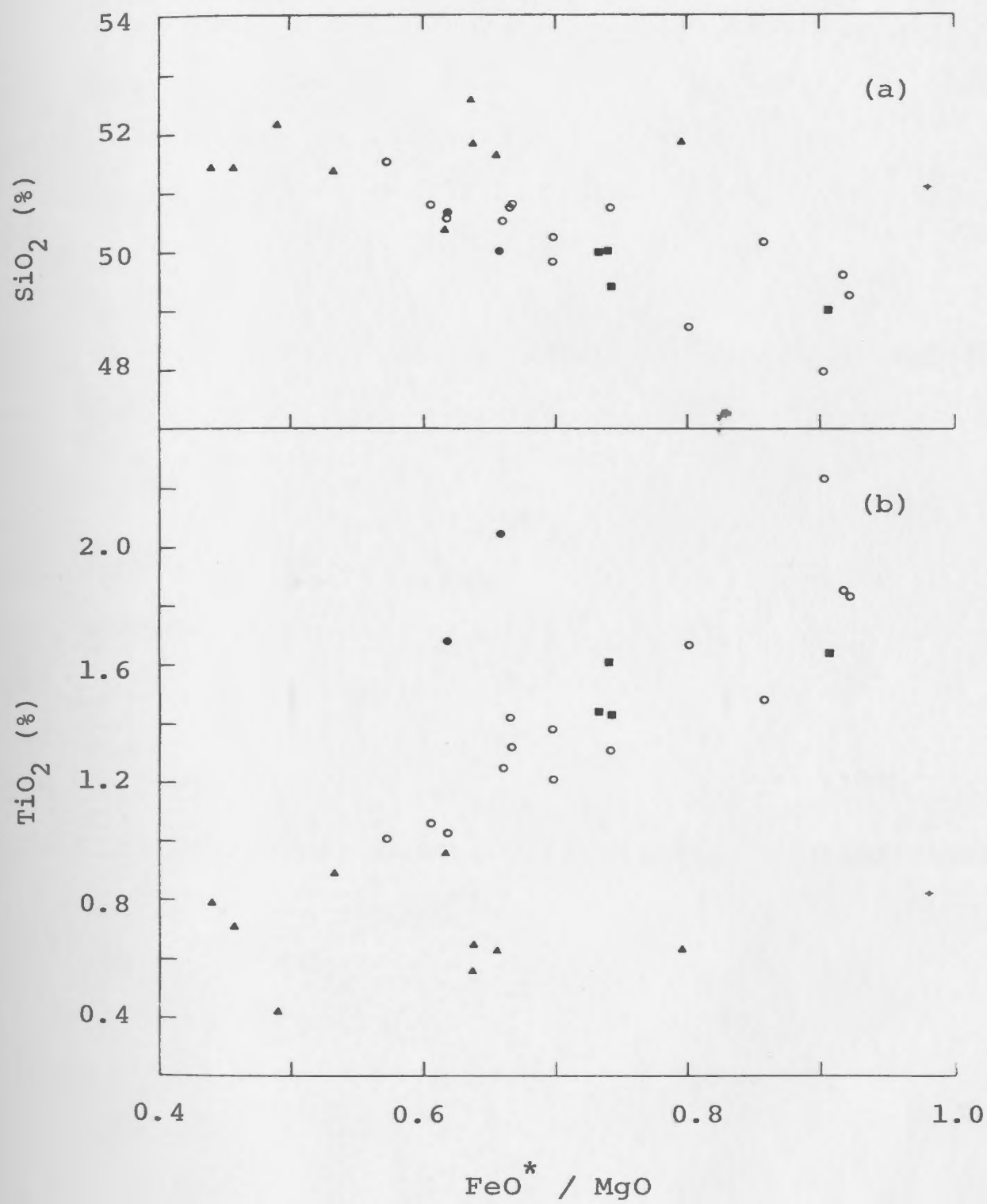


FIGURE 11. Compositional variation of relict clinopyroxenes (see Table 4) from rocks of the Blue Hills Sequence plotted in terms of enstatite (EN) - diopside (DI) - hedenbergite (HD) - ferrosilite (FS). Field boundaries after Deer et al. (1971).

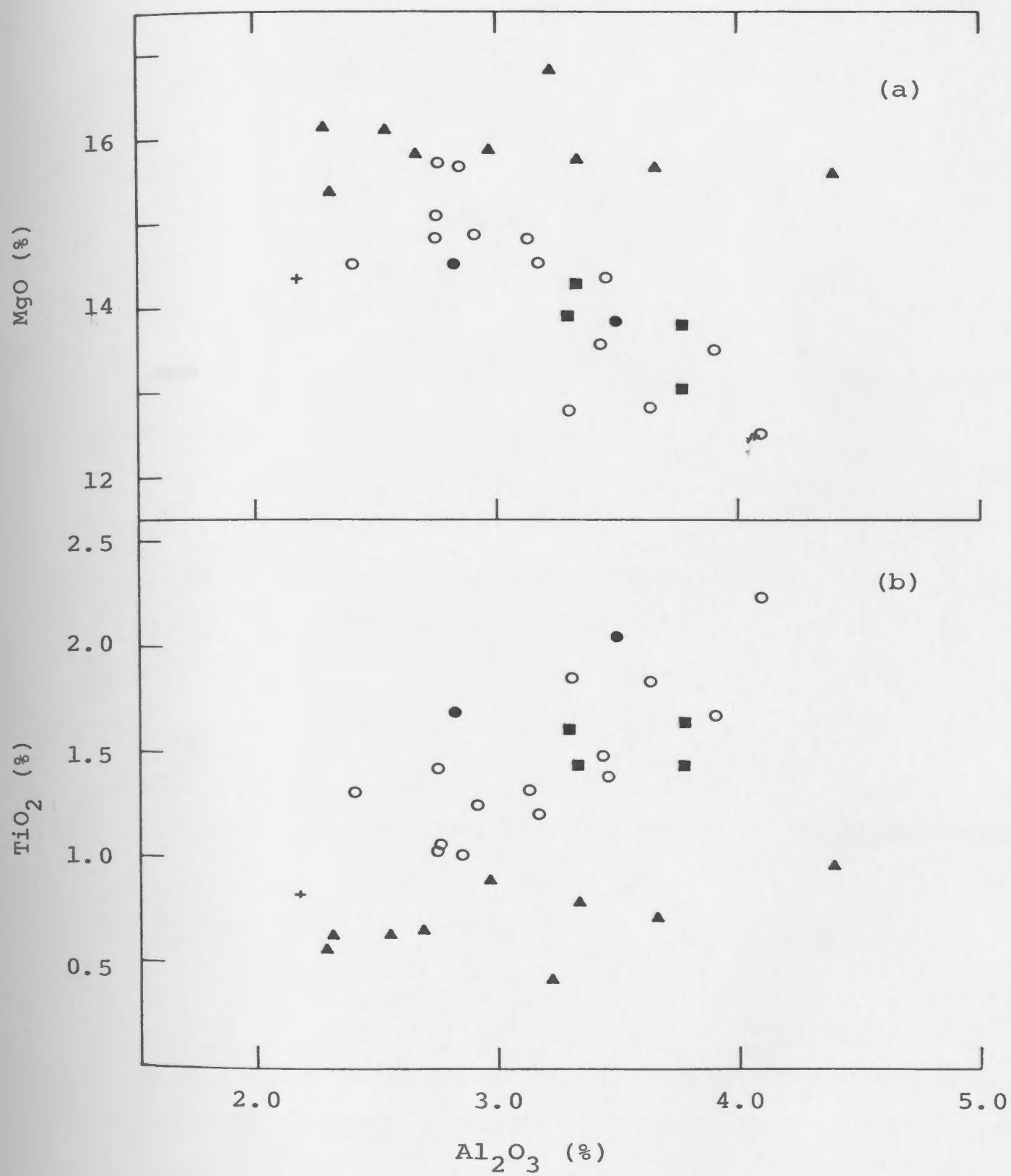
FIGURE 12. (a)  $\text{SiO}_2$  and (b)  $\text{TiO}_2$  versus  $\text{FeO}^*/\text{MgO}$  variation diagrams for clinopyroxenes in rocks of the Blue Hills Sequence. Symbols as for host rocks:  $\blacktriangle$ , pyroxene-phyric basaltic lavas;  $\bigcirc$ , aphyric basalt lavas;  $\bullet$ , Brigus Junction Inlier lavas;  $\blacksquare$ , sills;  $+$ , dyke. Note that pyroxenes in the stratigraphically lower rocks are characterised by relatively consistent low  $\text{TiO}_2$  and high  $\text{SiO}_2$  contents whereas the remainder of the pyroxenes display decreasing  $\text{SiO}_2$  and increasing  $\text{TiO}_2$  with increasing fractionation. For comparison with bulk rock compositions see Fig. 4.



In a scheme similar to that employed for whole rock chemistry, the pyroxenes from the various units display distinct trends on variation diagrams. In Figure 12 it can be seen that pyroxenes from the basal units show very little variation in  $\text{TiO}_2$  or  $\text{SiO}_2$  with increasing  $\text{FeO}^*/\text{MgO}$ . On the other hand, the main series of basalts contain pyroxenes displaying increasing  $\text{TiO}_2$  and decreasing  $\text{SiO}_2$  contents with increasing differentiation.

Figure 13 also displays two distinct compositional trends in the pyroxenes. The pyroxene-phyric lavas exhibit very little variation in  $\text{TiO}_2$  with change in  $\text{Al}_2\text{O}_3$ . Pyroxenes in the remainder of the rock units show a positive correlation between  $\text{TiO}_2$  and  $\text{Al}_2\text{O}_3$  - again reflecting the relative stratigraphic position of the samples. One observation which can explain the  $\text{TiO}_2$  -  $\text{Al}_2\text{O}_3$  correlation is linked to the variation of  $\text{MgO}$  with stratigraphic height, which has already been discussed. Since  $\text{Al}_2\text{O}_3$  and  $\text{TiO}_2$  both show a negative correlation with  $\text{MgO}$ , they must have been concentrated in the melt during the early stages of crystallisation (Schweitzer et al., 1979). Thus, the trends displayed in these diagrams can be explained by increasing degrees of fractional crystallisation which corresponds well with increasing stratigraphic position.

FIGURE 13. (a) Plot of MgO and (b)  $\text{TiO}_2$  against  $\text{Al}_2\text{O}_3$  content in clinopyroxenes of the Blue Hills Sequence. Symbols as for host rocks:  $\blacktriangle$ , pyroxene-phyric basaltic lavas;  $\bigcirc$ , aphyric basalt lavas;  $\bullet$ , Brigus Junction Inlier lavas;  $\blacksquare$ , sills; +, dyke. Again, phenocrysts from the stratigraphically lower pyroxene-phyric lavas display a slightly different trend than the remainder of the plotted analyses.



*A theory is a tool - not a creed. -- J.J. Thomson*

## CHAPTER 5

### RECOGNITION OF PRIMARY MAGMATIC AFFINITIES

#### 5.1 INTRODUCTION

This chapter is organised in a similar manner to the previous one, in that the magmatic affinities of the rocks will be discussed first with reference to their whole rock chemistry and then in terms of data from clinopyroxene chemistry.

#### 5.2 MAGMATIC AFFINITIES BASED ON WHOLE ROCK CHEMISTRY

##### 5.2.1 Major Oxides

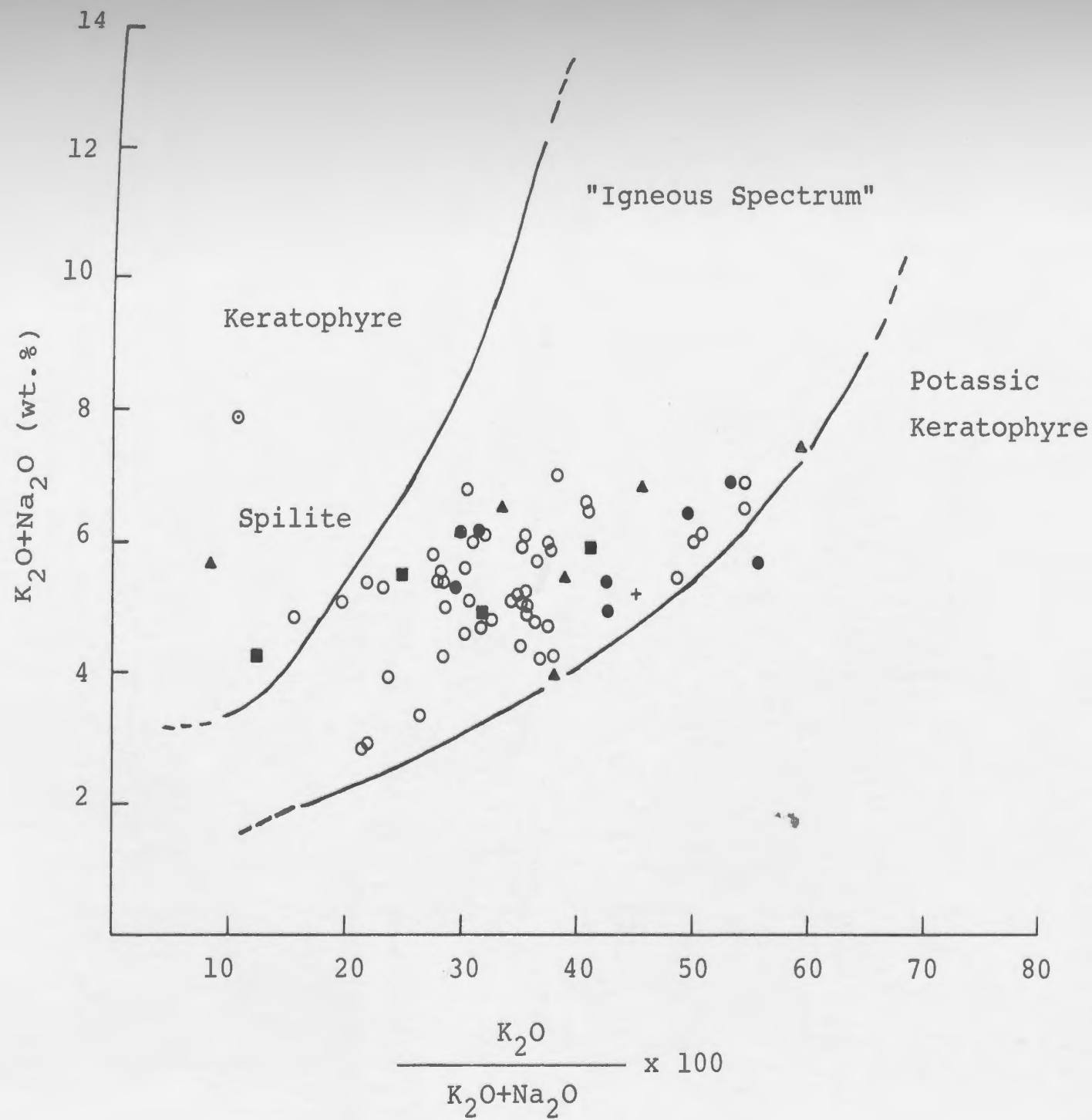
It is now generally accepted that during low-grade metamorphism many of the major elements may be considered mobile. This is particularly true of  $K_2O$ ,  $Na_2O$ ,  $CaO$ , and sometimes  $SiO_2$ . Although alteration of these rocks is evident from their petrography, a plot of alkali parameters

(Hughes, 1973) (Fig. 14) shows that only a few of the total number of analysed samples fall outside the 'Igneous Spectrum'. This suggests that even though there has been alkali mobility (recognised in the alteration of primary mineralogy) this may have resulted only in a reconstitution of components (eg. Ca-plagioclase to epidote) with only minor loss of elements. This process may also be responsible for the relative depletion of LREE mentioned earlier (see Ch. 4).

Similarly a plot of total alkalis ( $\text{Na}_2\text{O} + \text{K}_2\text{O}$ ) against  $\text{SiO}_2$  values indicates that the majority of the samples have alkaline affinities (Fig. 15). Again caution must be exercised in interpreting diagrams of this nature due to the suspected mobility of the alkali elements. However, if the samples had been originally subalkaline, then the implication is that many of the samples would have had to gain as much as 4-5 wt.% total alkalis. If this had occurred, then severe alteration would be apparent, but petrography of the samples does not support this suggestion. On the other hand, the concept of reconstitution of mineral components with no significant gain or loss of alkalis seems more plausible.

In Figure 16 the samples are plotted in terms of  $\text{Na}_2\text{O} + \text{K}_2\text{O} - \text{FeO}^* - \text{MgO}$  (AFM). All the rock units have subalkaline character here. However, the stratigraphically higher Brigus Junction lavas appear distinct from the rest of the lavas in that they exhibit an enrichment in iron and the

FIGURE 14. Plot of alkali parameters (Hughes, 1973) for rocks of the Blue Hills Sequence. Symbols for samples: ⊙, 058-1; ▲, pyroxene-phyric basaltic lavas; ○, aphyric basalt lavas; ●, Brigus Junction Inlier lavas; ■, sills; +, dyke.



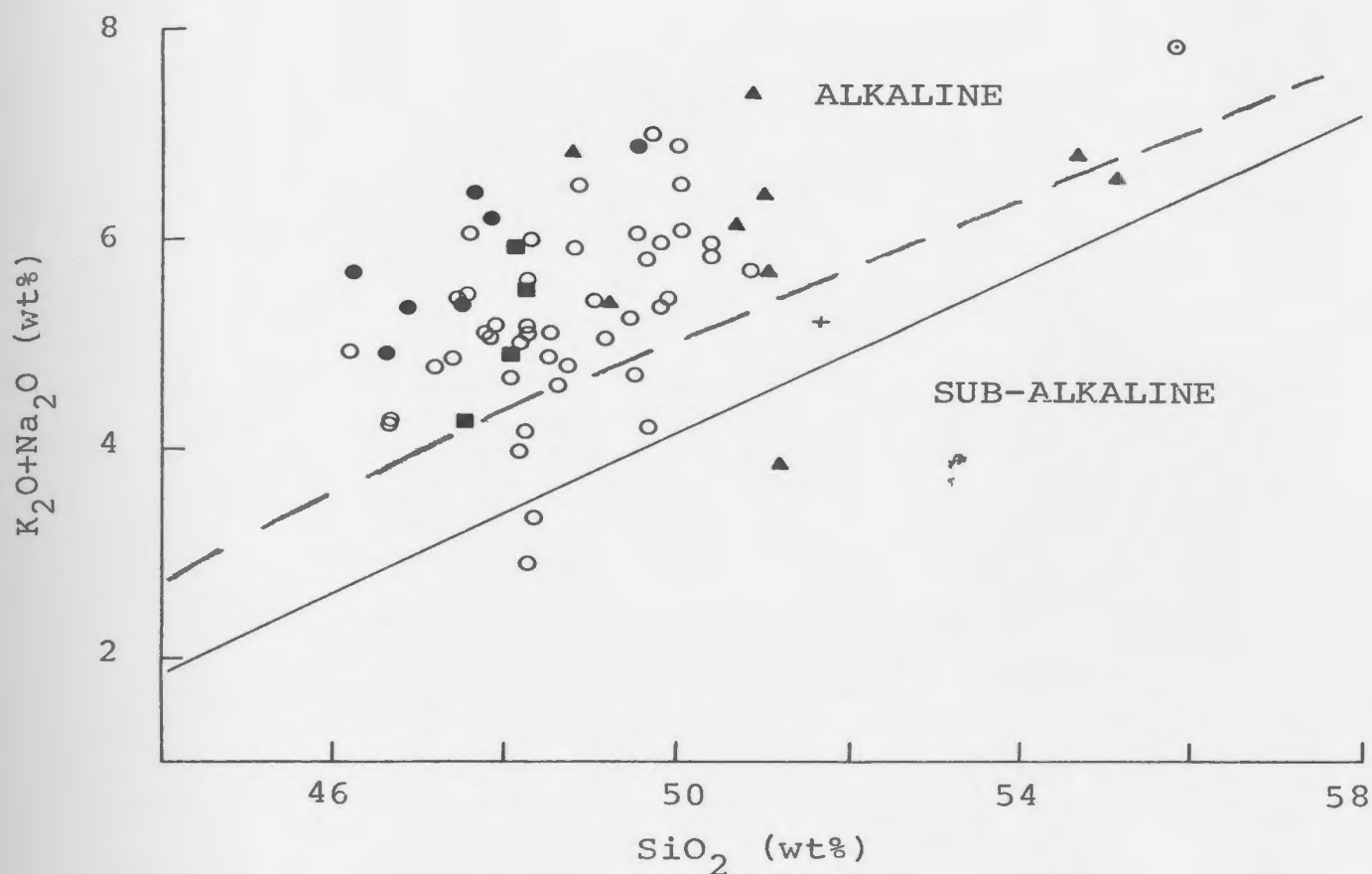
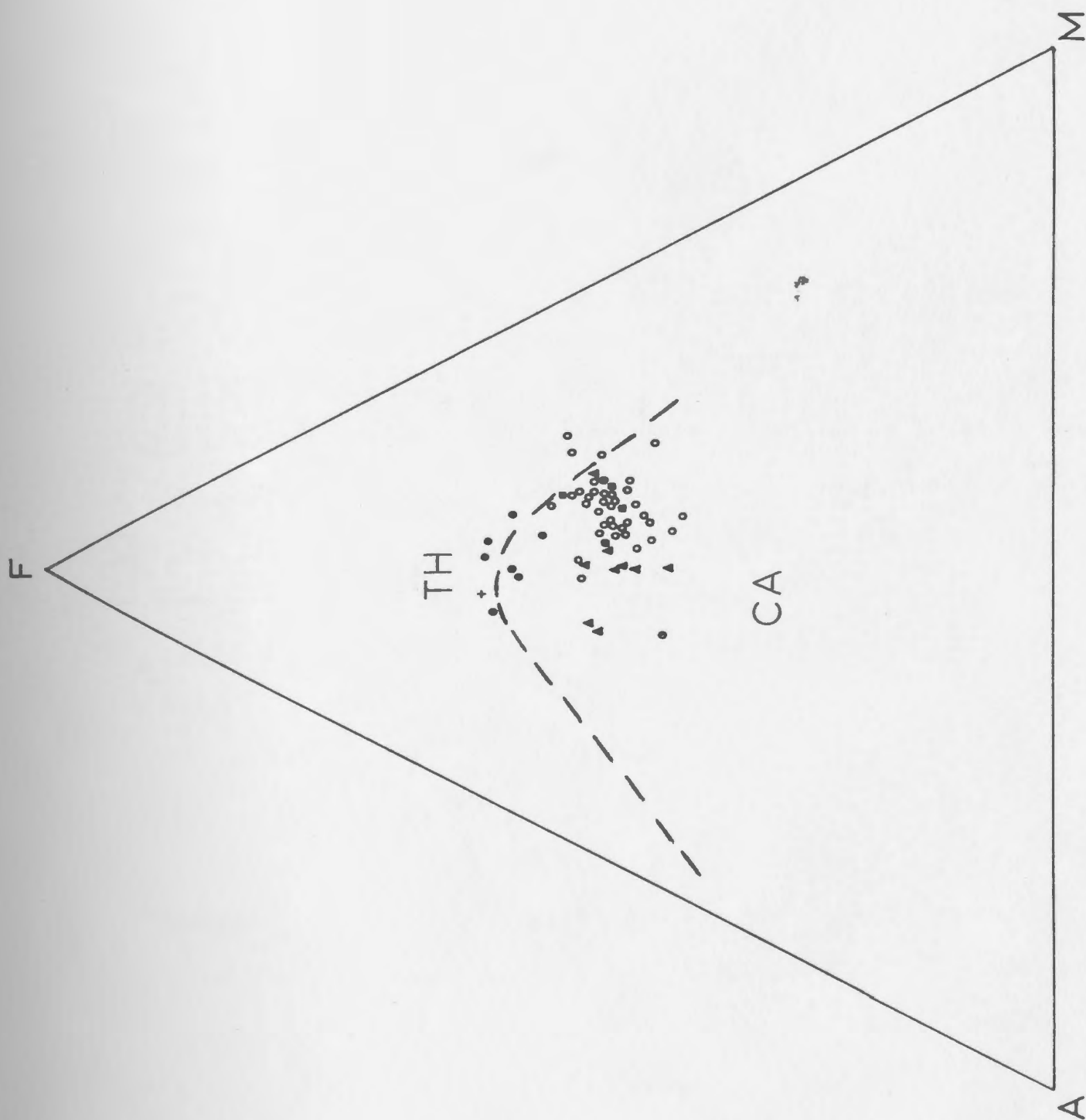


FIGURE 15. Alkali-silica plot for the Blue Hills Sequence.

The dashed line separating alkaline - subalkaline fields is from Irvine and Baragar (1971); the solid dividing line is from MacDonald and Katsura (1961).

Symbols for samples: ⊙, 058-1; ▲, pyroxene-phyric basaltic lavas; ○, aphyric basalt lavas; ●, Brigus Junction Inlier lavas; ■, sills; +, dyke.

FIGURE 16. AFM plot of Blue Hills Sequence rocks.  
A= $\text{Na}_2\text{O}+\text{K}_2\text{O}$ ; F=total iron as FeO; M=MgO.  
Tholeiitic (TH) - Calc-alkaline (CA) dividing  
line from Irvine and Baragar (1971). Symbols  
for samples: ⊙, 058-1; ▲, pyroxene-phyric  
basaltic lavas; ○, aphyric basalt lavas;  
●, Brigus Junction Inlier lavas; ■, sills;  
+, dyke.



stratigraphically lower pyroxene-phyric lavas display an apparent alkali-enrichment. The ambiguous information derived from the AFM diagram (especially when compared with the results of the previous diagrams) strengthens the argument that extreme caution must be taken when interpreting the results of variation diagrams employing major oxides, particularly the alkali elements. Therefore greater emphasis should be placed on using trace elements to determine the magmatic affinities of these lavas.

#### 5.2.2 Trace Elements

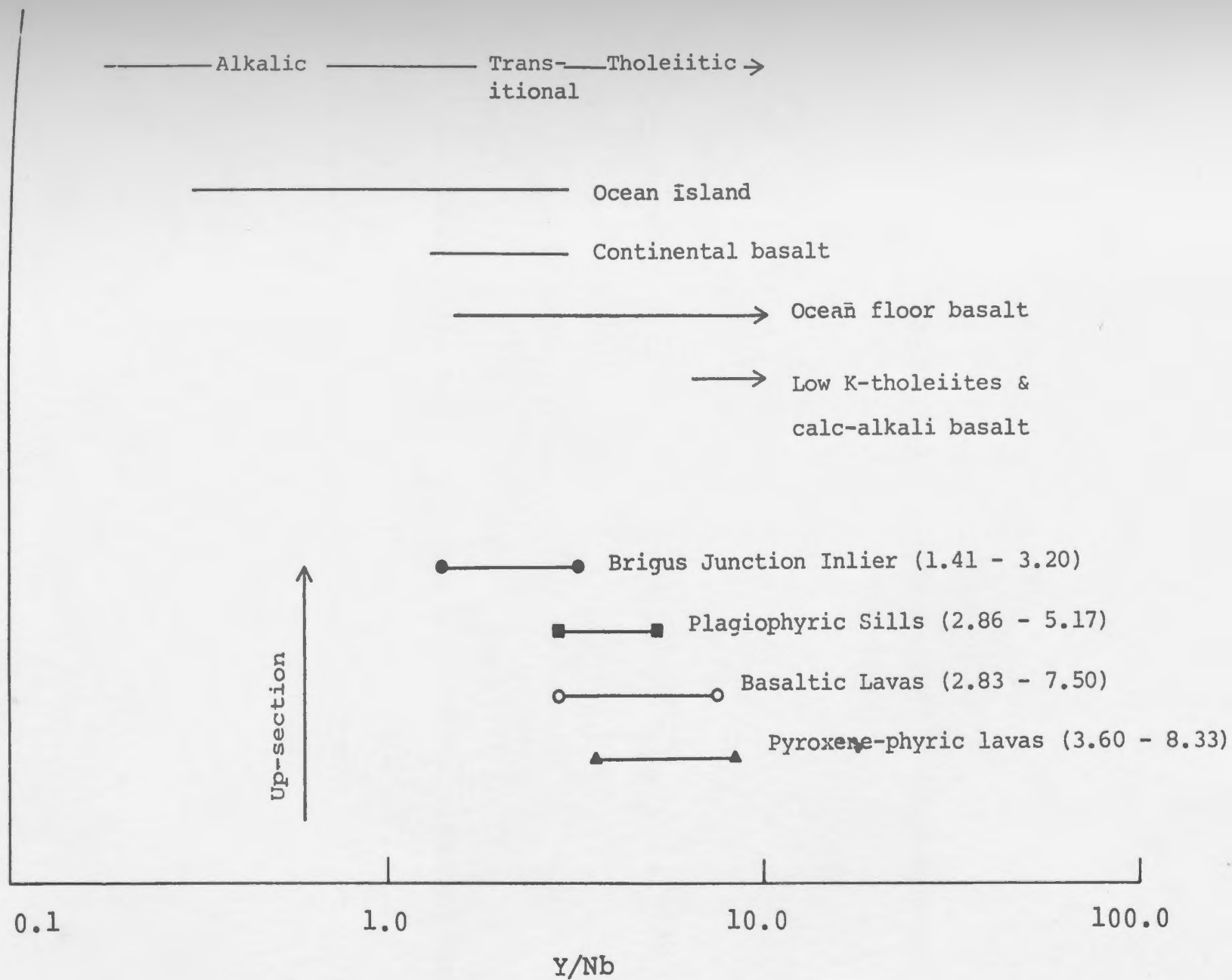
Although a knowledge of the major element composition of basaltic rock suites is necessary to understand their petrogenesis, the minor and trace element data can be used to further constrain petrogenetic models for the origin and subsequent history of the magmas. A study of trace element compositions is particularly useful because some trace elements are considered to be relatively unaffected by low-grade metamorphism (Cann, 1970; Pearce and Cann, 1973; Floyd and Winchester, 1975; Winchester and Floyd, 1976, 1977), which usually modifies the major element composition of flows from deeper parts of thick basaltic lava piles.

The apparent preservation of the expected igneous relationship between Nb and Zr (Fig. 9, Ch. 4) indicates either that these two elements are immobile during metamorphism or that the concentration of both elements

changed in such a way as to preserve the original abundance ratio. Because zircon, which contains most of the Zr, is stable even during amphibolite grade metamorphism, it is more likely that Zr and, therefore, Nb were immobile during the low-grade metamorphism that has affected the Blue Hills sequence. The Zr-Y and Nb-Y plots (Fig. 9, Ch. 4) show very limited scatter and this suggests that Y was also immobile during the low-grade metamorphism. From these arguments and others presented in the previous chapter, it appears that the trace elements Zr, Nb, Y<sub>sp</sub> and some of the minor elements have not been significantly mobilised during low-grade metamorphism. These are the main elements which will be used to deduce the magmatic and tectonic affinities of these rocks.

The ratio Y/Nb is often used as an index of alkalinity in mafic rock suites. Pearce and Cann (1973) suggest that a Y/Nb ratio of 1.0 provides a convenient divider between tholeiitic and alkaline basalts, although some fresh continental alkali basalts do contain a Y/Nb ratio slightly exceeding 1.0 (Floyd and Winchester, 1975). The Y/Nb ratio in samples from the Blue Hills Sequence ranges from 8.33 in one of the pyroxene-phyric lavas to 1.41 in a Brigus Junction Inlier sample. The range of values for the individual units of the sequence are shown in Figure 17. Clearly there is a trend of increasing alkalinity upwards in the stratigraphic section. Compared with other rock types, the stratigraphically lower pyroxene-phyric lavas appear

FIGURE 17. Variation in Y/Nb ratio of the various rock units of the Blue Hills Sequence with their ranges in brackets. The Y/Nb ratio is often used as an index of alkalinity in volcanic rock suites. For comparison, Y/Nb ranges for various types of volcanic groups (Pearce and Cann, 1973) are also shown.



tholeiitic while the Brigus Junction lavas have transitional to mildly alkaline affinities. It is also known that alkali basalts have higher contents of  $\text{TiO}_2$  than tholeiitic basalts. The trend of increasing  $\text{TiO}_2$  content with decreasing Y/Nb ratio in these rocks (Fig. 18) supports the increasingly alkaline nature of these rocks.

In a similar manner, the Zr and  $\text{P}_2\text{O}_5$  contents can be used to distinguish magmatic affinities of mafic volcanic rock suites (Winchester and Floyd, 1976). Subalkaline basalts are characterised by low  $\text{P}_2\text{O}_5$  values. Although many of the pyroxene-phyric samples plot just within the alkaline field of the diagram, the positive correlation between Zr and  $\text{P}_2\text{O}_5$  in rocks of the Blue Hills Sequence reaffirms the subalkaline nature of the lower sections with increasing alkalinity upwards (Fig. 19).

The Zr/ $\text{P}_2\text{O}_5$  ratio produces a similar discrimination relationship as the Y/Nb ratio when plotted against  $\text{TiO}_2$  (Fig. 20). Although the samples straddle the alkaline-subalkaline boundary, the result is a nearly vertical trend with the entire suite displaying only minor variation in Zr/ $\text{P}_2\text{O}_5$  over a relatively wide  $\text{TiO}_2$  range. The stratigraphically lower lavas generally plot in the subalkaline field, or near the alkaline/subalkaline boundary, with the uppermost lavas plotting well within the alkaline field.

FIGURE 18. Distribution of  $\text{TiO}_2$  and the Y/Nb ratio in analysed samples from the Blue Hills Sequence. Symbols for samples:  $\odot$ , 058-1;  $\blacktriangle$ , pyroxene-phyric basaltic lavas;  $\bigcirc$ , aphyric basalt lavas;  $\bullet$ , Brigus Junction Inlier lavas;  $\blacksquare$ , sills;  $+$ , dyke.

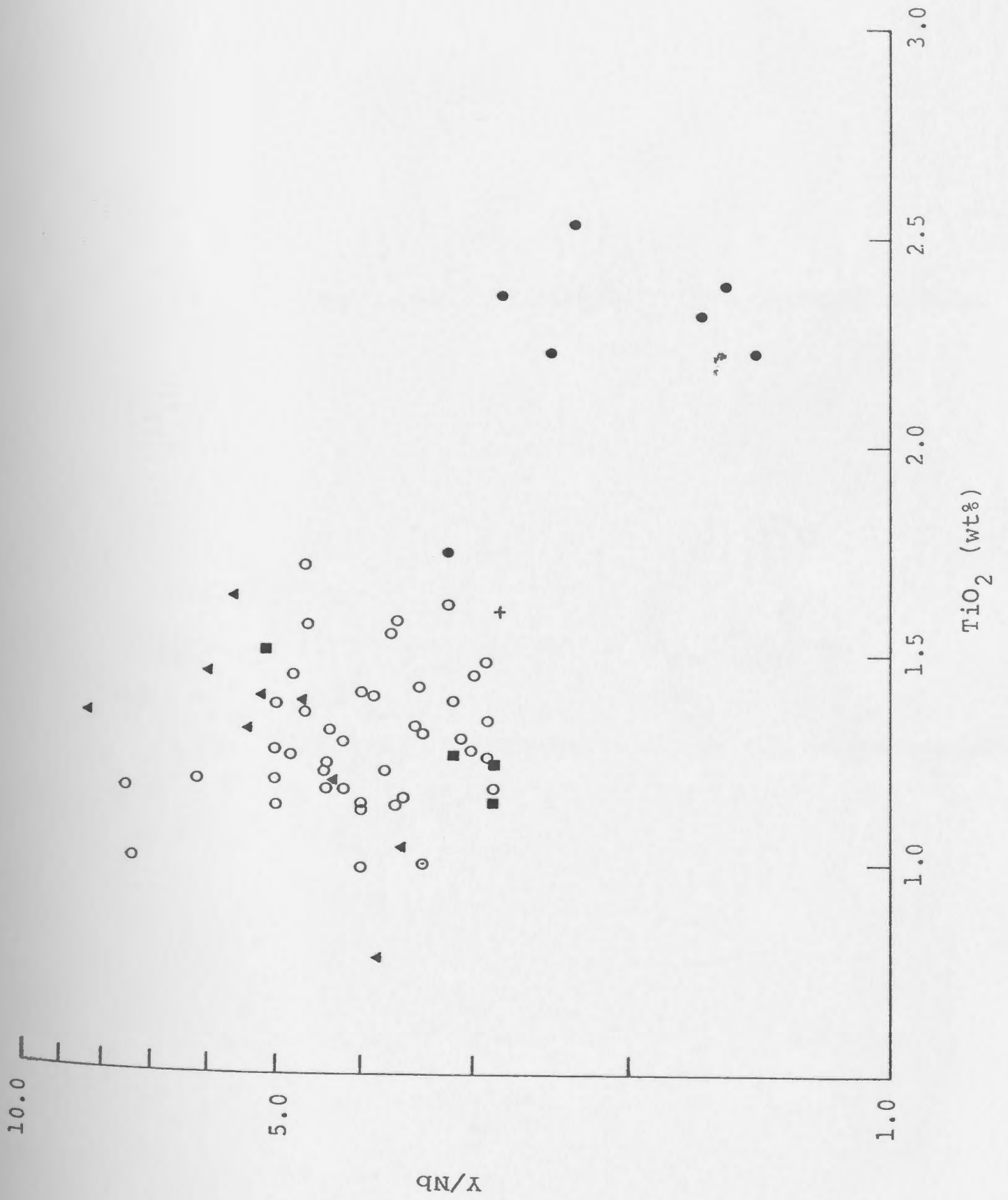


FIGURE 19.  $P_2O_5$  - Zr diagram showing the petrologic character of the Blue Hills Sequence. Symbols for samples:  $\odot$ , 058-1;  $\blacktriangle$ , pyroxene-phyric basaltic lavas;  $\circ$ , aphyric basalt lavas;  $\bullet$ , Brigus Junction Inlier lavas;  $\blacksquare$ , sills;  $+$ , dyke. The group displays subalkaline affinities in the stratigraphically lower rocks, transitional to alkaline rocks of the Brigus Junction Inlier. Alkaline - subalkaline dividing line is from Winchester and Floyd (1976).

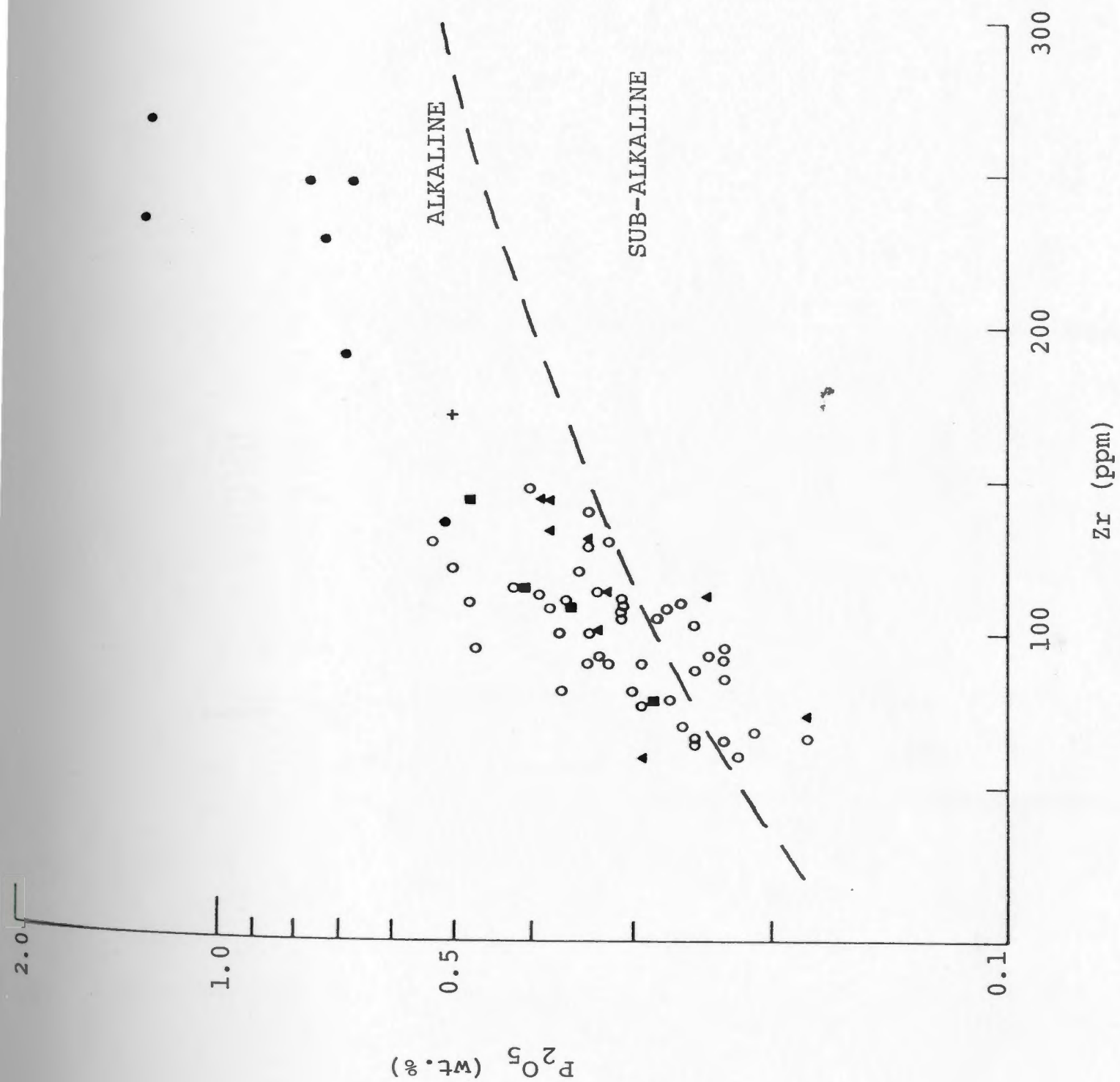


FIGURE 20. Distribution of samples from the Blue Hills Sequence on the  $\text{TiO}_2$  -  $\text{Zr/P}_2\text{O}_5$  diagram. Symbols for samples:  $\odot$ , 058-1;  $\blacktriangle$ , pyroxene-phyric basaltic lavas;  $\circ$ , aphyric basalt lavas;  $\bullet$ , Brigus Junction Inlier lavas;  $\blacksquare$ , sills;  $+$ , dyke. Field boundaries after Winchester and Floyd (1976). As in Fig. 17, there is an overall trend of increasing alkalinity in the samples which can be correlated with increasing stratigraphic position of the samples.



### 5.3 MAGMATIC AFFINITIES BASED ON CLINOPYROXENE COMPOSITION

The compositions of clinopyroxenes from mafic rocks are very useful because they may be directly compared to one another and to pyroxenes from recent rocks of known magmatic/tectonic settings (see also section 6.3). The above comparisons are not true for most whole rock analyses since depositional and post-depositional conditions may vary greatly, and to a considerable extent unpredictably affect the initial elemental concentrations.

Kushiro (1960) has shown that clinopyroxene crystallising from a  $\text{SiO}_2$  saturated melt has a higher proportion of Si and less Al in the tetrahedral site, whereas clinopyroxene crystallising from a  $\text{SiO}_2$  undersaturated melt has a higher proportion of tetrahedral Al ( $\text{Al}_z$ ) and relatively lower proportions of tetrahedral Si. Increases in  $\text{Al}_z$  are compensated by additional Tivi, Alvi, and  $\text{Fe}^{3+}$  in the y-site of the pyroxene structure to maintain the charge balance. Thus Si varies antithetically with  $\text{Al}_z$  and Ti, and likewise, Ti and  $\text{Al}_z$  vary sympathetically.

LeBas (1962) applied Kushiro's Si-Al relations by directly correlating the percentage of Al in the z-position with Si and Ti to define the alkalinity in some recent igneous suites. LeBas (1962) showed that the proportions of these components in clinopyroxene change systematically depending on the magma type and fractionation stage. When these components are plotted for pyroxenes from fresh rocks

they separate into three well-defined fields designated as subalkaline, alkaline, and peralkaline.

Figures 21 ( $\text{Al}_2\text{O}_3$  vs  $\text{SiO}_2$ ) and 22 ( $\text{Al}_2\text{O}_3$  vs  $\text{TiO}_2$ ) indicate that all clinopyroxenes from the stratigraphically lower flows of the Blue Hills Sequence are subalkaline, while the remainder of the analysed pyroxenes are transitional between subalkaline and alkaline in character. The trends on both of these diagrams exactly reflect the position of the samples in the stratigraphy even more effectively than the whole rock geochemical data. As is evident from Figure 21 the  $\text{Al}_2\text{O}_3/\text{SiO}_2$  weight ratio increases with stratigraphic height. In pyroxenes from tholeiitic, high-alumina, and calc-alkaline rocks, the  $\text{Al}_2\text{O}_3/\text{SiO}_2$  ratio is low and usually decreases with fractionation. In normal alkaline pyroxenes, the  $\text{Al}_2\text{O}_3/\text{SiO}_2$  ratio is slightly higher and it increases with fractionation (LeBas, 1962). In a similar manner, an increase in  $\text{Al}_2\text{O}_3$  with rising  $\text{TiO}_2$  is characteristic of fractionation in an alkaline basalt suite.

Leterrier et al. (1982) have constructed discriminant diagrams which enable the separation of rock types based upon clinopyroxene compositions. They have based their study on pyroxenes from fresh rocks of known geological settings and, unlike previous workers, have used a large data base, incorporated both phenocryst and groundmass clinopyroxene compositions, and have tested their model on several palaeo-volcanic sequences with success. Figure 23 shows the result of plotting clinopyroxene compositions from

FIGURE 21. Plot of silica versus alumina for relict clinopyroxenes from rocks of the Blue Hills Sequence. Symbols as for host rocks: ▲, pyroxene-phyric basaltic lavas; ○, aphyric basalt lavas; ●, Brigus Junction Inlier lavas; ■, sills; +, dyke. Boundaries of fields for pyroxenes from different rock types after LeBas (1962). Note the good positive correlation between increasing alkaline nature and increasing stratigraphic position of the samples.

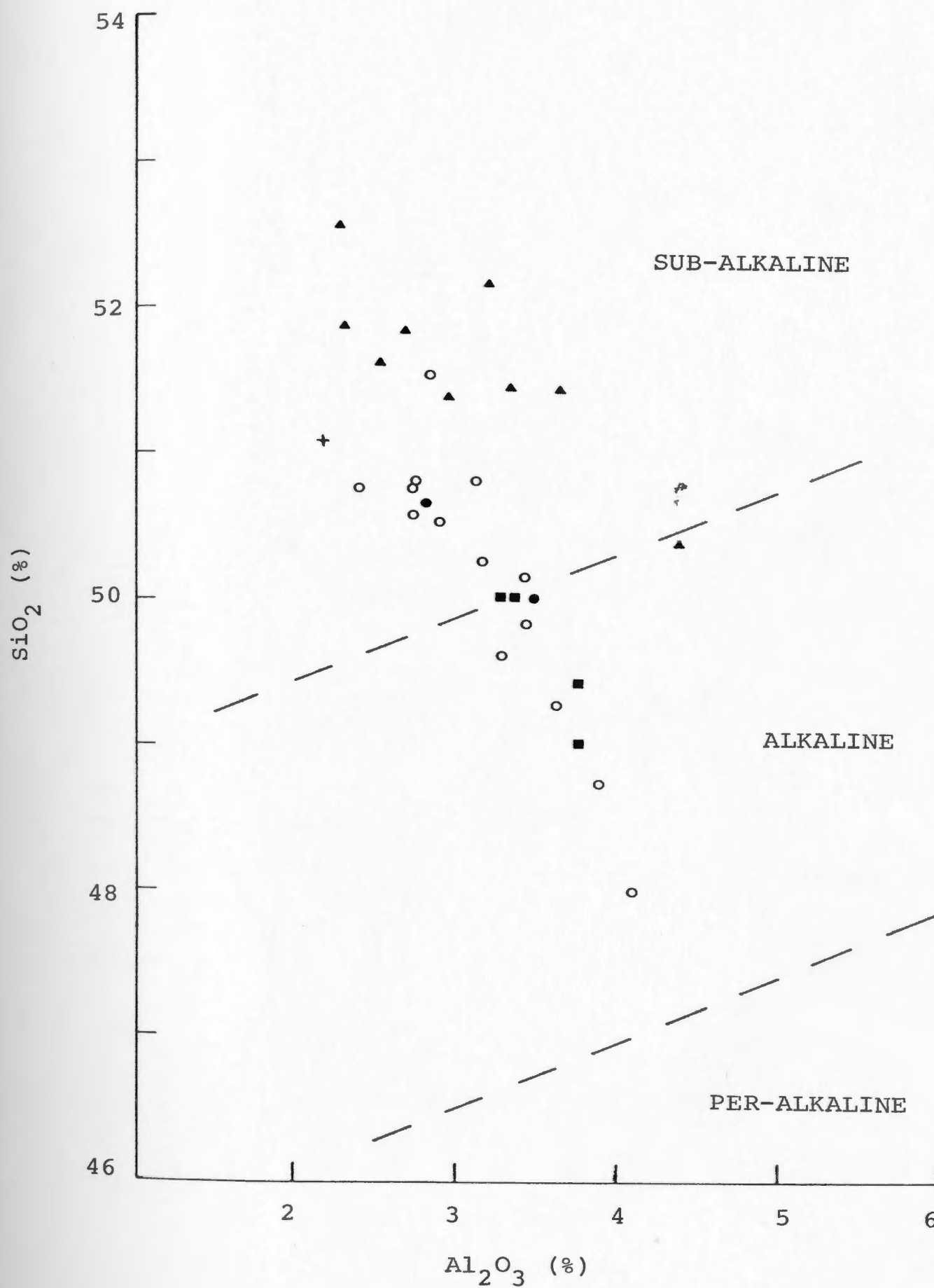


FIGURE 22. Plot of  $Al_2$  against  $TiO_2$  content in clinopyroxenes from rocks of the Blue Hills Sequence. Symbols as for host rocks: ▲, pyroxene-phyric basaltic lavas; ○, aphyric basalt lavas; ●, Brigus Junction Inlier lavas; ■, sills; +, dyke.

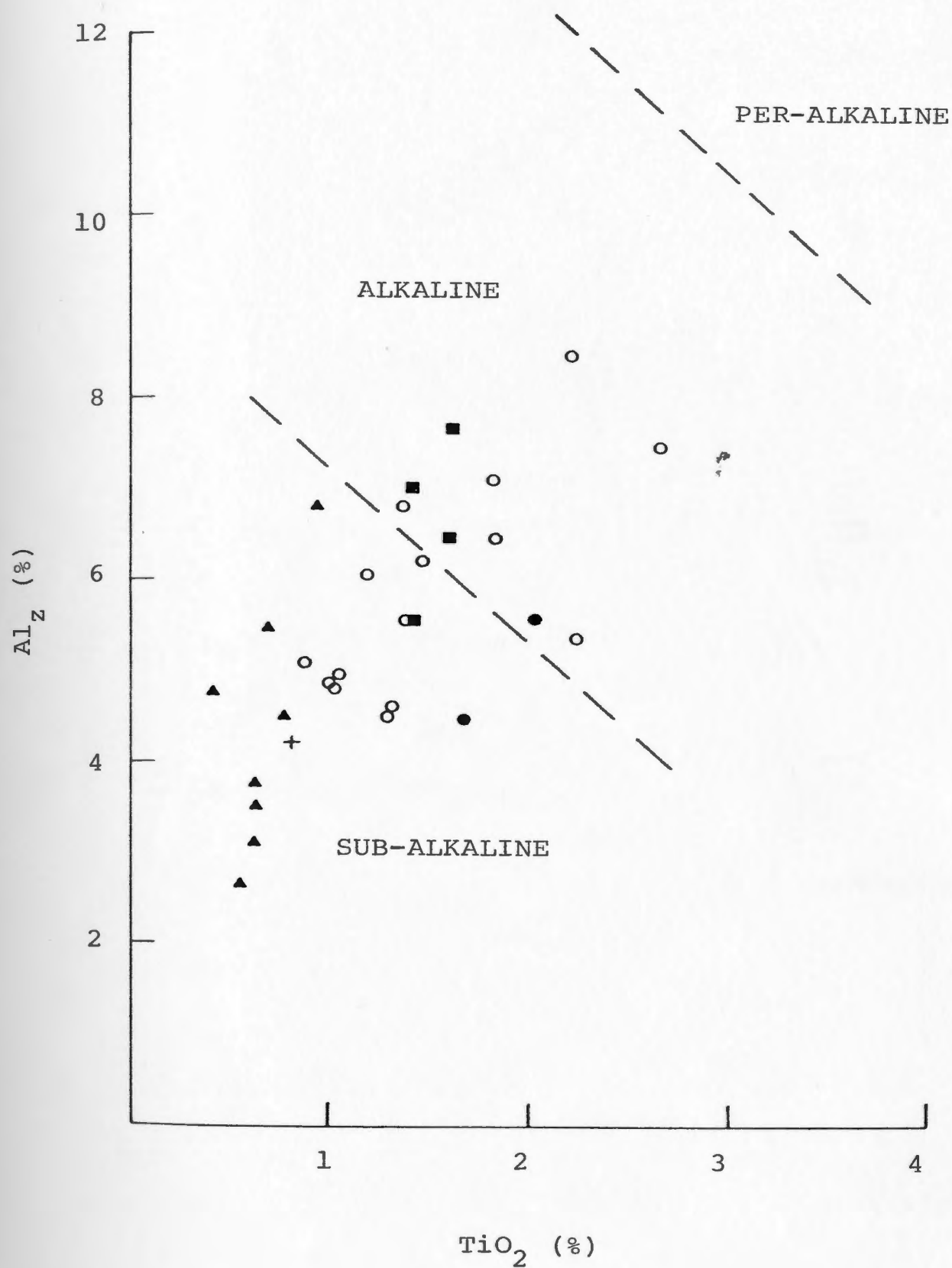
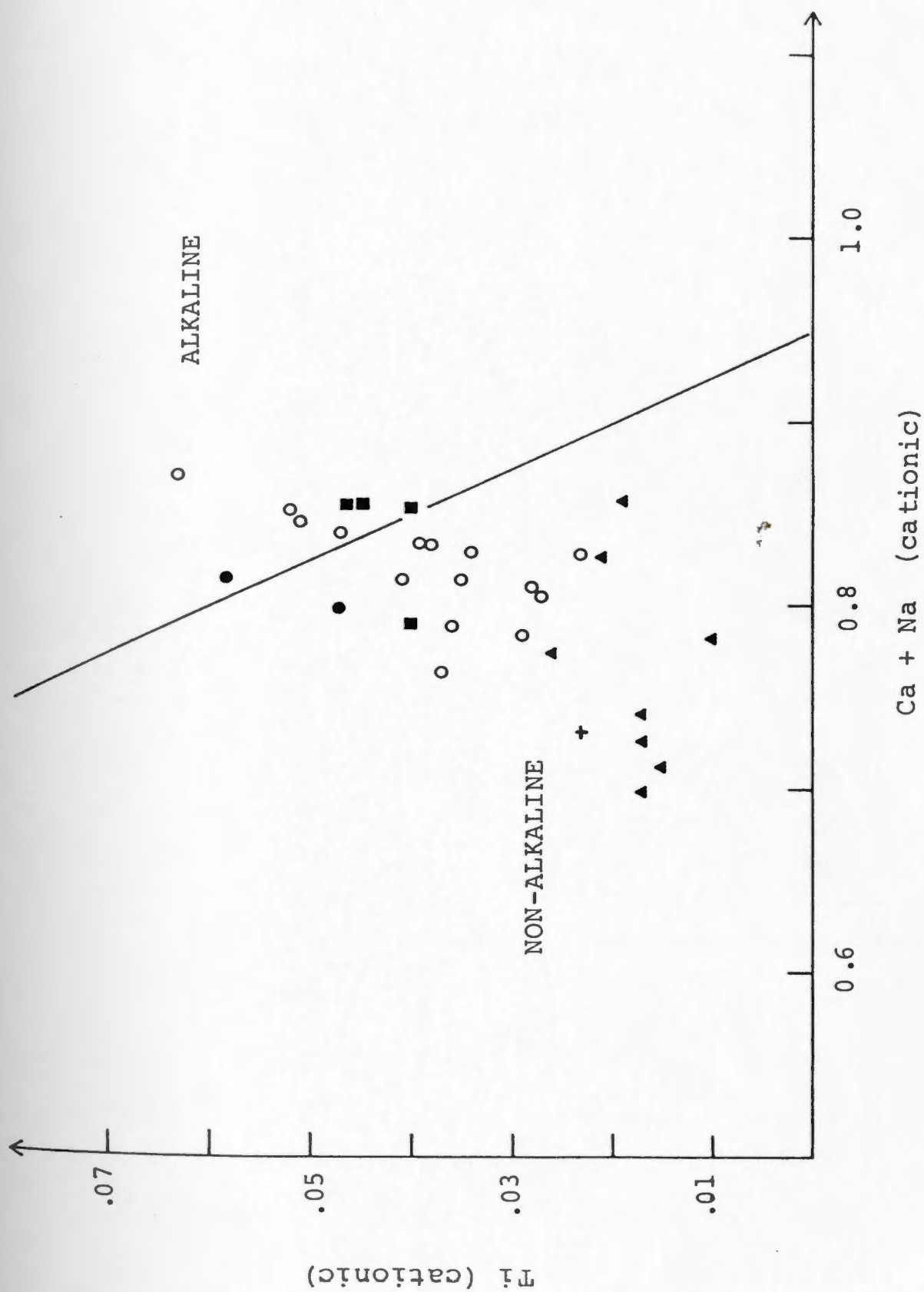


FIGURE 23. Characterisation of the magmatic parentage of the Blue Hills Sequence using the compositions of relict clinopyroxenes in the discriminant diagram of Leterrier et al. (1982). Symbols as for host rocks: ▲, pyroxene-phyric basaltic lavas; ○, aphyric basalt lavas; ●, Brigus Junction Inlier lavas; ■, sills; +, dyke. Note that this diagram displays a similar trend as observed in the previous diagrams (Figs. 21, 22) of increasing alkaline character with increasing stratigraphic position of the samples.



the Blue Hills Sequence on one of these diagrams. This plot is in general agreement with the LeBas (1962) diagrams and strengthens the positive correlation between increasing alkalinity with increasing stratigraphic height in the sequence.

*The present is the key to the past. -- Sir A. Geike*

## CHAPTER 6

### RECOGNITION OF TECTONIC AFFINITIES

#### 6.1 INTRODUCTION

Many people working in ancient geologic terranes rely heavily on volcanic rocks to provide evidence of palaeotectonic settings. It is therefore important to be able to recognise in which tectonic regime a lava sequence was erupted. In some cases this is easily achieved from field relations, petrography, and conventional major element diagrams. Often, however, the effects of deformation and/or metamorphism mask these lines of evidence so that less direct means of geochemical characterisation must be applied.

Several geologists (Miyashiro, 1973, 1974; Martin and Piwinski, 1972; Pearce, 1975, 1980; Pearce and Cann, 1973) have shown that basaltic rocks are characterised either by a relative enrichment or depletion of particular elements. As

a result of extensive sampling and comparison of geochemical trends in modern volcanic rocks, it has been possible to assign different basalt types to distinctive tectonic settings (ie. island-arc, ocean floor, continental rift, oceanic island, etc.). By careful selection of variables, discrimination diagrams can be drawn which highlight these various characteristics and therefore enable the distinction of basalts erupted in different tectonic settings, especially where geological evidence is ambiguous.

Existing models proposed for the evolution of the Avalon Zone suggest that the Harbour Main Group is related to either a late Precambrian rifting event (Papezik, 1972; Strong et al., 1978), or else it developed as an archipelago of volcanic islands related to subduction (Hughes, 1971; Rast et al., 1976). Until now, discrimination between these models has been rather subjective, as geochemical data, particularly in terms of immobile element abundances, were either unavailable or incomplete in previous studies. In this chapter the geochemical criteria which may be useful in the interpretation of the geologic and tectonic environment of formation of the Harbour Main Group are discussed.

## **6.2 TECTONIC AFFINITIES BASED ON WHOLE ROCK CHEMISTRY**

### **6.2.1 Major Oxides**

Because of the susceptibility of most of the major

elements to alteration, only  $\text{TiO}_2$ ,  $\text{FeO}^*$ , and  $\text{MgO}$  may be useful in determining tectonic environments. Although oxidation and alteration have probably changed the original abundances of  $\text{Fe}^{2+}$  and  $\text{Fe}^{3+}$  in these rocks, it is likely that the ratio  $\text{FeO}^*/\text{MgO}$  (total iron as  $\text{FeO}$ ) has changed little except possibly for extremely altered samples.

Figure 24 shows a trend of increasing  $\text{TiO}_2$  content with increasing  $\text{FeO}^*/\text{MgO}$  ratio in the volcanics of the Blue Hills Sequence. Bebie (1980) recognised that the patterns of variation of  $\text{TiO}_2$  content during magmatic evolution are different in the so-called 'orogenic' and 'non-orogenic' basic rock associations. Orogenic magmas are characterised by monotonically low  $\text{TiO}_2$  contents whereas non-orogenic basaltic rocks are distinguished by enrichment in  $\text{TiO}_2$  with fractional crystallisation. Figure 24 also shows trends of some typical orogenic and non-orogenic rock suites for comparison.

### 6.2.2 Trace Elements

In terms of trace elements, the most valuable for determining tectonic setting are Zr, Nb, and Y, all of which have previously been shown to be relatively unaffected by low-grade metamorphism and other secondary processes in these rocks (see Fig. 9 and section 5.3). In Figure 25,  $\text{Zr/Y}$  is plotted against  $\text{Ti/Y}$ . This discrimination diagram is analogous to the triangular Ti-Zr-Y diagram of Pearce and

FIGURE 24. Plot of  $\text{TiO}_2 - \text{FeO}^*/\text{MgO}$  for rocks of the Blue Hills Sequence. Symbols for samples:  $\odot$ , 058-1;  $\blacktriangle$ , pyroxene-phyric basaltic lavas;  $\circ$ , aphyric basalt lavas;  $\bullet$ , Brigus Junction Inlier lavas;  $\blacksquare$ , sills;  $+$ , dyke. The dividing line between 'non-orogenic' (NO) and 'orogenic' (OR) mafic suites is from Bebout (1982). For comparison, fractionation trends for: Skaergaard liquid (A), abyssal tholeiites (B), island arc tholeiite series (C,D), and island arc calc-alkaline series (E,F) are shown (after Miyashiro, 1973).

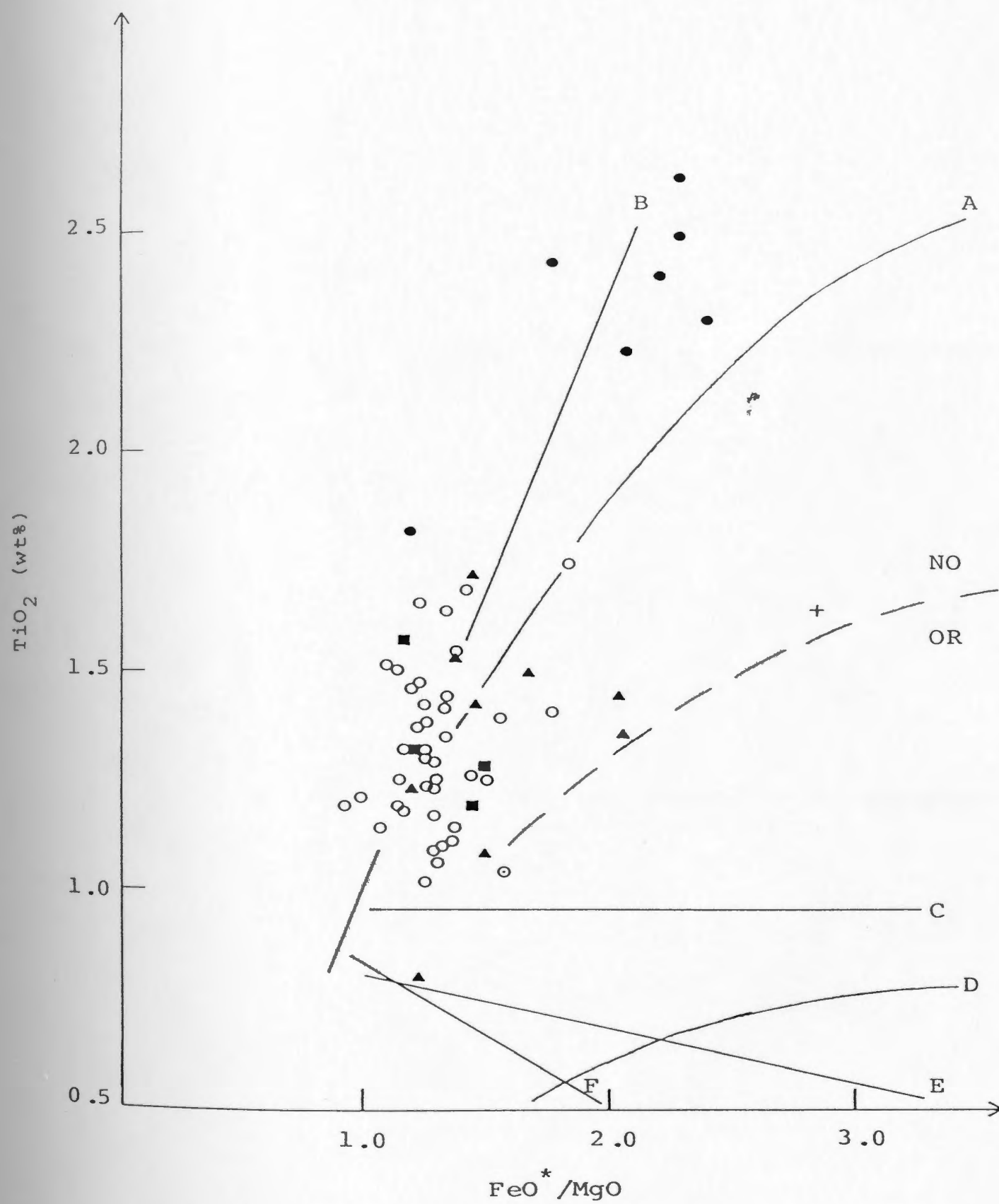
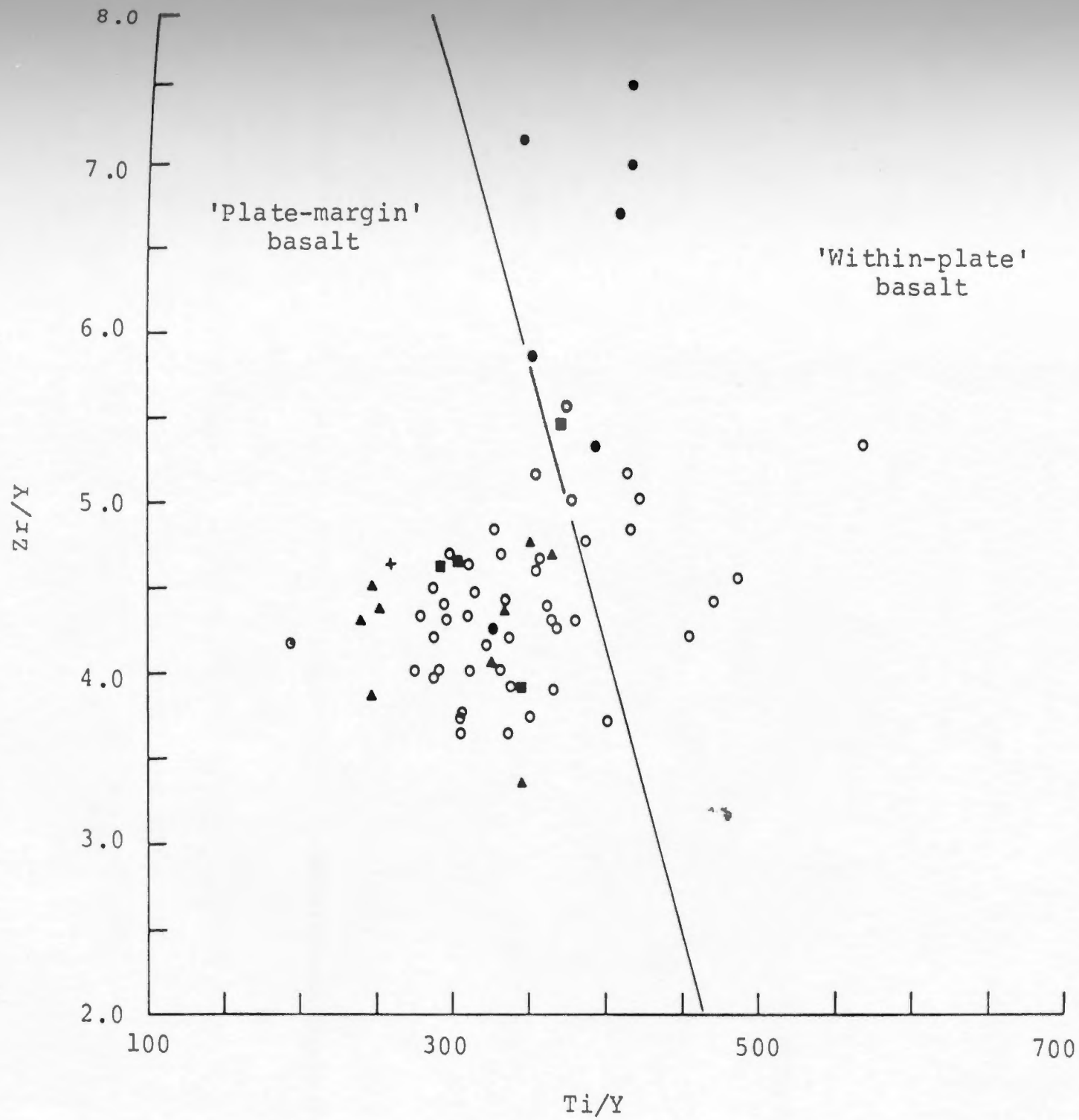


FIGURE 25. Samples from the various units of the Blue Hills Sequence plotted on the Zr/Y - Ti/Y discrimination diagram of Pearce and Gale (1977) (analogous to the Ti - Zr - Y diagram of Pearce and Cann, 1973). The diagram separates volcanics of within-plate affinity from magma types of other tectonic settings. Symbols for samples: ⊙, 058-1; ▲, pyroxene-phyric basaltic lavas; ○, aphyric basalt lavas; ●, Brigus Junction Inlier lavas; ■, sills; +, dyke.

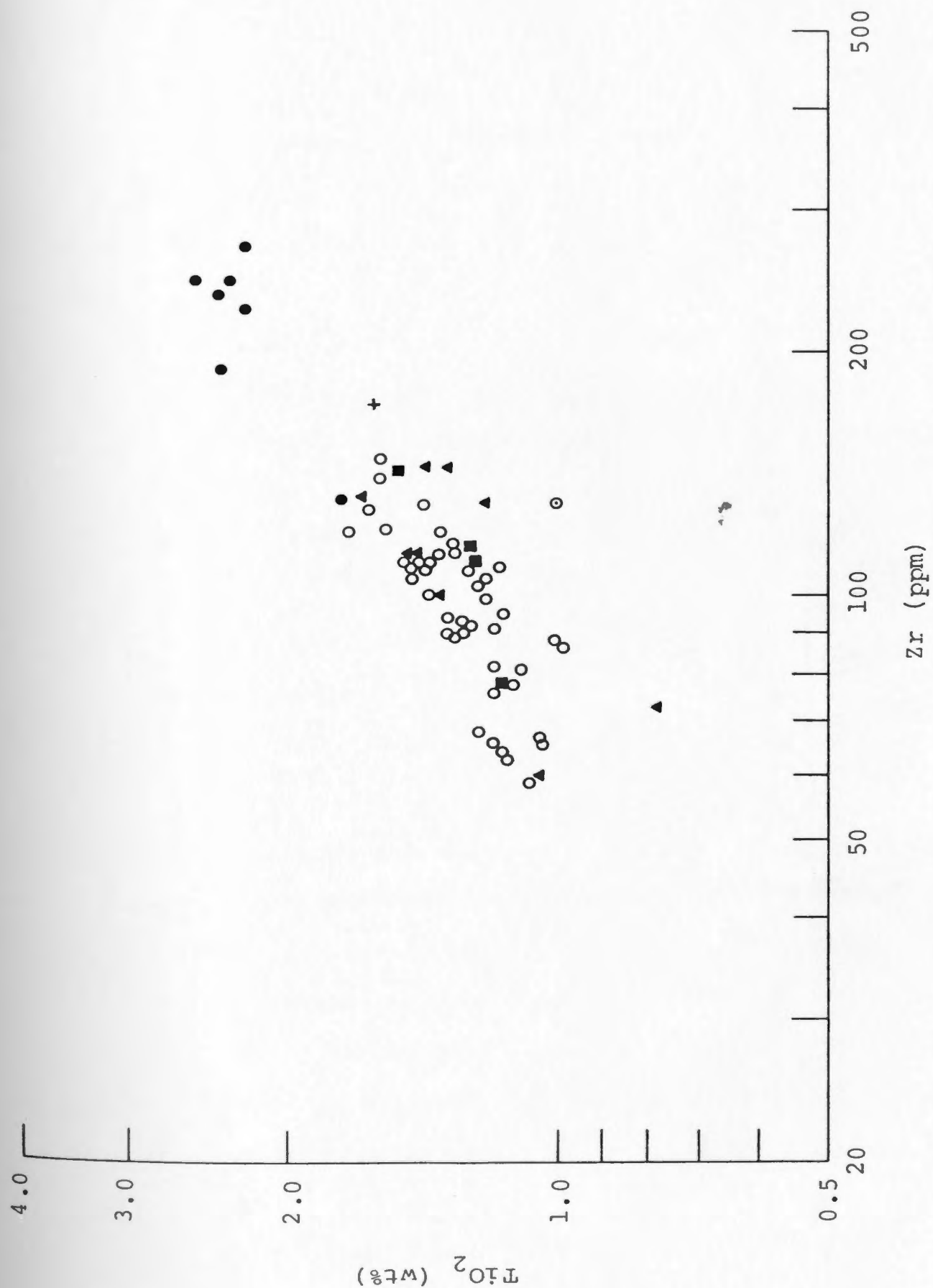


Cann (1973), which sometimes produces misleading results because the 'ocean-floor basalt' field has been shown to include all tholeiitic basalts formed in a rifting environment (mid-oceanic ridge, continental rifting, etc.) (Floyd and Winchester, 1975; Cameron, 1980; Holm, 1982). The Zr/Y versus Ti/Y diagram distinguishes 'within plate' from 'other' (plate margin) magma types. Although the analysed samples straddle this boundary, there is an apparent trend. The stratigraphically lower lavas lie furthest in the 'plate-margin' field, and there is a gradual transition into the 'within-plate' field with increased stratigraphic height in the section.

Pearce and Cann (1973), Pearce and Gale (1981), Gale and Pearce (1982) have shown that a plot of  $\text{TiO}_2$  versus Zr can be useful as an indicator of tectonic affinity in altered volcanic rocks because these elements are only slightly, if at all, affected by alteration and low-grade metamorphism. Figure 26 exhibits a positive correlation between the incompatible elements  $\text{TiO}_2$  and Zr in the analysed samples. The trend displayed by these lavas is similar to recent mafic suites erupted at extensional tectonic settings. In contrast, basalts from compressional tectonic settings (eg. volcanic arcs) show little or no increase in  $\text{TiO}_2$  with increasing Zr contents, thus producing a near horizontal trend on this discrimination diagram (Pearce, 1982).

In a similar manner, Pearce and Norry (1979) prepared a

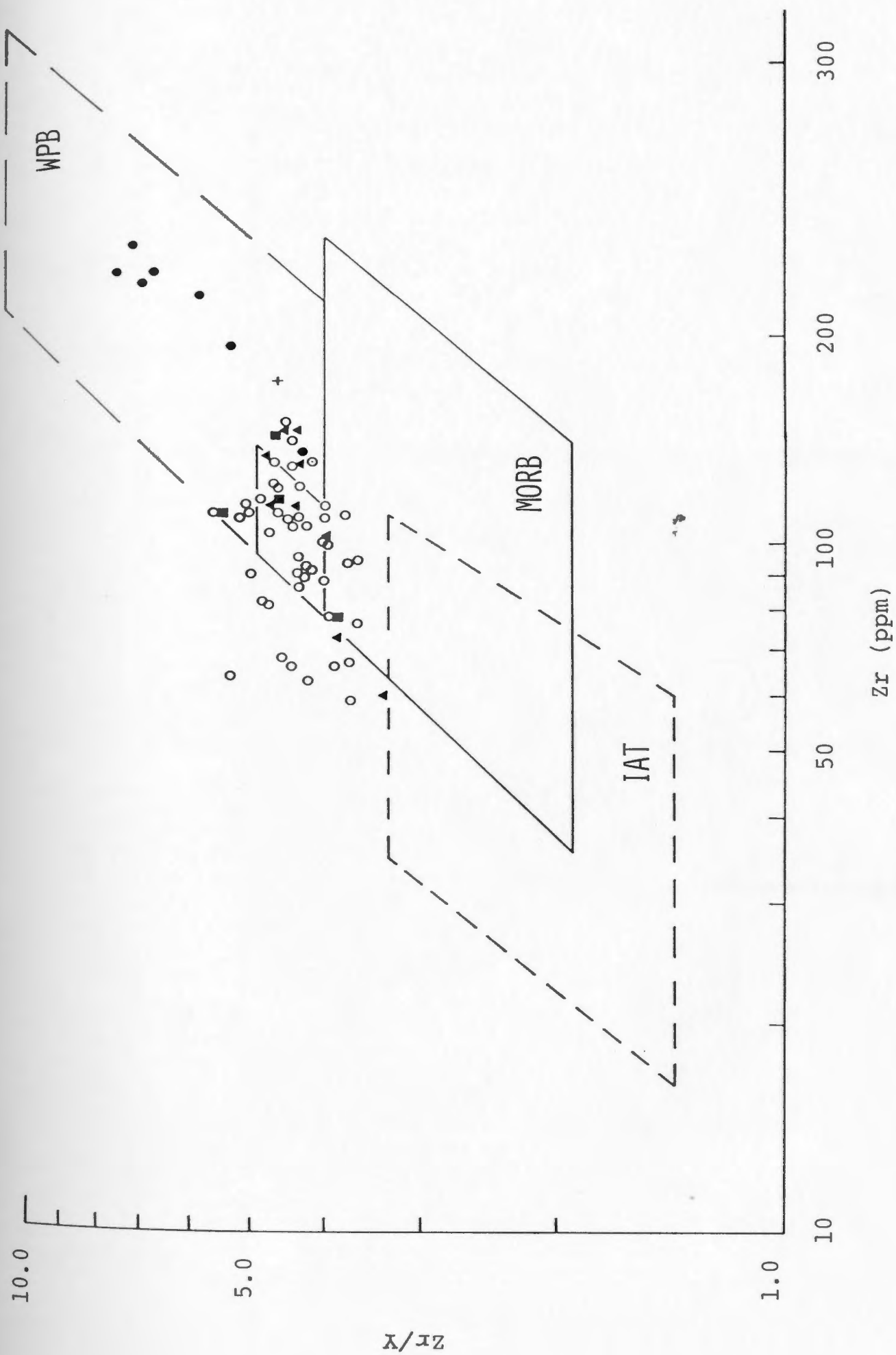
FIGURE 26. Plot of  $\text{TiO}_2$  versus Zr content in rocks of the Blue Hills Sequence. Symbols for samples:  $\odot$ , 058-1;  $\blacktriangle$ , pyroxene-phyric basaltic lavas;  $\circ$ , aphyric basalt lavas;  $\bullet$ , Brigus Junction Inlier lavas;  $\blacksquare$ , sills; +, dyke. Diagram is modified after Pearce and Cann (1973) and Pearce (1980). Mafic volcanic rocks from non-orogenic tectonic settings are characterised by a positive correlation in titanium and zirconium values such as is displayed here, whereas orogenic lavas display a progressive increase in Zr while  $\text{TiO}_2$  remains relatively constant.



plot of  $Zr/Y$  against  $Zr$  in order to discriminate between basaltic suites from different tectonic settings. Although there is some overlap between field boundaries it should be noted that island-arc tholeiites (IAT) are characterised by low  $Zr/Y$  ratios and lower  $Zr$  values than mid-ocean ridge basalts (MORB) or within-plate basalts (WPB). As with the previous diagrams the result of plotting analysed samples from the Blue Hills Sequence is a general trend with positive correlation on this diagram (Fig. 27). Samples from the stratigraphically lower lavas and most of the main series are classified as 'ocean-floor basalts', while the Brigus Junction Inlier lavas and others from the main series appear as 'within-plate basalts'. This is in general agreement with Figures 25 and 26.

Table 2 (Ch. 4) reports  $Ti/V$  values for the analysed samples and these may be used both as indicators of alkalinity and tectonic setting of basaltic rocks (Shervais, 1982). MORBs are confined almost entirely to  $Ti/V$  ratios between 20 and 50 regardless of whether they are 'normal' or 'enriched' ocean-floor basalts. Continental flood basalts have the same range in  $Ti/V$  as MORB, but tend to have higher absolute abundances. Volcanic rocks from island arc-related settings have  $Ti/V$  ratios generally less than 20. Calc-alkaline series from volcanic arc associations have slightly higher  $Ti/V$  ratios but produce negatively sloped trends on a  $Ti-V$  diagram, which implies magnetite fractionation throughout their evolution (Shervais, 1982).

FIGURE 27. Discriminant diagram of Zr/Y ratio against Zr showing the tectonic affinities of analysed samples from the Blue Hills Sequence. Symbols for samples:  $\odot$ , 058-1;  $\blacktriangle$ , pyroxene-phyric basaltic lavas;  $\circ$ , aphyric basalt lavas;  $\bullet$ , Brigus Junction Inlier lavas;  $\blacksquare$ , sills;  $+$ , dyke. Field boundaries for mid-ocean ridge basalt (MORB), island arc tholeiites (IAT), and within plate basalt (WPB) are after Pearce and Norry (1979). Although some of the samples straddle boundaries, this diagram indicates a non-orogenic setting for these rocks.



Alkaline rocks have Ti/V ratios generally greater than 50. Figure 28 shows that rocks of the Blue Hills Sequence have Ti/V ratios between 20 and 50, with the exception of two samples from the Brigus Junction Inlier which have Ti/V slightly higher than 50.

### 6.3 TECTONIC AFFINITIES BASED ON CLINOPYROXENE COMPOSITION

Just as with whole rock chemical data, there are significant differences between clinopyroxenes from basalts of different tectonic settings. Clinopyroxenes from within-plate alkali basalts characteristically have high Na and Ti and low Si contents. Pyroxenes from within-plate tholeiites and ocean-floor basalts can usually be distinguished from volcanic arc basalts by their higher Ti, Fe, and Mn contents.

A  $\text{SiO}_2$ - $\text{TiO}_2$  diagram (Nisbet and Pearce, 1977) enables basaltic magmas to be characterised on the basis of pyroxene compositions. Results of analysed relict pyroxenes in rocks from the Blue Hills Sequence reaffirm the findings from whole rock data and indicate a stratigraphic progression from subalkaline rocks with transitional or 'plate-boundary' affinities to more alkaline samples with distinct 'within-plate' tendencies (Fig. 29).

This result is in good agreement with the discriminant diagram of Leterrier et al. (1982). Based on a statistical study of the Ti, Cr, and Ca contents of calcic

FIGURE 28. Ti - V (whole-rock chemistry) plot of mafic samples from the Blue Hills Sequence. Symbols for samples:  $\odot$ , 058-1;  $\blacktriangle$ , pyroxene-phyric basaltic lavas;  $\circ$ , aphyric basalt lavas;  $\bullet$ , Brigus Junction Inlier lavas;  $\blacksquare$ , sills;  $+$ , dyke. Volcanic rocks from modern island arcs have Ti/V ratios of  $\leq 20$ ; MORB and continental flood basalts, 20-50; alkaline rocks are generally  $\geq 50$ ; and back-arc basin basalts may have either arc-like or MORB-like Ti/V ratios (Shervais, 1982).

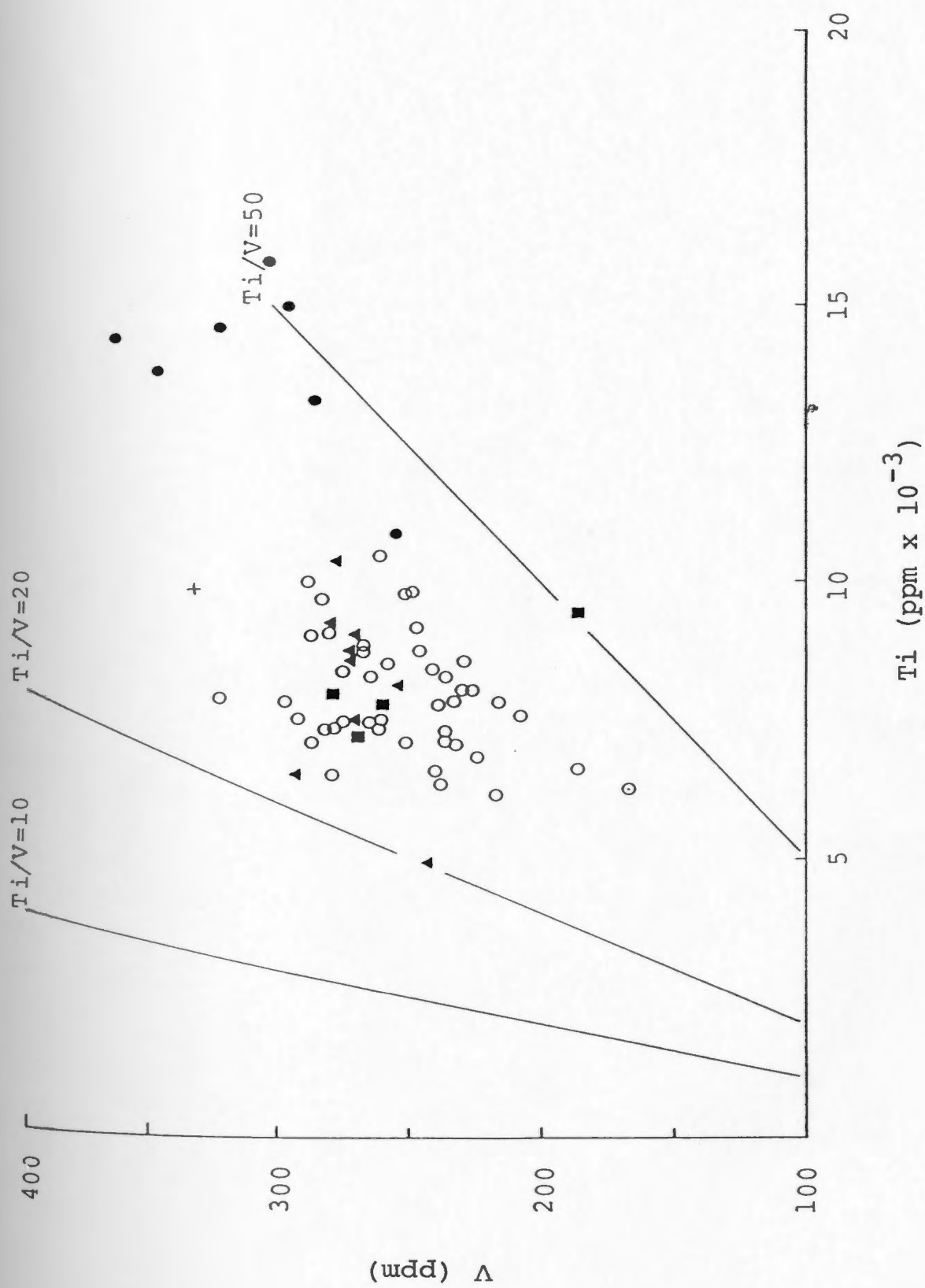
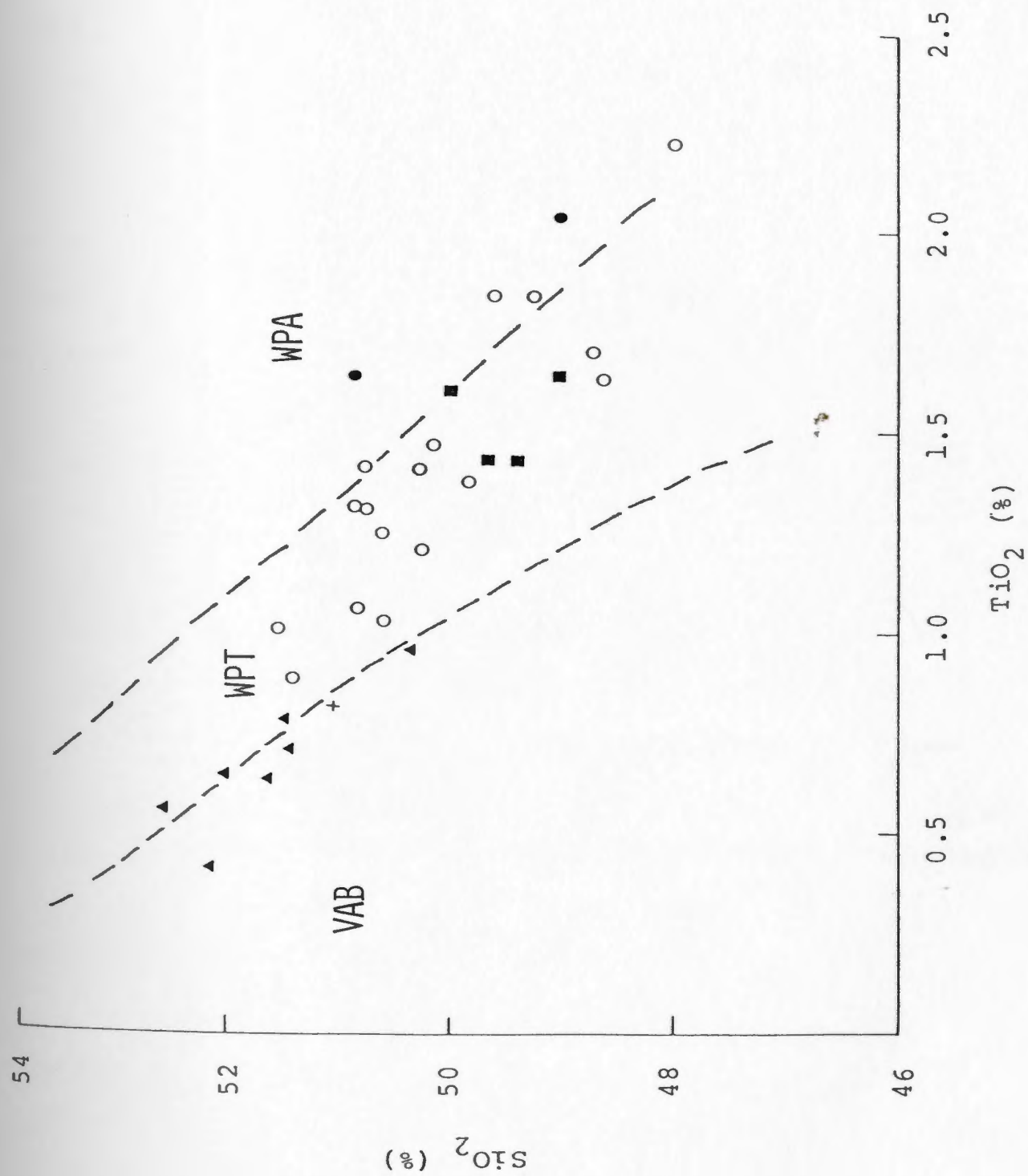


FIGURE 29. Tectonic setting of rocks from the Blue Hills Sequence based on the  $\text{SiO}_2$  -  $\text{TiO}_2$  covariation in relict clinopyroxenes. Symbols as for host rocks:  $\blacktriangle$ , pyroxene-phyric basaltic lavas;  $\circ$ , aphyric basalt lavas;  $\bullet$ , Brigus Junction Inlier lavas;  $\blacksquare$ , sills;  $+$ , dyke. The diagram indicates that pyroxenes from the stratigraphically lower lavas are similar in composition to those of volcanic arc basalts (VAB), while the majority of analysed pyroxenes are comparable to within-plate tholeiites (WPT) and a few are like those found in modern-day within-plate alkaline (WPA) varieties. Field boundaries are from Nisbet and Pearce (1977).



clinopyroxenes, they have been able to distinguish between rocks of 'non-orogenic' and 'orogenic' tectonic regimes. Using this diagram, the host rocks of the Blue Hills Sequence clinopyroxene are non-orogenic basalts (Fig. 30). Again there is good correlation between increasing stratigraphic height and increasingly non-orogenic character in the samples, with the stratigraphically lower pyroxene-phyric lavas actually straddling the boundary between the two fields.

#### 6.4 DISCUSSION OF RESULTS

It is clear from the foregoing that the tectonic evolution of this particular part of the Harbour Main Group of volcanics is complex and that simply looking at fields of a diagram into which analyses plot is not sufficient to define the tectonic setting of these rocks. More important are the trends defined on the various diagrams by the samples, combined with the knowledge of stratigraphic position of the rock units within the Blue Hills Sequence and information based upon field observations. What is consistent throughout all diagrams employed here is a trend indicative of an evolving rock suite by fractional crystallisation.

The obvious subaerial nature of lava flows from the Blue Hills Sequence (eg. oxidised and brecciated flow tops) and associated interflow terrestrial sediments makes it

FIGURE 30. Discriminant diagram of Leterrier et al. (1982) for determining the tectonic character of host volcanic rocks based upon the (Ti + Cr) and Ca contents of clinopyroxenes. Symbols for host rocks: ▲, pyroxene-phyric basaltic lavas; ○, aphyric basalt lavas; ●, Brigus Junction Inlier lavas; ■, sills; +, dyke. The majority of the analysed clinopyroxenes suggest a non-orogenic (NO) as opposed to an orogenic (OR) setting for rocks of the Blue Hills Sequence. This is in general agreement with other diagrams using pyroxene data as well as those plotted from whole rock compositions.



highly unlikely that these rocks represent a MORB-related tectonic environment as suggested by several of the discriminant diagrams. There is, however, a strong overall suggestion that these rocks were erupted in a non-orogenic environment which was undergoing extensional tectonic activity, with probable transitional affinities. As more data becomes available it seems that transitional tectonic settings may be more common than once realised. For example, transitional MORB/WPB types can be found in such spreading centres as Iceland or Afar (Pearce, 1980). Tectonic environments which appear transitional between WPB/IAT types may be formed above subduction zones in areas where continental back-arc rifting is taking place and close to trench-transform fault intersections (DeLong et al., 1976). These 'ensialic back-arc basins', the continuations of back-arc basins on continents, are reported to be volcano-tectonic rift zones characterised by rhyolite ash-flow tuffs, such as the Taupo Zone of New Zealand (Cole, 1981; Cole et al., 1983; Reid, 1983) and the Basin and Range Province of the southwestern United States (Scholz et al., 1971; Elston, 1976). Ash-flow tuff eruptions occur before tensional spreading of the back-arc basin. During spreading, volcanism is dominantly basaltic. Although difficult to fully substantiate, this style or pattern of volcanism is remarkably similar to what is observed in this area of the Harbour Main volcanics; that is, a thick sequence of ash-flow tuffs directly overlain by a series of

basaltic lava flows. A possible scenario of the tectonic evolution of this area which seems compatible with the transitional chemical data and field observations is that the extensive high-silica, high-alkali rhyolitic ash-flow tuffs of Nixon (1975) represent the last event in a compressional-related (transpressional?) volcanic episode. The release of compressive stress resulted in crustal extension, block faulting, and dominantly extensional-related basaltic volcanism which resulted in the Blue Hills Sequence.

*When you know a thing, to hold that you know it; and when you do not know a thing, to allow you do not know it - this is knowledge. -- Confucious*

## CHAPTER 7

### SUMMARY AND DISCUSSION

#### 7.1 SUMMARY

This study is concerned with a series of mafic lava flows and minor intrusives which constitute part of the late Precambrian Harbour Main Group in the southern part of Conception Bay, central Avalon Peninsula. Because of the observed field relationships of this sequence (Blue Hills Sequence) with the overlying basal Conception Group in the area, these rocks almost certainly represent the highest stratigraphy and perhaps the last geological expression of the Harbour Main Group.

Petrography, whole rock and mineral geochemistry indicate the presence of three distinct rock units within the Blue Hills Sequence; each representing a different stratigraphic level. The lowest section of the stratigraphy

is characterised by lavas rich in clinopyroxene phenocrysts and display sub-alkaline chemical tendencies. The bulk of the lava pile consists of sub-alkaline, transitional to mildly alkaline mafic varieties. The stratigraphically highest lavas from the Brigus Junction Inlier, are more alkaline in nature and display characteristics similar to volcanics erupted in non-orogenic tectonic settings. In addition to these three main units, there are plagiophyric sills which intrude all levels of the stratigraphy and chemically most resemble samples from the main part of the sequence. Although there are definite chemical and petrographic differences between the bottom of the stratigraphy and the highest level of the lava pile, chemical studies show that there are no significant compositional gaps from one stratigraphic level to the next. The overall trend of the entire sequence strongly suggests that the lavas are a result of differentiation from a common parent through fractionation of olivine, clinopyroxene, and plagioclase.

Compared to modern-day volcanics, the Blue Hills Sequence may represent a transitional type of tectonic setting where the stratigraphically lower lavas may be representative of a transpressional (Keppie, 1981) regime. The stratigraphically higher lavas represent a progressive change to a more tensional environment which perhaps may be viewed in terms of pull-apart basins bounded by block-faults (analogous to the Basin-Range Province). Basement to the

sequence may represent a transitional type of tectonic setting where the stratigraphically lower lavas may be representative of a transpressional (Keppie, 1981) regime. The stratigraphically higher lavas represent a progressive change to a more tensional environment which perhaps may be viewed in terms of pull-apart basins bounded by block-faults (analogous to the Basin-Range Province). Basement to the Harbour Main Group has not been identified, but the abundance of subaerial volcanism, the terrestrial sedimentary rocks, and essentially bimodal volcanism with a high felsic to mafic ratio in the map area suggests that the Group was deposited on continental crust. With minor modifications, these findings are consistent with those of Papezik (1972) and Strong and Minatidis (1975) among others who have been cited previously.

## 7.2 POSSIBLE REGIONAL CORRELATIONS

Previous workers (Rast et al., 1976; Giles and Ruitenberg, 1977; Keppie et al., 1979; Strong et al., 1979; Williams, 1979; O'Brien et al., 1983; Strong et al., 1984) have noted the widespread occurrence of Precambrian volcanics in the Avalon Zone of the Canadian Appalachians (Fig. 31). Many of these authors maintain that most, if not all, of these widespread rock groups are correlatives of one another. This has led to much confusion in terms of reconciling the tectonic significance of these

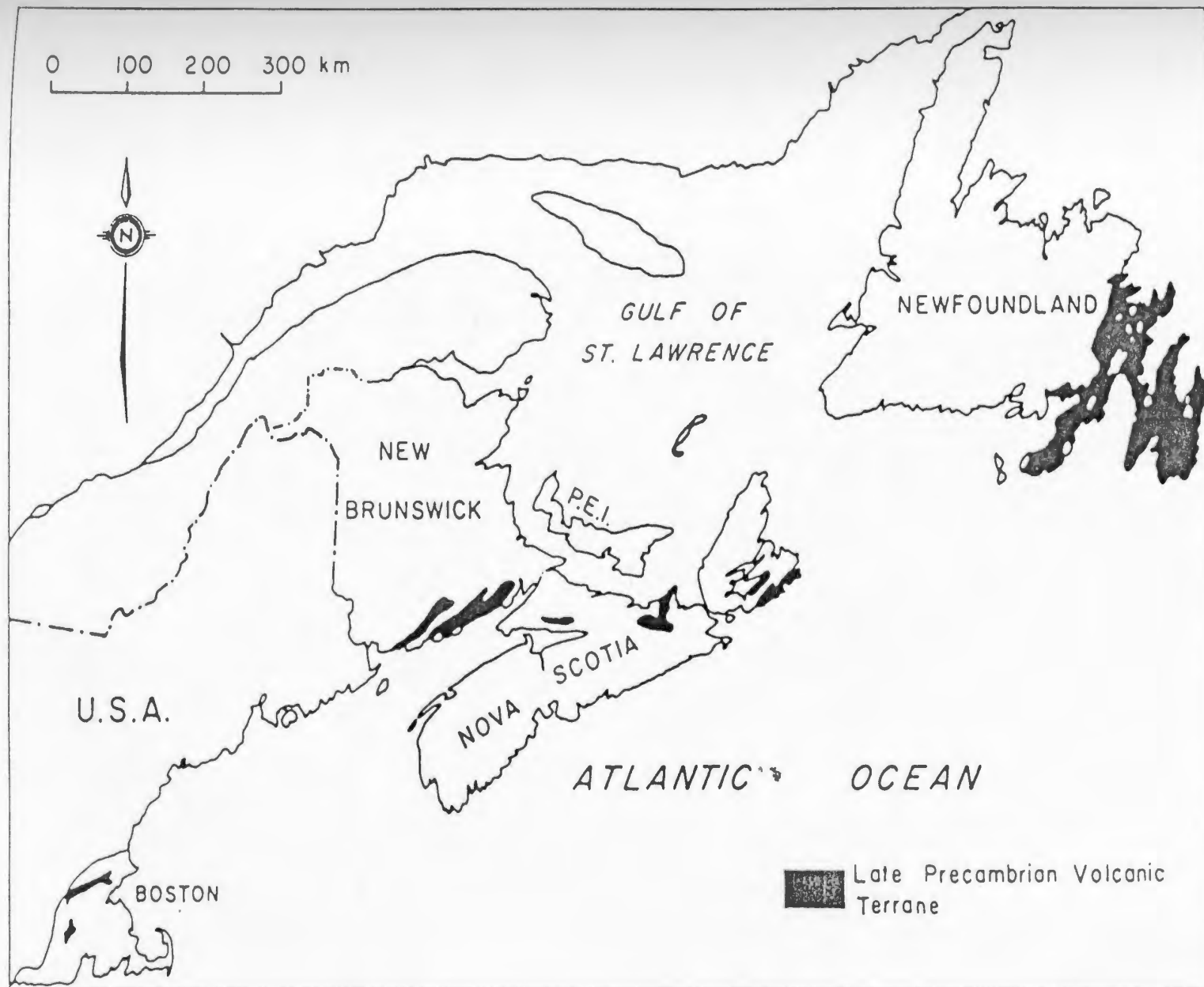


FIGURE 31. Map showing distribution of Late Precambrian volcanic rocks in the Avalon Zone of the northern Appalachians (from Keppie et al., 1979).

volcanics. It is true that the general lithologies of these volcanic groups are very similar, generally consisting of ash-flow tuffs, pyroclastics, mafic lavas, and interbedded terrestrial sediments. However, it should be realised that lithologies in modern-day volcanic terranes from widely different tectonic settings may exhibit very similar lithologies. (In short, a basalt looks like a basalt - no matter where you observe it.)

One reason for the confusion over the interpretations of tectonic significance of the various Precambrian Avalonian volcanics may be that many of the correlations have been based upon inadequate geochemical information. Much of the previous work in this area has dealt with major element analyses mainly of felsic volcanic members, neither of which is sufficiently diagnostic enough when dealing with ancient volcanic rock suites. In most instances the rocks involved have been subjected to secondary alteration processes which have undoubtedly affected the original bulk composition. In some recent work (eg. Strong et al., 1984), greater use is being made of 'immobile' trace element contents of mafic members of the various volcanic groups; both of which have been shown to be more useful in determining the tectonic signature of the rocks under study. Much more detailed geochemical information of this nature is required to more fully understand the significance of the Avalon Zone in the Appalachian Orogen.

In addition, it is unfortunate that there are so few precise age dates (for example, U-Pb ages from zircons) available for Precambrian volcanics of the Avalon Zone. Accurate and reliable age-dating of the various volcanic groups involved would greatly help to reconcile the many problems facing the understanding of the Precambrian development of the Avalon Zone. In particular, such information should be capable of resolving the question of whether these 'equivalent' rock units actually represent the same time span of the Precambrian.

**REFERENCES**

*Give every man thine ear, but few thy voice;  
Take every man's censure, but reserve thy judgement.*  
-- Shakespeare

- Abbey, S., 1983. Studies in "standard samples" of silicate rocks and minerals, 1969-1982. Geological Survey of Canada Paper 83-15, 114 pp.
- American Geological Institute, 1972. Glossary of Geology: Washington, D.C., 805 pp.
- Bebien, J., 1980. Magmatismes basiques dits "orogeniques" et "anorogeniques" et teneurs en  $\text{TiO}_2$ : Les associations "isotitanees" et "anisotitanees". Journal of Volcanology and Geothermal Research, 8: 337-342.
- Black, W.W., 1980. Chemical characteristics of metavolcanics in the Carolina Slate Belt. In: Proceedings, "The Caledonides in the U.S.A.". International Geological Correlation Project: Caledonide Orogen; I.G.C.P., 27, Blacksburg, Virginia: 271-278.
- Cameron, K.J., 1980. Geochemistry and petrogenesis of volcanic rocks from the Bourinot Group, Cape Breton Island, Nova Scotia. Unpublished B.Sc. Honours Thesis, St. Mary's University, Halifax, Nova Scotia, 123 pp.
- Cann, J.R., 1970. Rb, Sr, Y, Zr, Nb in some ocean-floor basaltic rocks. Earth and Planetary Science Letters, 10: 7-11.
- Cole, J.W., 1981. Genesis of lavas of the Taupo Volcanic Zone, North Island, New Zealand. Journal of Volcanology and Geothermal Research, 10: 317-337.
- Cole, J.W., Cashman, K.V., and Rankin, P.C., 1983.

rare-earth element geochemistry and the origin of andesites and basalts of the Taupo Volcanic Zone, New Zealand. *Chemical Geology*, 38: 255-274.

Cowie, J.W., 1964. The Cambrian Period. In: The Phanerozoic timescale. *Quarterly Journal of the Geological Society of London*, 120S: 254-259.

Dallmeyer, R.D., 1980. Geochronology report. In: Current Research, C.F. O'Driscoll and R.V. Gibbons (editors), Newfoundland Dept. of Mines and Energy, Report 80-1: 143-146.

Dallmeyer, R.D., Blackwood, R.F., and Odom, A.L., 1981. Age and origin of the Dover Fault: tectonic boundary between the Gander and Avalon Zones of the northeastern Newfoundland Appalachians. *Canadian Journal of Earth Sciences*, 8: 1431-1442.

Deer, W.A., Howie, R.A., and Zussman, J., 1971. 'An Introduction to the Rock-Forming Minerals'. Longman, London, 528 pp.

DeLong, S.E., Hodges, F.N., and Arculus, R.J., 1976. Ultramafic and mafic inclusions, Kanaga Island, Alaska, and occurrence of alkaline rocks in island arcs. *Geological Society of America Bulletin*, 87: 275-288.

Eby, N., 1972. Determination of rare-earth, yttrium, and scandium abundances in rocks and minerals by an ion exchange - X-ray fluorescence procedure. *Analytical Chemistry*, 44: 2137-2143.

Elston, W.E., 1976. Tectonic significance of mid-Tertiary

volcanism in the Basin and Range Province: A critical review with special reference to New Mexico. In: Cenozoic Volcanism in Southwestern New Mexico, W.E. Elston and S.A. Northrop (editors), New Mexico Geological Society, Special Publication No. 5: 93-102.

Fairbairn, H.W., Bottino, M.L., Pinson, W.H., Jr., and Hurley, P.M., 1966. Whole-rock age and initial  $^{87}\text{Sr}/^{86}\text{Sr}$  of volcanics underlying fossiliferous Lower Cambrian in the Atlantic Provinces of Canada. Canadian Journal of Earth Sciences, 3: 509-521.

Floyd, P.A. and Winchester, J.A., 1975. Magma type and tectonic setting discrimination using immobile elements. Earth and Planetary Science Letters, 27: 211-218.

Frith, R.A. and Poole, W.H., 1972. Late Precambrian rocks of eastern Avalon Peninsula, Newfoundland - A volcanic island complex: Discussion. Canadian Journal of Earth Sciences, 9: 1058-1059.

Fryer, B.J., 1977. Rare-earth evidence in iron formations for changing oxidation states. Geochimica et Cosmochimica Acta, 41: 361-367.

Gale, G.H. and Pearce, J.A., 1982. Geochemical patterns in Norwegian greenstones. Canadian Journal of Earth Sciences, 19: 385-397.

Giles, P.S. and Ruitenberg, A.A., 1977. Stratigraphy, palaeogeography, and tectonic setting of the Coldbrook

- Group in the Caledonia Highlands of southern New Brunswick. Canadian Journal of Earth Sciences, 14: 1263-1275.
- Greene, B.A. and Williams, H., 1974. New fossil localities and the base of the Cambrian in southeastern Newfoundland. Canadian Journal of Earth Sciences, 11: 319-323.
- Haworth, R.T. and LeFort, J.P., 1979. Geophysical evidence for the extent of the Avalon Zone in Atlantic Canada. Canadian Journal of Earth Sciences, 16: 552-567.
- Hellman, P.L. and Henderson, P., 1977. Are rare-earth elements mobile during spilitisation? Nature, 267: 38-40.
- Hellman, P.L., Smith, R.E., and Henderson, P., 1979. The mobility of the rare-earth elements: Evidence and implications from selected terrains affected by burial metamorphism. Contributions to Mineralogy and Petrology, 71: 23-44.
- Henderson, E.P., 1972. Surficial geology of the Avalon Peninsula, Newfoundland. Geological Survey of Canada, Memoir 368, 121 pp.
- Holm, P.E., 1982. Non-recognition of continental tholeiites using the Ti-Y-Zr diagram. Contributions to Mineralogy and Petrology, 79: 308-310.
- Howell, B.F., 1925. The faunas of the Cambrian Paradoxides beds at Manuels, Newfoundland. Bulletin of American Paleontology, 11: 1-140.

- Hughes, C.J., 1970. The late Precambrian Avalonian Orogeny in Avalon, southeast Newfoundland. *American Journal of Science*, 269: 183-190.
- Hughes, C.J., 1972. Geology of the Avalon Peninsula, Newfoundland and its possible correspondence with Morocco. *Notes et Memoires du Service Geologique de Maroc*, No. 236: 265-275.
- Hughes, C.J., 1973. Spilites, keratophyres, and the igneous spectrum. *Geological Magazine*, 109: 513-527.
- Hughes, C.J. and Bruckner, W.D., 1971. Late Precambrian rocks of eastern Avalon Peninsula, Newfoundland - A volcanic island complex. *Canadian Journal of Earth Sciences*, 8: 899-915.
- Humphris, S.E., Morrison, M.A., and Thompson, R.N., 1978. Influence of rock crystallisation history upon subsequent lanthanide mobility during hydrothermal alteration of basalts. *Chemical Geology*, 23: 125-137.
- Hutchinson, R.D., 1953. Geology of Harbour Grace map-area, Newfoundland. *Geological Survey of Canada, Memoir 275*.
- Irvine, T.N. and Baragar, W.R.A., 1971. A guide to the chemical classification of the common volcanic rocks. *Canadian Journal of Earth Sciences*, 8: 523-548.
- Jenness, S.E., 1963. Terra Nova and Bonavista map areas, Newfoundland *Geological Survey of Canada, Memoir 327*, 184 pp.
- Keppie, J.D., 1977. Tectonics of southern Nova Scotia. *Nova Scotia Dept. of Mines, Paper 77-1*, 34 pp.

- Keppie, J.D., 1981. Plate tectonics and tectonic mapping. Episodes, 1981: 11-14.
- Keppie, J.D., Dostal, J., and Murphy, J.B., 1979. Petrology of the late Precambrian Fourchu Group in the Louisbourg area, Cape Breton Island. Nova Scotia Dept. of Mines and Energy, Paper 79-1, 18 pp.
- King, A.F., 1980. The birth of the Caledonides: Late Precambrian rocks of the Avalon Peninsula, Newfoundland and their correlatives in the Appalachian Orogen. In: Proceedings, "The Caledonides in the U.S.A." International Geological Correlation Project: Caledonide Orogen; I.G.C.P., 27, Blacksburg, Virginia: 3-8.
- King, A.F., Brueckner, W.D., Anderson, M.M., and Fletcher, T., 1974. 'Late Precambrian and Cambrian sedimentary sequences of eastern Newfoundland'. Geological Association of Canada, Annual Meeting, Field Trip Manual B-6, 59 pp.
- Krogh, T.E., Strong, D.F., and Papezik, V.S., 1983. Precise U-Pb ages of zircons from volcanic and plutonic units in the Avalon Peninsula. Geological Society of America, Abstracts with Programs, N.E. Section, 15: p.135.
- Kushiro, I., 1960. Si-Al relations of clinopyroxenes from igneous rocks. American Journal of Science, 258: 548-554.
- LeBas, M.J., 1962. The role of aluminum in igneous

- clinopyroxenes with relation to their parentage. American Journal of Science, 260: 267-288.
- Leeman, W.P., Budahn, J.R., Gerlach, D.G., Smith, D.R., and Powell, B.N., 1980. Origin of Hawaiian tholeiites: Trace element constraints. American Journal of Science, 280-A: 794-819.
- Leterrier, J., Maury, R.C., Thonon, P., Girard, D., and Marchat, M., 1982. Clinopyroxene composition as a method of identification of the magmatic affinities of paleo-volcanic series. Earth and Planetary Science Letters, 59: 139-154.
- Lilly, H.D., 1966. Late Precambrian and Appalachian tectonics in light of submarine exploration of the Great Bank of Newfoundland and in the Gulf of St. Lawrence: Preliminary views. American Journal of Science, 264: 569-574.
- Long, L.T., 1979. The Carolina Slate Belt - Evidence of a continental rift zone. Geology, 7: 180-184.
- Martin, R.F. and Piwinski, A.J., 1972. Magmatism and tectonic settings. Journal of Geophysical Research, 77: 4966-4975.
- MacDonald, G.A., 1972. 'Volcanoes'. Prentice Hall, Englewood Cliffs, New Jersey, 510 pp.
- MacDonald, G.A. and Katsura, T., 1961. Chemical composition of Hawaiian lavas. Journal of Petrology, 5: 82-133.
- McCartney, W.D., 1967. Whitbourne map-area, Newfoundland.

Geological Survey of Canada, Memoir 341, 135 pp.

Miyashiro, A., 1973. The Troodos ophiolitic complex was probably formed in an island arc. *Earth and Planetary Science Letters*, 19: 218-224.

Miyashiro, A., 1974. Volcanic rock series in island arcs and active continental margins. *American journal of Science*, 274: 321-355.

Moorhouse, W.W., 1970. A comparative atlas of textures of Archean and younger volcanic rocks. Geological Association of Canada, Special Paper, No. 7 (edited by J.J. Fawcett).

Morrison, M.A., 1978. The use of 'immobile' trace elements to distinguish the palaeotectonic affinities of metabasalts: Applications to the Palaeocene basalts of Mull and Skye, northwest Scotland. *Earth and Planetary Science Letters*, 39: 407-416.

Murray, D.P., Rast, N., and Skehan, S.J., 1978. The convergence of the Caledonian and Variscan (Alleghanian) Episodes in the northern Appalachians. In: *Abstracts with Programs, I.G.C.P.: Caledonide Orogen, Dublin, Ireland.*

Nisbet, E.G. and Pearce, J.A., 1977. Clinopyroxene composition in mafic lavas from different tectonic settings. *Contributions to Mineralogy and Petrology*, 63: 149-160.

Nixon, G.T., 1975. Late Precambrian (Hadrynian) ash-flow tuffs and associated rocks of the Harbour Main Group

- near Colliers, Avalon Peninsula, southeastern Newfoundland. Unpublished M.Sc. Thesis, Memorial University of Newfoundland, St. John's, Newfoundland.
- Nixon, G.T. and Papezik, V.S., 1979. Late Precambrian ash-flow tuffs and associated rocks of the Harbour Main Group near Colliers, eastern Newfoundland: Chemistry and magmatic affinities. *Canadian Journal of Earth Sciences*, 16: 167-181.
- O'Brien, S.J., 1979. Volcanic stratigraphy, petrology, and geochemistry of the Marystown Group, Burin Peninsula, Newfoundland. Unpublished M.Sc. Thesis, Memorial University of Newfoundland, St. John's, Newfoundland, 253 pp.
- O'Brien, S.J., Strong, D.F., Strong, P.G., Taylor, S.W., and Wilton, D.H., 1976. South-eastern Newfoundland: Continental margin, island arc, aulacogen, or ocean basin? *Geological Association of Canada, Program and Abstracts*, p. 81.
- O'Brien, S.J., Strong, P.G., and Evans, J.L., 1977. Geology of the Grand Bank and Lamaline map-areas, Newfoundland. Newfoundland Dept. of Mines and Energy, Mineral Development Division, Report 77-7.
- O'Brien, S.J., Wardle, R.J., and King, A.F., 1983. The Avalon Zone: A Pan-African terrane in the Appalachian Orogen of Canada. *Geological Journal*, 18: 195-222.
- Papezik, V.S., 1969. Late Precambrian ignimbrites on the Avalon Peninsula, Newfoundland. *Canadian Journal of*

Earth Sciences, 6: 1405-1414.

papezik, V.S., 1970. Petrochemistry of volcanic rocks of the Harbour Main Group, Avalon Peninsula, Newfoundland. Canadian Journal of Earth Sciences, 7: 1485-1498.

papezik, V.S., 1972. Late Precambrian ignimbrites in eastern Newfoundland and their tectonic significance. In: Proceedings, 24th International Geological Congress, Section 1: 147-152.

papezik, V.S., 1974. Prehnite-pumpellyite facies metamorphism of late Precambrian rocks of the Avalon Peninsula, Newfoundland. Canadian Mineralogist, 12: 463-468.

Pearce, J.A., 1975. Basalt geochemistry used to investigate past tectonic environments on Cyprus. Tectonophysics, 25: 41-67.

Pearce, J.A., 1980. Geochemical evidence for the genesis and eruptive setting of lavas from Tethyan ophiolites. In: Panayiotou, A. (ed.) 'Ophiolites': Proceedings, International Ophiolite Symposium, Cyprus, 1979. The Geological Survey Dept., Cyprus. pp. 261-272.

Pearce, J.A., 1982. Trace element characteristics of lavas from destructive plate boundaries. In: Thorpe, R.S. (ed.), 'Orogenic Andesites'. J. Wiley and Sons, New York, pp. 525-548.

Pearce, J.A. and Cann, J.R., 1973. Tectonic setting of basic volcanic rocks determined using trace element analyses. Earth and Planetary Science Letters, 19:

290-300.

- pearce, J.A. and Gale, G.H., 1977. Identification of ore deposition environment from trace element geochemistry of associated igneous host rocks. In: Volcanic Processes in Ore Genesis. Geological Society of London, Special Publication, 7: 14-24.
- pearce, J.A. and Norry, M.J., 1979. Petrogenetic implications of Ti, Zr, Y, and Nb variations in volcanic rocks. Contributions to Mineralogy and Petrology, 69: 33-47.
- Poole, W.H., 1976. Plate tectonic evolution of the Canadian Appalachian region. In: Geological Survey of Canada, Paper 76-1B, pp. 113-126.
- Rast, N., O'Brien, B.H., and Wardle, R.J., 1976. Relationships between Precambrian and lower Palaeozoic rocks of the "Avalon Platform" in New Brunswick, the northeast Appalachians, and the British Isles. Tectonophysics, 30: 315-338.
- Reid, F., 1983. Origin of the rhyolitic rocks of the Taupo Volcanic Zone, New Zealand. Journal of Volcanology and Geothermal Research, 15: 315-338.
- Rodgers, J., 1970. 'The Tectonics of the Appalchians', J. Wiley and Sons, New York, 271 pp.
- Rodgers, J., 1972. Latest Precambrian (Post-Grenville) rocks of the Appalachian region. American Journal of Science, 272: 507-520.
- Rose, E.R., 1952. Torbay map-area, Newfoundland.

Geological survey of Canada, Memoir 265.

Ross, C.S. and Smith, R.L., 1961. Ash-flow tuffs: Their origin, geologic relations, and identification. United States Geological Survey, Professional Paper 366, 81 pp.

Schenk, P.E., 1971. Southeastern Atlantic Canada, northwestern Africa and continental drift. Canadian Journal of Earth Sciences, 8: 1218-1251.

Scholz, C.H., Barazangi, M., and Sbar, M.L., 1971. Late Cenozoic evolution of the Great Basin, western United States, as an ensialic interarc basin. Geological Society of America Bulletin, 82: 2979-2990.

Schweitzer, E.L., Papike, J.J., and Bence, A.E., 1979. Statistical analysis of clinopyroxenes from deep-sea basalts. American Mineralogist, 64: 501-513.

Shervais, J.W., 1982. Ti-V plots and the petrogenesis of modern and ophiolitic lavas. Earth and Planetary Science Letters, 59: 101-118.

Strong, D.F., 1979. Proterozoic tectonics of northwestern Gondwanaland: new evidence from eastern Newfoundland. Tectonophysics, 54: 81-101.

Strong, D.F., Dickson, W.L., O'Driscoll, C.F., and Kean, B.F., 1974. Geochemistry of eastern Newfoundland granitoid rocks. Newfoundland Dept. of Mines and Energy, Mineral Development Division, Report 74-3, 140 pp.

Strong, D.F. and Minatidis, D.G., 1975. Geochemistry and

tectonic setting of the late Precambrian Holyrood plutonic series of eastern Newfoundland. *Lithos*, 8: 283-295.

Strong, D.F., O'Brien, S.J., Taylor, S.W., Strong, P.G., and Wilton, D.H., 1978. Aborted Proterozoic rifting in eastern Newfoundland. *Canadian Journal of Earth Sciences*, 15: 117-131.

Strong, D.F., O'Brien, S.J., and Dostal, J., 1984. Petrochemical evolution of Late Proterozoic rocks of the Avalon Zone type-area in Newfoundland. *Geological Society of America, Abstracts with Programs, N.E. Section*, 16: p.65.

Stukas, V., 1977. Plagioclase release patterns: a high resolution  $^{40}\text{Ar}/^{39}\text{Ar}$  study. Unpublished PhD. Thesis, Dalhousie University, Halifax, Nova Scotia.

Taylor, S.R. and Gorton, M.P., 1977. Geochemical application of spark source mass spectrography - III. Element sensitivity, precision and accuracy. *Geochimica et Cosmochimica Acta*, 41: 1375-1380.

Thompson, R.N., Gibson, I.L., Marriner, G.F., Matthey, D.P., and Morrison, M.A., 1980. Trace-element evidence of multistage mantle fusion and polybaric fractional crystallisation in the Palaeocene lavas of Skye, N.W. Scotland. *Journal of Petrology*, 21: 265-293.

Whitney, J.A. Paris, T.A., Carpenter, R.H., and Hartley, M.E., III, 1978. Volcanic evolution of the Southern Slate Belt of Georgia and South Carolina: A primitive

- oceanic island arc. *Journal of Geology*, 86: 173-192.
- Williams, H., (compiler), 1978. Tectonic-lithofacies map of the Appalachian Orogen. Memorial University of Newfoundland, Map No. 1.
- Williams, H., 1979. Appalachian Orogen in Canada. *Canadian Journal of Earth Sciences*, 16: 792-807.
- Williams, H., 1984. Miogeoclines and suspect terranes of the Caledonian- Appalachian Orogen: Tectonic patterns in the North Atlantic region. *Canadian Journal of Earth Sciences*, 21: 887-901.
- Williams, H., Kennedy, M.J., and Neale, E.R.W., 1972. The Appalachian structural province. In: Price, R.A. and Douglas, R.J.W. (eds.), *Variations in Tectonic Styles in Canada*. Geological Association of Canada, Special Paper, 11: pp. 183-261.
- Williams, H. and King, A.F., 1979. Trepassey map-area, Newfoundland. Geological Survey of Canada, Memoir 389, 24 pp.
- Winchester, J.A. and Floyd, P.A., 1976. Geochemical magma type discrimination: Application to altered and metamorphosed basic igneous rocks. *Earth and Planetary Science Letters*, 28: 459-469.
- Winchester, J.A. and Floyd, P.A., 1977. Geochemical discrimination of different magma series and their differentiation products using immobile elements. *Chemical Geology*, 20: 325-343.
- Wise, D.U., 1982. Linesmanship and the practice of linear

geo-art. Geological Society of America Bulletin, 93: 886-888.

Wood, D.A., Gibson, I.L., and Thompson, R.N., 1976. Elemental mobility during zeolite facies metamorphism of the Tertiary basalts of eastern Iceland. Contributions to Mineralogy and Petrology, 55: 241-254.

Wright, J.E. and Seiders, V.M., 1980. Age of zircon from volcanic rocks of the central North Carolina Piedmont and tectonic implications for the Carolina Slate Belt. Geological Society of America Bulletin, 91: 287-294.

*When we look at a thing, we must examine its essence and treat its appearance merely as an usher at the threshold, and once we cross the threshold, we must grasp the essence of the thing; this is the only reliable and scientific method of analysis. -- Mao*

## APPENDIX A

### ANALYTICAL METHODS

#### A.1 SAMPLING PROCEDURE

Specimens for chemical analyses were collected with the aim of obtaining as representative a sampling as possible of the various stratigraphic units of the Blue Hills Sequence. Certain difficulties encountered with sampling are noted here. An inherent problem of mapping and sampling in volcanic terranes (especially ancient ones) is that in most cases the lava flows are not uniform in thickness throughout their distribution and very seldom do they cover an entire area. This problem is compounded in ancient volcanic fields which have been folded, faulted, and are otherwise structurally complicated. Although exposure in the Blue

Hills Sequence is generally good, in many cases individual flows cannot be traced along strike for more than a few hundred metres. In the Brigus Junction Inlier exposure is generally poor with only a few areas having continuous outcrop. In addition, a large proportion of the material exposed here consists of pyroclastic and epiclastic rock types. As a result only a few samples representative of lavas in this area have been analysed.

Analysed samples for this study have been taken primarily from the massive central portions of thicker flows and mafic units. Efforts were made to avoid sampling rocks which showed any obvious macroscopic evidence of alteration (eg. amygdules, veining, oxidation). Wherever possible, a single bulk sample of about 1 to 2 kg was taken for analysis. In some cases, however, it was necessary to take chip samples from an outcrop to make up a representative sample. Further screening of specimens was done during petrographic study of these rocks carried out prior to analysis.

## A.2 SAMPLE PREPARATION

After removing the weathered surfaces, samples chosen for analysis were broken into 3-4 cm pieces using a hydraulic press. These were then crushed to chips (5-10 mm) using a Braun 'chipmunk' jaw-crusher. The plates of this machine were brushed and scrubbed between each sample to

minimise contamination. Each sample was checked visually for any contamination from the steel plates of the jaw-crusher. The rock chips were shaken in a plastic bag to ensure homogeneity. A portion of the chips was pulverised in a Siebtechnik tungsten-carbide 'TEMA' swing mill for 1-2 minutes. The powder should be between 100 and 200 mesh. To ensure homogeneity, the powder was mixed and sample splits were taken. The tungsten-carbide bowl and rings were cleaned between each sample. The risk of contamination was lessened by crushing and discarding a portion of sample in the precleaned bowl before the main bulk of the sample was pulverised. After every third sample, silica sand was pulverised, discarded, and the bowl washed to further ensure clean grinding conditions.

### A.3 MAJOR OXIDE ANALYSIS (AND PHOSPHORUS AND L.O.I.)

Major and minor oxides were determined on a Perkin Elmer model 2380 atomic absorption spectrophotometer at Memorial University. Samples were prepared according to the method outlined below:

1. Exactly 0.1000 gram of rock powder is weighed out and placed in a clean, labelled, 'Nalgene' polycarbonate digestion bottle.
2. Using a precise volume dispenser, 5 mls HF (stock solution) is added to each digestion bottle to effect

dissolution of the powder. The mixture is heated on a steam-bath for about 1/2 hour.

3. After cooling of the solution, 50 mls of saturated boric acid solution ( $\text{H}_3\text{BO}_4$ ) is added (using an automatic pipette) to complex undissolved fluorides. The bottle is returned to the steam-bath until solution is clear.
4. After cooling, exactly 145 mls distilled water is added (using an automatic pipette) and the mixture is shaken.

Phosphorus was determined by dilution and treatment of a 5 ml aliquot of the sample solution. The samples were then analysed on a Bausch and Lomb Spectronic 20 colourimeter.

Samples were analysed and compared to standard solutions and standard blends by G. Andrews. Precision of major element analysis, as determined by replicate analysis of a representative sample (172-2), is generally better than 5% for most elements (Table A-1).

Loss on ignition (L.O.I.) was determined by weighing an amount of sample into a porcelain crucible, heating in a muffle furnace at  $1050^\circ\text{C}$  for 2 hours, cooling in a dessicator, and re-weighing to determine the percent weight loss of volatiles.

#### A.4 TRACE ELEMENT ANALYSIS

Trace element contents in the samples were determined using a Philips 1450 fully automated sequential X-ray

TABLE A-1.      PRECISION OF MAJOR ELEMENT ANALYSIS  
(Sample 172-2)

	$\bar{X}$	s	C
SiO <sub>2</sub> (wt.%)	46.5	0.21	0.45
TiO <sub>2</sub>	1.41	0.01	0.71
Al <sub>2</sub> O <sub>3</sub>	16.57	0.29	1.75
Fe <sub>2</sub> O <sub>3</sub> *	11.64	0.12	1.03
MnO	0.21	0.01	4.76
MgO	8.85	0.23	2.60
CaO	5.94	0.03	0.51
Na <sub>2</sub> O	3.25	0.09	2.77
K <sub>2</sub> O	1.70	0.02	1.18
P <sub>2</sub> O <sub>5</sub>	0.33	0.02	6.06
L.O.I.	3.97	0.17	4.37

Notes:    \* Total iron as Fe<sub>2</sub>O<sub>3</sub>

n = 3

$\bar{X}$  = mean

s = one standard deviation (n-1)

C = coefficient of variation  $\frac{s}{\bar{X}} \times 100$

fluorescence spectrometer equipped with a self-feeding sample tray and linked to an HP-85 mini-computer. All trace elements were analysed using a rhodium target X-ray tube.

Pressed powder pellets used for trace element analyses are prepared in the following manner:

1. Rock powders are mixed in their vials to ensure homogeneity.
2. Approximately 10 grams of powder is weighed into a precleaned and labelled dry mixing bottle. To this is added 1.4 to 1.5 grams of a phenyl formaldehyde binder (low density Union Carbide Phenolic Resin material BRP-5933). Two stainless steel ball bearings are placed into each bottle which are then capped and swirled manually for a few seconds to ensure initial mixing of rock powder and binder. The sample is then mixed for about 10 minutes.
3. The homogenised sample is loaded into the 40 mm diameter die of a Herzog hydraulic press and subjected to a pressure of 50 MPa (~20 tons p.s.i.) for 10 seconds.
4. The pressed pellet is removed from the press and placed on an aluminum tray. After each sample the die on the press is thoroughly cleaned with methanol.
5. The pressed discs are heated in an oven (200°C) for 15 minutes. After cooling, the pellets are labelled and stored for later analysis.

During analysis, representative samples were chosen

to act as internal standards and, along with several U.S.G.S. rock standards, were analysed on the X.R.F. for the determination of precision and accuracy. (Tables A-2,3).

#### A.5 RARE-EARTH ELEMENT ANALYSIS

Rare-earth element abundances were determined by a thin film X-ray fluorescence method of Eby (1972) modified by Fryer (1977). A summary of the method follows:

1. Approximately 1.5 grams of rock powder is weighed into a clean 100 ml Teflon beaker (amount of sample used depends upon trace element concentration).
2. Exactly 2.5 ml of 25  $\mu\text{g}/\text{ml}$  Tm spike solution (approximately 50  $\mu\text{g}$  in solution) is pipetted into the beaker. To this is added 15 mls HF and 2 mls  $\text{HClO}_4$ . The sample is evaporated to dryness.
3. Another 15 mls HF are added and evaporated to complete dryness.
4. 15 mls 2N HCl plus 2 mls  $\text{HClO}_4$  are added and evaporated again to dryness.
5. Another 15 mls 2N HCl are added, and the sample is again evaporated to complete dryness.
6. 5 mls 2N HCl are added and warmed to dissolve the precipitate. When dissolved, the sample is diluted to a 1N HCl solution.
7. The solution is transferred to a centrifuge tube, topped

TABLE A-2. PRECISION OF TRACE ELEMENT ANALYSIS BY X-RAY FLUORESCENCE (all values in ppm)

		022-1	108-3	136-1	145-2	172-2	221-2
	$\bar{X}$	49	35	27	78	42	41
Rb	s	0.84	2.51	0.84	2.17	2.88	3.96
	C	1.71	7.17	3.11	2.78	6.86	9.66
	$\bar{X}$	692	659	585	568	599	707
Sr	s	5.36	0.84	3.78	2.61	5.46	5.70
	C	0.77	0.13	0.65	0.46	0.91	0.81
	$\bar{X}$	1493	905	166	1009	938	540
Ba	s	29.74	27.28	31.05	8.71	25.82	39.75
	C	1.99	3.01	18.70	0.86	2.75	7.36
	$\bar{X}$	20	18	15	47	24	16
Y	s	1.41	0.89	1.14	1.92	2.00	2.19
	C	7.05	4.94	7.6	4.09	8.33	13.69
	$\bar{X}$	91	71	59	245	104	67
Zr	s	2.92	2.30	1.82	2.30	2.68	1.52
	C	3.21	3.24	3.08	0.94	2.58	2.27
	$\bar{X}$	4	4	2	17	6	3
Nb	s	0.71	0.55	0.89	1.00	1.14	1.64
	C	17.75	13.75	44.5	5.88	19.0	54.67
	$\bar{X}$	282	243	189	300	273	278
V	s	5.43	5.79	2.77	1.95	4.72	3.58
	C	1.93	2.38	1.47	0.65	1.73	1.29
	$\bar{X}$	84	142	57	68	125	70
Cr	s	3.83	5.63	3.36	2.79	2.17	4.22
	C	4.56	3.96	5.89	4.10	1.74	6.03
	$\bar{X}$	88	66	80	80	100	94
Ni	s	2.00	3.21	1.82	2.12	2.45	3.42
	C	2.27	4.86	2.28	2.65	2.45	3.64
	$\bar{X}$	15	16	17	16	16	17
Ga	s	2.59	1.30	1.82	3.70	2.61	1.41
	C	17.27	8.13	10.71	23.13	16.31	8.29

Notes: n = 5

 $\bar{X}$  = mean

s = one standard deviation (n-1)

C = coefficient of variation  $\frac{s}{\bar{X}} \times 100$

TABLE A-3. ACCURACY OF TRACE ELEMENT ANALYSIS BY X-RAY FLUORESCENCE (all values in ppm)

		BCR-1	AGV-1	BHVO-1	GSP-1	G-2	W-1
	n	15	11	5	3	3	4
Rb	$\bar{X}$	51	73	14	254	170	28
	s	3.33	2.2	7.43	7.77	3.21	4.03
	R	47	67	10	250	170	21
Sr	$\bar{X}$	328	656	389	229	459	186
	s	4.39	5.99	7.43	4.04	6.00	1.26
	R	330	660	420	240	480	190
Ba	$\bar{X}$	767	1238	210	1236	1859	232
	s	41.13	29.74	17.69	85.05	55.86	31.03
	R	680	1200	135	1300	1900	160
Y	$\bar{X}$	45	23	30	34	10	26
	s	2.34	1.62	3.29	4.93	3.61	3.00
	R	40	19	27	29	11	25
Zr	$\bar{X}$	189	232	175	500	302	96
	s	3.48	3.14	4.34	6.35	1.15	1.71
	R	185	230	180	500	300	105
Nb	$\bar{X}$	15	16	22	29	15	10
	s	1.46	1.45	2.00	3.61	4.93	2.22
	R	19	16	19	23	13	9.5
V	$\bar{X}$	413	125	297	48	32	255
	s	8.98	4.71	5.81	4.04	1.41	8.37
	R	420	125	320	54	36	260
Cr	$\bar{X}$	14	2	208		4	90
	s	3.44	1.37	5.00		3.79	5.72
	R	15	10	300		8	115
Ni	$\bar{X}$	15	15	117	24	7	77
	s	3.14	1.14	2.19	17.62	1.41	4.11
	R	10	15	120	9	3.5	76
Ga	$\bar{X}$	21	22	21	23	23	17
	s	2.14	2.66	2.92	4.16	5.2	2.36
	R	22	21	21	23	23	16

Notes: n = number of determinations  
 $\bar{X}$  = mean  
s = one standard deviation (n-1)  
R = recommended value from Abbey, 1983

- with distilled water, and centrifuged for 2-3 minutes.
8. The sample is returned to its 100 ml Teflon beaker.
  9. The solution is filtered into a previously cleaned and pH balanced column containing a strong cation exchange resin (Fisher-Rexyn 10 Na-form).
  10. To remove all cations up to and including Sr, 105 mls 2N HCl is added (add 5 mls and then 100 mls so as not to disturb the resin bed). The eluted solution is discarded.
  11. The REE are collected in clean Teflon beakers by eluting the column with 100 mls 6N HCl. This solution is evaporated to dryness.
  12. The solid is re-dissolved in 20 mls distilled water and 2 drops of concentrated  $\text{H}_2\text{SO}_4$  is added (to precipitate Ba as  $\text{BaSO}_4$ ). The sample is heated for 1 hour, filtered, and heated again until dry.
  13. The sample is dissolved in 5 mls 2N HCl, warmed, and diluted with distilled water. The sample is passed through the recleaned cation exchange column a second time (see steps 10 and 11).
  14. The REE are collected in 100 mls 6N HCl, a drop of  $\text{HClO}_4$  is added to the beaker and the solution is evaporated until it covers just the bottom of the beaker. This is transferred to a 30 ml Teflon beaker and evaporated to complete dryness.
  15. The dried sample is dissolved by adding 50 ul of a very

dilute HCl solution using an Eppendorf pipette. Pick up the sample solution with the Eppendorf and place it in the middle of a prepared ion exchange resin paper. After drying the sample is stored in a labelled coin envelope for later analysis.

#### A.6 RELICT CLINOPYROXENE ANALYSIS

Representative thin sections containing relict clinopyroxene grains were first polished using a 1 micron aluminum oxide abrasive powder and finished with a 0.3 micron powder slurry. The thin sections were placed in an ultrasonic cleaner for several seconds to remove any remaining polishing agent. The slides were then coated with carbon in a Varian vacuum evaporator.

Analysis of relict pyroxenes was carried out on an automated JEOL JXA-50A electron probe microanalyser, equipped with Krisel Control through a PDP-11 computer, at Memorial University. Operating conditions consisted of an acceleration potential of 15 kV and a beam current of 20 microamperes. The width of the electron beam is approximately 1 micron. Compositions of the analysed pyroxenes were computer calculated by reference to calibration curves based on analysis of established standard materials.

**APPENDIX B****CIPW NORMS**

## INTRODUCTION

Calculated CIPW norms (wt.%) for analysed samples from the Blue Hills Sequence are presented in Table B-1. The norms were calculated on an anhydrous basis after adjusting  $\text{Fe}_2\text{O}_3/\text{FeO}$  to 0.25. This is a suitable ratio as these mafic flows were erupted in a subaerial environment.

Normative minerals listed in Table B-1 are abbreviated as follows:

Q	quartz	hy	hypersthene
or	orthoclase	ol	olivine
ab	albite	fo	forsterite
an	anorthite	fa	fayalite
ne	nepheline	mt	magnetite
di	diopside	il	ilmenite
wo	wollastonite	cr	chromite
en	enstatite	ap	apatite
fs	ferrosilite	C	corundum

TABLE B-1. CIPW WEIGHT NORMS. BLUE HILLS SEQUENCE, HARBOUR MAIN GROUP

		PYROXENE-PHYRIC LAVAS									
		058-1	014-1	108-3	109-4	118-1	119-3	132-2	197-1	235-1	236-1
Q		--	--	--	--	1.36	--	--	--	--	--
or		5.02	12.47	8.72	13.12	15.94	12.21	10.93	26.03	18.52	2.93
ab		59.28	24.95	20.22	34.95	33.11	40.40	34.48	25.54	23.37	41.20
an		6.21	30.57	29.99	24.50	17.96	17.22	25.35	19.73	26.43	20.21
ne		--	1.67	--	0.52	--	--	1.10	--	4.48	1.63
di	wo	--	5.14	6.15	0.90	3.45	3.87	.47	--	0.37	5.93
	en	--	2.84	3.64	0.51	1.74	1.98	1.43	--	0.22	3.46
	fs	--	2.11	2.20	0.36	1.63	1.79	0.93	--	0.13	2.18
hy	en	7.44	--	13.54	--	9.56	6.68	--	0.94	--	--
	fs	5.55	--	8.17	--	8.99	6.05	--	0.53	--	--
ol	fo	3.81	7.71	1.52	10.92	--	1.72	9.94	12.38	11.86	9.08
	fa	3.13	6.30	1.01	8.58	--	1.72	7.12	7.63	8.03	6.30
mt		2.42	2.78	2.82	2.87	2.78	2.71	2.73	2.68	2.83	2.86
il		1.99	2.85	1.54	2.05	2.56	2.74	2.70	2.36	2.93	3.28
cr		--	0.03	0.06	0.02	--	--	0.03	0.03	0.03	0.03
ap		0.78	0.57	0.43	0.70	0.93	0.92	0.80	0.82	0.79	0.93
C		4.37	--	--	--	--	--	--	1.34	--	--

Note: Norms calculated on anhydrous basis after adjusting  $\text{Fe}_2\text{O}_3/\text{FeO}$  to 0.25

TABLE B-1 (continued).

BASALTIC LAVAS										
	022-1	035-5	037-1	039-1	046-1	048-1	053-1	067-1	073-1	076-3
Q	--	--	--	--	--	--	--	--	--	--
or	12.27	8.96	17.75	15.88	9.05	10.85	10.45	9.50	10.33	10.36
ab	30.91	30.83	19.42	36.76	22.45	25.75	24.99	22.21	26.43	28.23
an	26.94	27.93	33.09	12.10	33.64	29.60	31.75	31.87	31.30	29.96
ne	--	0.96	3.29	--	--	1.45	--	--	0.08	0.02
di	wo	--	3.69	0.84	--	3.67	1.71	4.15	2.33	0.72
	en	--	2.16	0.49	--	2.20	1.04	2.47	1.36	0.42
	fs	--	1.35	0.30	--	1.27	0.58	1.47	0.86	0.26
hy	en	6.62	--	--	1.00	3.58	--	2.49	10.93	--
	fs	5.32	--	--	0.55	2.07	--	1.49	6.92	--
ol	fo	5.98	11.01	11.61	14.05	9.69	13.76	9.34	4.44	13.95
	fa	5.30	7.62	7.88	8.48	6.15	8.54	6.14	3.10	9.27
mt	3.07	2.84	2.66	2.99	2.93	3.04	2.73	3.05	3.25	3.13
il	2.39	2.10	2.02	2.50	2.49	2.60	1.96	2.56	3.12	3.13
cr	0.03	0.03	0.03	0.05	0.06	0.06	0.03	0.06	0.05	0.03
ap	0.57	0.51	0.61	0.59	0.76	1.02	0.56	0.80	0.83	0.99
C	0.61	--	--	5.05	--	--	--	--	--	--

Note: Norms calculated on anhydrous basis after adjusting  $\text{Fe}_2\text{O}_3/\text{FeO}$  to 0.25

TABLE B-1 (continued).

BASALTIC LAVAS										
	082-2	087-2	092-1	092-2	100-2	101-5	102-3	104-1	111-2	111-3
Q	--	--	--	--	--	--	--	--	--	--
or	5.27	9.19	5.59	8.82	12.76	9.05	7.19	13.08	9.26	3.77
ab	20.90	30.80	25.86	25.42	33.19	29.66	34.32	30.87	27.47	19.31
an	32.72	26.25	31.49	28.68	21.47	23.95	26.54	23.30	30.33	35.87
ne	--	1.42	--	0.96	--	1.89	--	--	--	--
di	wo	5.51	--	4.80	4.63	--	6.56	1.39	2.66	3.33
	en	3.31	--	2.55	2.75	--	3.76	0.83	1.57	2.02
	fs	1.91	--	2.10	1.65	--	2.51	0.49	0.95	1.13
hy	en	8.47	--	4.66	--	1.89	--	0.43	0.09	13.57
	fs	4.89	--	3.84	--	1.08	--	0.26	0.06	7.59
ol	fo	6.29	14.32	5.99	12.42	13.04	9.53	13.51	11.80	4.02
	fa	4.00	9.58	5.43	8.23	8.21	7.02	8.82	7.91	2.48
mt	3.11	3.29	3.48	3.15	3.06	2.98	3.10	2.86	3.02	3.13
il	2.72	3.09	3.34	2.48	2.79	2.41	2.35	2.25	2.50	2.82
ap	0.82	1.22	0.84	0.75	1.28	0.61	0.71	0.56	0.70	0.88
C	--	0.79	--	--	1.18	--	--	--	--	--

Note: Norms calculated on anhydrous basis after adjusting  $\text{Fe}_2\text{O}_3/\text{FeO}$  to 0.25

TABLE B-1 (continued).

BASALTIC LAVAS										
	115-1	125-1	135-2	136-1	136-2	137-1	138-1	140-3	163-2	166-1
Q	--	--	--	--	--	--	--	--	--	--
or	8.91	8.26	10.07	5.88	12.39	18.23	15.74	11.54	10.20	9.31
ab	23.57	27.32	29.37	29.27	27.76	19.27	15.34	31.02	22.84	27.08
an	31.91	29.67	27.61	29.14	27.54	28.87	31.65	24.06	29.18	29.85
ne	--	--	2.00	2.83	2.56	3.31	4.52	2.25	2.45	1.60
di	wo	0.49	3.06	0.16	5.39	0.85	--	5.11	4.51	1.19
	en	0.30	1.80	0.10	3.13	0.50	--	3.02	2.41	0.71
	fs	0.16	1.10	0.06	2.01	0.31	--	1.84	1.96	0.42
hy	en	1.52	2.96	--	--	--	--	--	--	--
	fs	0.81	1.80	--	--	--	--	--	--	--
ol	fo	16.01	10.17	14.63	9.88	13.27	15.10	9.95	8.23	14.38
	fa	9.33	6.82	9.49	7.00	8.86	8.92	6.67	7.38	10.36
mt		3.36	3.09	3.15	2.81	3.01	2.95	2.77	3.00	3.63
il		2.88	2.73	2.52	2.11	2.34	2.26	2.57	2.68	3.20
cr		0.08	0.06	0.05	0.02	--	0.03	0.05	0.03	0.05
ap		0.68	1.15	0.80	0.53	0.61	0.66	0.78	0.94	0.82
C	--	--	--	--	--	0.41	--	--	--	--

Note: Norms calculated on anhydrous basis after adjusting  $\text{Fe}_2\text{O}_3/\text{FeO}$  to 0.25

TABLE B-1 (continued).

## BASALTIC LAVAS

	169-1	169-2	172-2	173-1	185-1	186-1	221-2	225-2	228-1	229-1
Q	--	--	--	--	--	--	--	--	--	--
or	10.65	13.31	10.67	7.16	10.99	7.98	8.43	9.31	9.52	10.27
ab	26.62	28.41	27.98	7.36	34.95	35.93	28.17	28.78	35.76	25.94
an	27.61	23.77	28.23	28.47	23.28	21.19	31.11	29.18	22.18	27.28
ne	0.43	1.76	--	4.55	--	--	1.05	0.71	--	--
di	wo	3.17	3.74	0.29	10.52	0.37	--	1.70	1.35	--
	en	1.85	2.21	0.18	5.86	0.22	--	1.00	0.83	--
	fs	1.17	1.34	0.10	4.25	0.14	--	0.62	0.44	--
hy	en	--	--	1.38	--	1.05	1.91	--	--	0.76
	fs	--	--	0.77	--	0.65	0.97	--	--	0.42
ol	fo	12.77	11.57	14.64	8.18	13.31	16.00	13.25	14.69	15.09
	fa	8.86	7.72	8.93	6.53	9.07	8.99	9.04	8.64	9.11
mt	3.31	2.90	3.23	3.27	3.23	3.28	3.08	2.99	3.09	3.09
il	2.93	2.38	2.79	2.64	2.67	2.89	2.09	2.40	2.26	2.28
cr	--	--	0.06	0.05	0.05	0.06	0.03	0.03	0.03	0.03
ap	0.63	0.90	0.76	1.15	0.02	0.93	0.44	0.63	0.61	0.56
C	--	--	--	--	--	0.77	--	--	1.17	1.41

Note: Norms calculated on anhydrous basis after adjusting  $\text{Fe}_2\text{O}_3/\text{FeO}$  to 0.25

TABLE B-1 (continued).

BASALTIC LAVAS					BRIGUS JUNCTION					
	232-1	234-1	239-1	240-1	144-1	145-1	145-2	146-1	150-1	
Q	--	--	--	--	--	--	--	--	--	
or	4.52	21.08	22.31	15.84	12.47	13.58	19.10	9.42	18.93	
ab	31.24	19.65	25.12	28.81	20.90	24.13	24.33	29.39	16.72	
an	26.96	28.49	20.13	20.04	28.15	23.00	17.48	15.74	16.74	
ne	2.00	2.98	0.80	2.13	1.63	1.21	1.78	1.48	2.57	
di	wo	4.19	0.14	--	2.21	2.87	5.17	3.98	6.09	7.90
	en	2.51	0.09	--	1.35	1.77	2.85	1.99	3.00	3.73
	fs	1.46	0.04	--	0.73	0.94	2.12	1.91	2.98	4.07
hy	en	--	--	--	--	--	--	--	--	
	fs	--	--	--	--	--	--	--	--	
ol	fo	12.52	14.23	16.69	14.21	14.70	10.23	9.08	9.98	8.46
	fa	8.00	7.75	8.58	8.45	8.59	8.40	9.58	10.90	10.17
mt	3.07	2.62	2.84	2.99	3.27	3.71	4.08	4.56	4.54	
il	2.65	2.18	2.32	2.40	3.43	4.64	5.03	4.60	4.40	
cr	0.06	0.03	0.09	0.09	0.05	0.03	0.03	--	--	
ap	0.83	0.73	0.66	0.76	1.23	0.94	1.63	1.85	1.77	
C	--	--	0.45	--	--	--	--	--	--	

Note: Norms calculated on anhydrous basis after adjusting  $\text{Fe}_2\text{O}_3/\text{Feo}$  to 0.25

TABLE B-1 (continued).

BRIGUS JCT.			SILLS				DYKE
	210-1	212-2	055-1	070-1	081-4A	118-4	202-1
Q	--	--	--	--	--	--	1.32
or	21.91	11.72	8.20	9.21	16.94	3.14	13.98
ab	27.38	36.07	33.19	28.38	22.60	27.42	24.36
an	13.45	16.18	25.58	29.23	29.45	31.30	23.30
ne	--	--	1.10	--	1.90	2.32	--
di	wo	1.25	--	--	0.60	5.24	4.47
	en	0.61	--	--	0.34	2.98	1.94
	fs	0.62	--	--	0.23	2.03	2.53
hy	en	6.83	--	3.03	--	--	8.74
	fs	9.15	--	1.60	--	--	11.41
ol	fo	3.58	14.75	13.13	12.12	11.04	--
	fa	5.28	9.25	7.61	9.33	8.31	--
mt	4.25	4.16	3.08	3.06	3.14	3.21	3.64
il	4.65	4.77	2.52	2.98	2.45	2.27	3.12
cr	--	--	0.05	0.05	0.03	0.08	--
ap	2.90	2.97	1.00	1.16	0.87	0.68	1.19
C	0.61	--	1.30	0.57	--	--	--

Note : Norms calculated on anhydrous basis after adjusting  $\text{Fe}_2\text{O}_3/\text{FeO}$  to 0.25



